1. Report No. NASA TM X-3315	2. Government Accession No.	3. Recipient's Catalog No.
4. Title and Subtitle SUPERSONIC DYNAMIC-STABILITY DERIVATIVES OF THE SPACE SHUTTLE LAUNCH VEHICLE		5. Report Date February 1976 6. Performing Organization Code
7. Author(s) Richmond P. Boyden, Delma C. Freeman, Jr., and Edwin E. Davenport		8. Performing Organization Report No. L-10494
9. Performing Organization Name and Address NASA Langley Research Center Hampton, Va. 23665		10. Work Unit No. 506-26-30-04 11. Contract or Grant No.
12. Sponsoring Agency Name and Address National Aeronautics and Space Administration Washington, D.C. 20546		13. Type of Report and Period Covered Technical Memorandum 14. Sponsoring Agency Code
15. Supplementary Notes		

16. Abstract

An investigation has been made to determine the dynamic-stability characteristics of a 0.015-scale model of the space shuttle launch vehicle at supersonic speeds. These tests were made at angles of attack from -10° to 10° at Mach numbers of 2.00, 2.86, 3.96, and 4.63. The complete launch vehicle, consisting of the orbiter, external tank, and solid rocket boosters, has positive damping in pitch, roll, and yaw over the angle-of-attack and Mach number range. The orbiter external-tank configuration has a region of negative pitch damping for small negative angles of attack at a Mach number of 2.00. At all other test conditions, the orbiter external-tank configuration has positive damping about all three axes.

17. Key Words (Suggested by Author(s)) Dynamic stability Shuttle launch vehicle Forced oscillations Aeronautics	18. Distribution Statement Unclassified Unlimited Subject Category 15		
19. Security Classif. (of this report) Unclassified	20. Security Classif. (of this page) Unclassified	21. No. of Pages 67	22. Price* $4.25

*For sale by the National Technical Information Service, Springfield, Virginia 22161

SUPERSONIC DYNAMIC-STABILITY DERIVATIVES OF THE SPACE SHUTTLE LAUNCH VEHICLE

Richmond P. Boyden, Delma C. Freeman, Jr.,
and Edwin E. Davenport
Langley Research Center

SUMMARY

An investigation has been made to determine the dynamic-stability characteristics of a 0.015-scale model of the space shuttle launch vehicle at supersonic speeds. These tests were made at angles of attack from -10° to 10° at Mach numbers of 2.00, 2.86, 3.96, and 4.63. The complete launch vehicle, consisting of the orbiter, external tank, and solid rocket boosters, has positive damping in pitch, roll, and yaw over the angle-of-attack and Mach number range. The orbiter external-tank configuration has a region of negative pitch damping for small negative angles of attack at a Mach number of 2.00. At all other test conditions, the orbiter external-tank configuration has positive damping about all three axes.

INTRODUCTION

As part of the space shuttle development effort, the Langley Research Center has sponsored a program to determine experimentally the dynamic-stability characteristics of the space shuttle vehicle. The aerodynamic damping derivatives have been determined for the orbiter at subsonic to hypersonic speeds (refs. 1 to 3) and for the launch vehicle during the ascent flight from lift-off to transonic speeds (ref. 4). As part of this study, forced-oscillation dynamic-stability tests of a 0.015-scale model of the space shuttle launch vehicle were made at supersonic speeds in the Langley Unitary Plan wind tunnel. These tests were made at Mach numbers from 2.00 to 4.63, measuring the pitch, roll, and yaw damping as well as the normal force due to pitch rate and the cross derivatives (yawing moment due to roll rate and rolling moment due to yaw rate). The complete launch configuration and the orbiter external-tank combination without the solid rocket boosters were tested. The center-of-oscillation position was changed during the tests to take into account the wide variation in center-of-gravity location during the flight of the launch vehicle.

SYMBOLS

The aerodynamic parameters in this paper are referred to the body system of axes as shown in figure 1. The axes originate at the assumed centers of oscillation which were located to correspond with the center-of-gravity (c.g.) positions shown in figure 2.

The reference length used to nondimensionalize all of the aerodynamic parameters was the orbiter body length which is 0.4916 m (for the 0.015-scale model). The reference area used to nondimensionalize the aerodynamic parameters was the orbiter wing area which is 0.05623 m^2 (for the 0.015-scale model).

Units of measurement are presented in the International System of Units (SI). See reference 5 for details on the use of the SI physical constants and conversion factors.

C_l rolling-moment coefficient, $\frac{\text{Rolling moment}}{q_\infty S\ell}$

$C_{l_p} = \frac{\partial C_l}{\partial\left(\frac{p\ell}{2V}\right)}$, per radian

$C_{l_{\dot{p}}} = \frac{\partial C_l}{\partial\left(\frac{\dot{p}\ell^2}{4V^2}\right)}$, per radian

$C_{l_p} + C_{l_{\dot{\beta}}} \sin \alpha$ damping-in-roll parameter, per radian

$C_{l_r} = \frac{\partial C_l}{\partial\left(\frac{r\ell}{2V}\right)}$, per radian

$C_{l_{\dot{r}}} = \frac{\partial C_l}{\partial\left(\frac{\dot{r}\ell^2}{4V^2}\right)}$, per radian

$C_{l_r} - C_{l_{\dot{\beta}}} \cos \alpha$ rolling moment due to yaw-rate parameter, per radian

$C_{l_\beta} = \frac{\partial C_l}{\partial \beta}$, per radian

$C_{l_{\dot{\beta}}} = \frac{\partial C_l}{\partial\left(\frac{\dot{\beta}\ell}{2V}\right)}$, per radian

$C_{l_\beta} \sin \alpha - k^2 C_{l_{\dot{p}}}$ rolling moment due to roll-displacement parameter, per radian

$C_{l_\beta} \cos \alpha + k^2 C_{l_{\dot{r}}}$ effective dihedral parameter, per radian

C_m pitching-moment coefficient, $\frac{\text{Pitching moment}}{q_\infty S \ell}$

$C_{m_q} = \frac{\partial C_m}{\partial\left(\frac{q\ell}{2V}\right)}$, per radian

$C_{m_{\dot{q}}} = \frac{\partial C_m}{\partial\left(\frac{\dot{q}\ell^2}{4V^2}\right)}$, per radian

$C_{m_q} + C_{m_{\dot{\alpha}}}$ damping-in-pitch parameter, per radian

$C_{m_\alpha} = \frac{\partial C_m}{\partial \alpha}$, per radian

$C_{m_{\dot{\alpha}}} = \frac{\partial C_m}{\partial\left(\frac{\dot{\alpha}\ell}{2V}\right)}$, per radian

$C_{m_\alpha} - k^2 C_{m_{\dot{q}}}$ oscillatory longitudinal-stability parameter, per radian

C_N normal-force coefficient, $\frac{\text{Normal force}}{q_\infty S}$

$C_{N_q} = \frac{\partial C_N}{\partial\left(\frac{q\ell}{2V}\right)}$, per radian

$C_{N_{\dot{q}}} = \frac{\partial C_N}{\partial\left(\frac{\dot{q}\ell^2}{4V^2}\right)}$, per radian

$C_{N_q} + C_{N_{\dot{\alpha}}}$ normal force due to pitch-rate parameter, per radian

$C_{N_\alpha} = \frac{\partial C_N}{\partial \alpha}$, per radian

$C_{N_{\dot{\alpha}}} = \frac{\partial C_N}{\partial\left(\frac{\dot{\alpha}\ell}{2V}\right)}$, per radian

$C_{N_\alpha} - k^2 C_{N_{\dot{q}}}$ normal force due to pitch-displacement parameter, per radian

C_n yawing-moment coefficient, $\frac{\text{Yawing moment}}{q_\infty S\ell}$

$C_{n_p} = \frac{\partial C_n}{\partial\left(\frac{p\ell}{2V}\right)}$, per radian

$C_{n_{\dot{p}}} = \frac{\partial C_n}{\partial\left(\frac{\dot{p}\ell^2}{4V^2}\right)}$, per radian

$C_{n_p} + C_{n_{\dot{\beta}}} \sin \alpha$ yawing moment due to roll-rate parameter, per radian

$C_{n_r} = \frac{\partial C_n}{\partial\left(\frac{r\ell}{2V}\right)}$, per radian

$C_{n_{\dot{r}}} = \frac{\partial C_n}{\partial\left(\frac{\dot{r}\ell^2}{4V^2}\right)}$, per radian

$C_{n_r} - C_{n_{\dot{\beta}}} \cos \alpha$ damping-in-yaw parameter, per radian

$C_{n_\beta} = \frac{\partial C_n}{\partial \beta}$, per radian

$C_{n_{\dot{\beta}}} = \frac{\partial C_n}{\partial\left(\frac{\dot{\beta}\ell}{2V}\right)}$, per radian

$C_{n_\beta} \cos \alpha + k^2 C_{n_{\dot{r}}}$ oscillatory directional-stability parameter, per radian

$C_{n_\beta} \sin \alpha - k^2 C_{n_{\dot{p}}}$ yawing moment due to roll-displacement parameter, per radian

f frequency of oscillation, hertz

k reduced-frequency parameter, $\frac{\omega \ell}{2V}$ in pitch, roll, and yaw, radians

ℓ reference length, orbiter body length, meters

M free-stream Mach number

p angular velocity of model about X-axis, radians/second

q angular velocity of model about Y-axis, radians/second

q_∞ free-stream dynamic pressure, newtons/meter^2

R Reynolds number, based on orbiter body length, ℓ

r angular velocity of model about Z-axis, radians/second

S reference area, meters^2

T tunnel-stagnation temperature, K

V free-stream velocity, meters/second

α angle of attack, degrees or radians

β angle of sideslip, radians

ϕ model roll-orientation angle, degrees

ω angular velocity, $2\pi f$, radians/second

A dot over a quantity indicates a first derivative with respect to time.

MODEL AND TEST APPARATUS

A drawing of the 0.015-scale model used for these tests is shown in figure 2. The model consisted of the space shuttle orbiter vehicle mounted above the external propellant tank and the solid rocket boosters (SRB) mounted on the sides of the propellant tank. The model could be tested as a complete launch vehicle (orbiter, external tank and SRB) or without the solid rocket boosters as the orbiter external-tank combination to represent the configuration after the solid rockets had been staged during launch or an abort situation. Details of the external propellant tank, solid rocket boosters, and the front and rear attachment points are presented in figure 3.

The supersonic forced-oscillation tests were made in the Langley Unitary Plan wind tunnel. Test section 1 was used for Mach numbers of 2.00 and 2.86 while Mach numbers of 3.96 and 4.63 were run in test section 2. The operating characteristics of the Unitary Plan Tunnel are given in reference 6. Figure 4 shows a photograph of the model mounted in the test section for the forced-oscillation tests. A description of the technique and the measurement and reduction of data for the small-amplitude, forced-oscillation, dynamic-stability tests are found in reference 2.

TESTS

The forced-oscillation dynamic-stability tests were made to determine the pitch $\left(C_{m_q} + C_{m_{\dot{\alpha}}}\right)$, yaw $\left(C_{n_r} - C_{n_{\dot{\beta}}} \cos \alpha\right)$, and roll damping $\left(C_{l_p} + C_{l_{\dot{\beta}}} \sin \alpha\right)$; the normal force due to pitch rate $\left(C_{N_q} + C_{N_{\dot{\alpha}}}\right)$; and the cross-derivative parameters: yawing moment due to roll rate $\left(C_{n_p} + C_{n_{\dot{\beta}}} \sin \alpha\right)$ and the rolling moment due to yaw rate $\left(C_{l_r} - C_{l_{\dot{\beta}}} \cos \alpha\right)$. The values of the nominal amplitude of the oscillation and of the range of the reduced-frequency parameter during the dynamic-stability tests were:

Oscillation axis	Amplitude of oscillation, degrees	Reduced-frequency parameter, k, radians
Pitch	1	0.0064 to 0.0174
Yaw	1	.0064 to .0159
Roll	2.5	.0109 to .0195

The longitudinal position of the model moment reference center was varied depending on the configuration. The definition of the positions used in the tests is presented in figure 2.

The tunnel dynamic pressure, velocity, stagnation temperature, and Reynolds number based on the orbiter body length were:

Mach number, M	Dynamic pressure, q_∞, kN/m^2	Velocity, V, m/sec	Stagnation temperature, T, K	Reynolds number, R
2.00	22.7	550	339	3.22×10^6
2.86	19.0	650	339	↓
3.96	14.1	733	353	↓
4.63	11.2	758	353	↓

For the Mach numbers of 2.00 and 2.86, three-dimensional roughness in the form of sparsely distributed No. 60 carborundum grains was applied in bands 0.16 cm wide located 1.27 cm from the leading edge of the orbiter wing and vertical tail. Similar bands were applied in rings around the nose of the orbiter, the external tank, and the solid rocket boosters, 3.05 cm rearward from the nose of each. For the higher Mach numbers of 3.96 and 4.63, single particles of No. 45 carborundum grains were spaced approximately 0.16 cm apart in the same locations as noted previously for the lower Mach numbers.

The angle of attack was varied from about -10° to 10°. Because the dynamic-stability sting is mounted 16.5 cm below the center line in both test sections of the Langley Unitary Plan wind tunnel, the model had to be inverted to obtain the negative angles of attack. No data were taken at a Mach number of 2.00 at angles of attack between -1° and -4° because of a reflected shock impingement upon the model vertical tail.

RESULTS AND DISCUSSION

The complexity of the flow field surrounding the launch vehicle configurations at supersonic speeds is illustrated by the series of typical schlieren photographs in figure 5. The photographs show the orbiter external-tank configuration at Mach numbers of 2.00 and 3.96 and the complete launch configuration at a Mach number of 4.63.

Pitch Oscillation Tests

The complete results of the pitch oscillation tests are presented in figures 6 to 9. The data in the figures are identified by model roll-orientation angle ϕ of either 0° or 180° because the model had to be inverted for the negative angles of attack.

The pitch-damping results for the shuttle launch configuration at the center-of-gravity position for both the maximum dynamic-pressure case (max. q_∞) and for the solid rocket

booster (SRB) burnout case are shown in figure 6. This configuration exhibited positive damping in pitch (negative values of $C_{m_q} + C_{m_{\dot{\alpha}}}$) throughout the range of angle of attack and Mach number. There are only small effects on the pitch damping from the change in center-of-gravity position while the change in level of the oscillatory longitudinal stability $(C_{m_\alpha} - k^2 C_{m_{\dot{q}}})$ is evident as expected from the shift in center of gravity. The center-of-gravity position for maximum dynamic pressure results in regions of low or slightly unstable values of the oscillatory longitudinal-stability parameter. The scatter evident in the data points for the two lower Mach numbers, 2.00 and 2.86, is greater than that at the two higher Mach numbers, 3.96 and 4.63. A similar effect may also be seen in the yaw and roll results. This scatter, evident at the lower Mach numbers, is thought to be a result of a higher level of tunnel turbulence in the low Mach number test section.

In order to provide information for use in abort and staging studies, tests were made on the orbiter external-tank combination with the center of gravity corresponding to the vehicle center of gravity after staging the solid rocket boosters. These results are shown in figure 7. There is a region of negative damping (positive values of $C_{m_q} + C_{m_{\dot{\alpha}}}$) at small negative angles of attack for a Mach number of 2.00. As previously mentioned, there is a gap in all of the $M = 2.00$ results because of a reflected shock wave striking the model when it was in the inverted position at low angles of attack. At $M = 2.00$, the value of the damping-in-pitch parameter was a strong function of angle of attack for the negative angle-of-attack range. For Mach numbers higher than 2.00 the damping in pitch for the orbiter external-tank combination was positive and relatively insensitive to angle of attack. The orbiter external-tank combination had stable values of the oscillatory longitudinal-stability parameter over the entire range of test conditions.

The normal force due to pitch rate and the normal force due to pitch-displacement results are shown in figures 8 and 9. Both the maximum dynamic-pressure configuration and the solid-rocket burnout configuration (fig. 8) have values that show only small changes in the normal force due to pitch rate with angle of attack. The normal force due to pitch-displacement parameter, which is analogous to the static C_{N_α}, decreases with increasing Mach number. The values of $C_{N_q} + C_{N_{\dot{\alpha}}}$ for the orbiter external-tank configuration (fig. 9) show more variation with angle of attack than did the other two configurations.

Yaw Oscillation Tests

For the yaw and roll tests, the launch configuration was tested only at the center-of-gravity position corresponding to the maximum dynamic-pressure condition. The results of the oscillation tests in yaw are contained in figures 10 and 11 where the damping-in-yaw parameter $(C_{n_r} - C_{n_{\dot{\beta}}} \cos \alpha)$ and the oscillatory directional-stability parameter $(C_{n_\beta} \cos \alpha + k^2 C_{n_{\dot{r}}})$ are

plotted against angle of attack. Both the mated vehicle and the orbiter external-tank combination are seen to have positive damping in yaw (negative values of $C_{n_r} - C_{n_{\dot{\beta}}} \cos \alpha$) over the angle-of-attack and Mach number range. The level of the yaw damping generally decreases with increasing Mach number. There are positive values of the oscillatory directional-stability parameter for both configurations over the range of test conditions, but the parameter generally decreases in value with both increasing angle of attack and Mach number. The orbiter external-tank configuration has a higher level of oscillatory directional stability than the launch configuration, but there is a large difference in center-of-gravity position between the two configurations.

The rolling moment due to yaw-rate parameter and the effective dihedral parameter are presented in figures 12 and 13 for the mated vehicle and for the orbiter external-tank combination. Both configurations have generally small positive values of the rolling moment due to yaw-rate parameter and negative values of the effective dihedral parameter indicating positive dihedral effect.

Roll Oscillation Tests

The results of the roll oscillation tests are shown in figures 14 and 15 in the form of the roll-damping parameter $(C_{l_p} + C_{l_{\dot{\beta}}} \sin \alpha)$ and the rolling moment due to roll-displacement parameter $(C_{l_\beta} \sin \alpha - k^2 C_{l_{\dot{p}}})$. The launch configuration and orbiter external-tank configuration have positive damping in roll (negative values of $C_{l_p} + C_{l_{\dot{\beta}}} \sin \alpha$) over the Mach number and angle-of-attack range. Only small differences in the level of roll damping are evident between the two configurations as a result of removing the solid rocket boosters.

The yawing moment due to roll-rate parameter $(C_{n_p} + C_{n_{\dot{\beta}}} \sin \alpha)$ and the yawing moment due to roll-displacement parameter $(C_{n_\beta} \sin \alpha - k^2 C_{n_{\dot{p}}})$ test results are contained in figures 16 and 17. Values of the yawing moment due to roll-rate parameter were positive throughout the range of test conditions for both the complete launch configuration and for the orbiter external-tank configuration.

SUMMARY OF RESULTS

An investigation has been made to determine the dynamic-stability characteristics of a 0.015-scale model of the space shuttle launch vehicle at supersonic speeds. These tests were made at angles of attack from -10° to 10° at Mach numbers of 2.00, 2.86, 3.96, and 4.63. The results of these tests may be summarized as follows:

1. The complete launch vehicle, consisting of the orbiter, external tank, and solid rocket boosters, has positive damping in pitch, roll, and yaw over the angle-of-attack and Mach number range.

2. The orbiter external-tank configuration has a region of negative pitch damping for small negative angles of attack at a Mach number of 2.00. At all other test conditions, the orbiter external-tank configuration has positive damping about all three axes.

Langley Research Center
National Aeronautics and Space Administration
Hampton, Va. 23665
December 8, 1975

REFERENCES

1. Boyden, Richmond P.; and Freeman, Delma C., Jr.: Subsonic and Transonic Dynamic Stability Characteristics of a Space Shuttle Orbiter. NASA TN D-8042, 1975.

2. Freeman, Delma C., Jr.; Boyden, Richmond P.; and Davenport, Edwin E.: Supersonic Dynamic Stability Characteristics of a Space Shuttle Orbiter. NASA TN D-8343, 1975.

3. Uselton, Bob L.; and Jenke, Leroy M.: Pitch-, Yaw-, and Roll-Damping Characteristics of a Shuttle Orbiter at $M_\infty = 8$. AEDC-TR-74-129, U.S. Air Force, May 1975.

4. Freeman, Delma C., Jr.; Boyden, Richmond P.; and Davenport, Edwin E.: Subsonic and Transonic Dynamic Stability Characteristics of the Space Shuttle Launch Vehicle. NASA TM X-3336, 1976.

5. Mechtly, E. A.: The International System of Units Physical Constants and Conversion Factors (Second Revision). NASA SP-7012, 1973.

6. Schaefer, William T., Jr.: Characteristics of Major Active Wind Tunnels at the Langley Research Center. NASA TM X-1130, 1965.

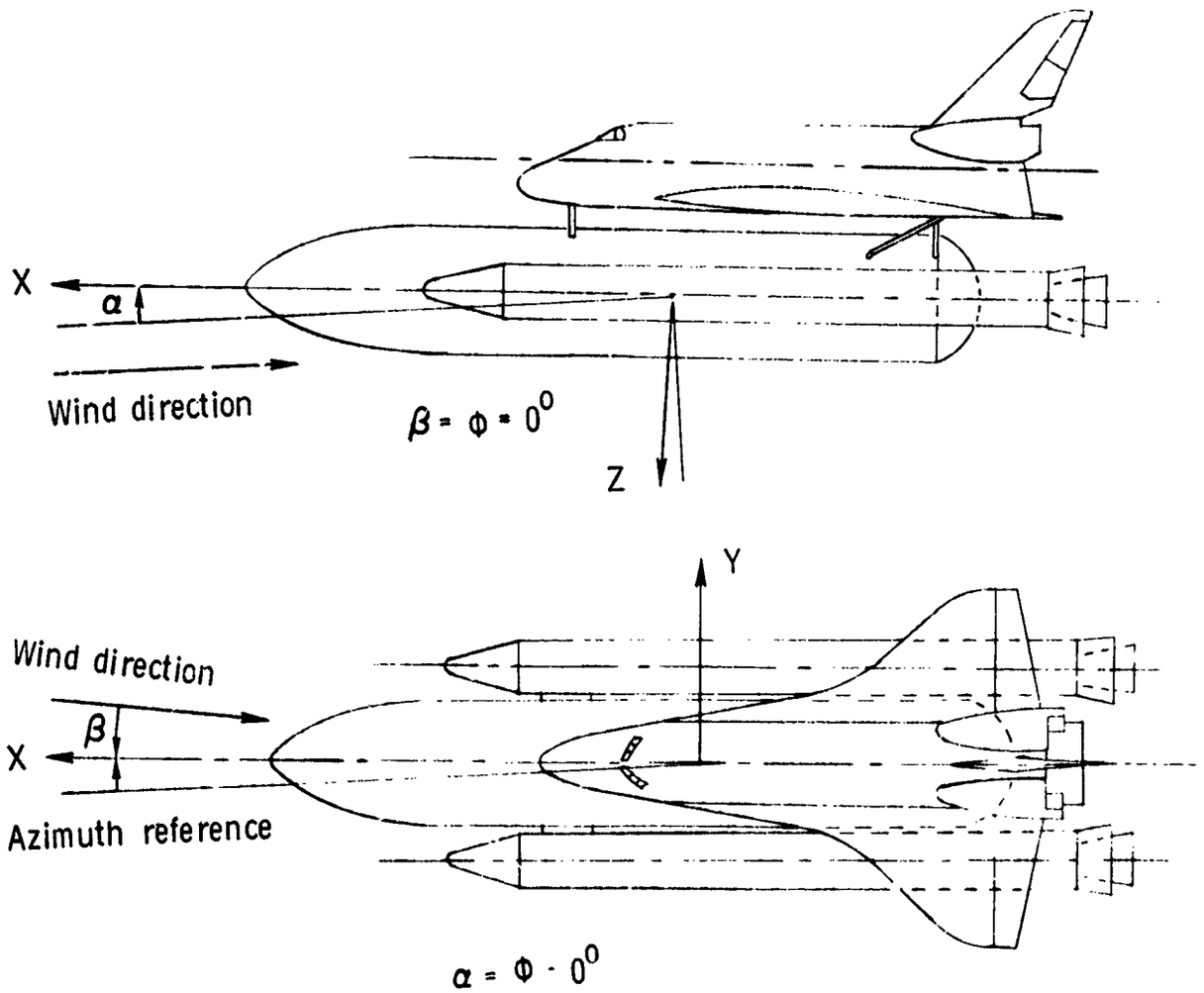

Figure 1.- System of axes.

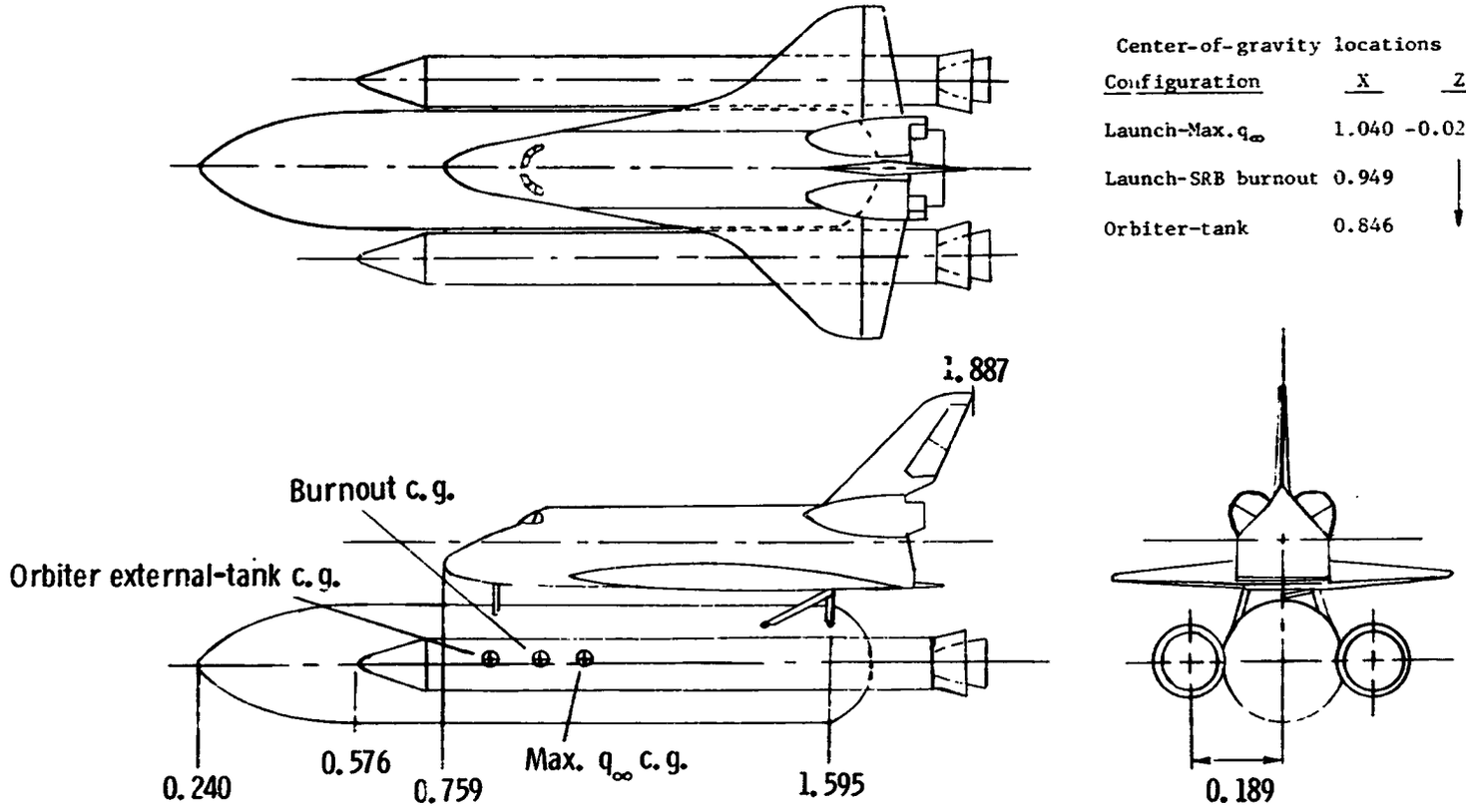

Figure 2.- Three-view drawing of model. All linear dimensions have been nondimensionalized by reference length ℓ (ℓ = 49.16 cm).

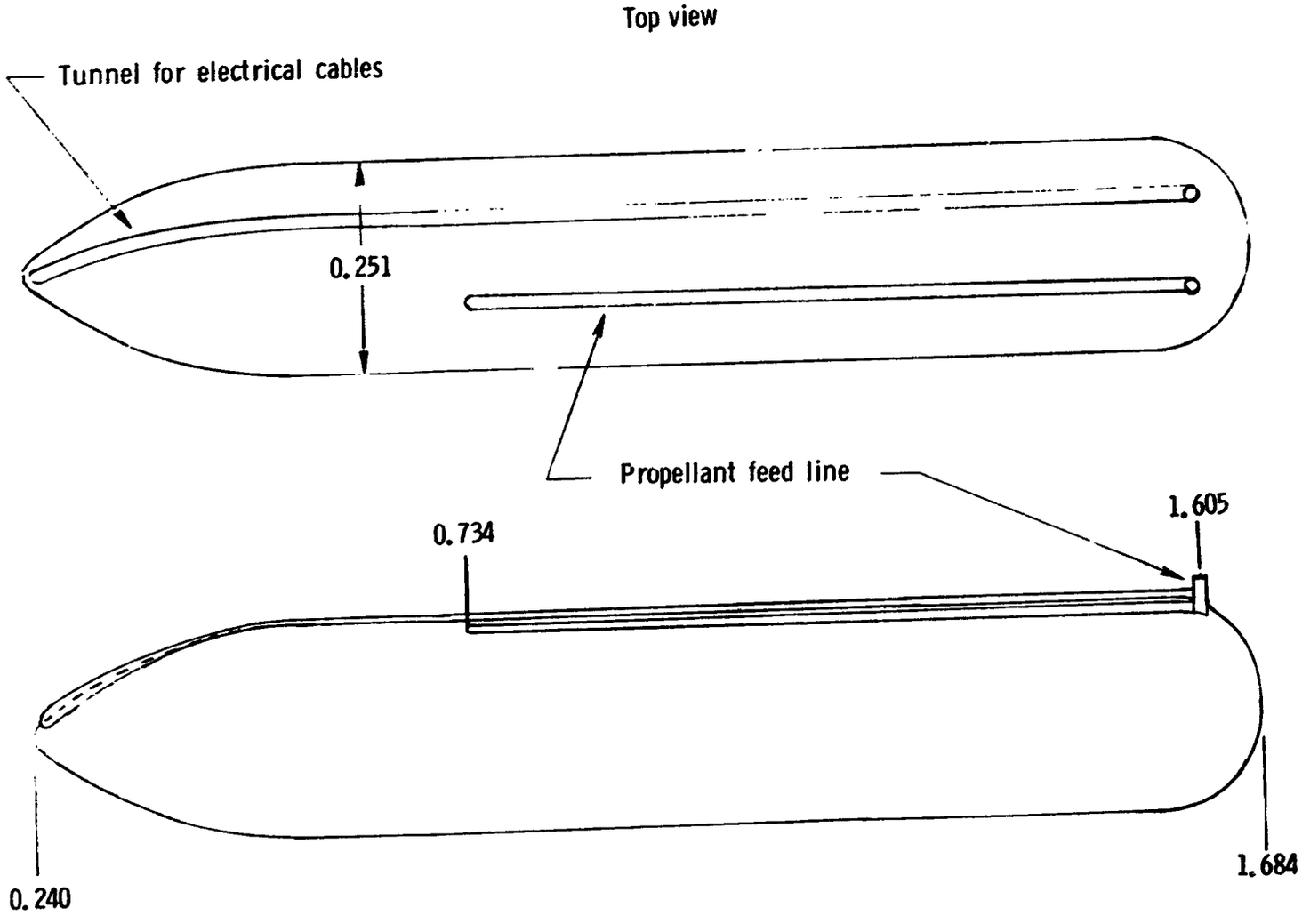

(a) External tank details.

Figure 3.- Detail drawings of model components. All linear dimensions have been nondimensionalized by reference length ℓ (ℓ = 49.16 cm).

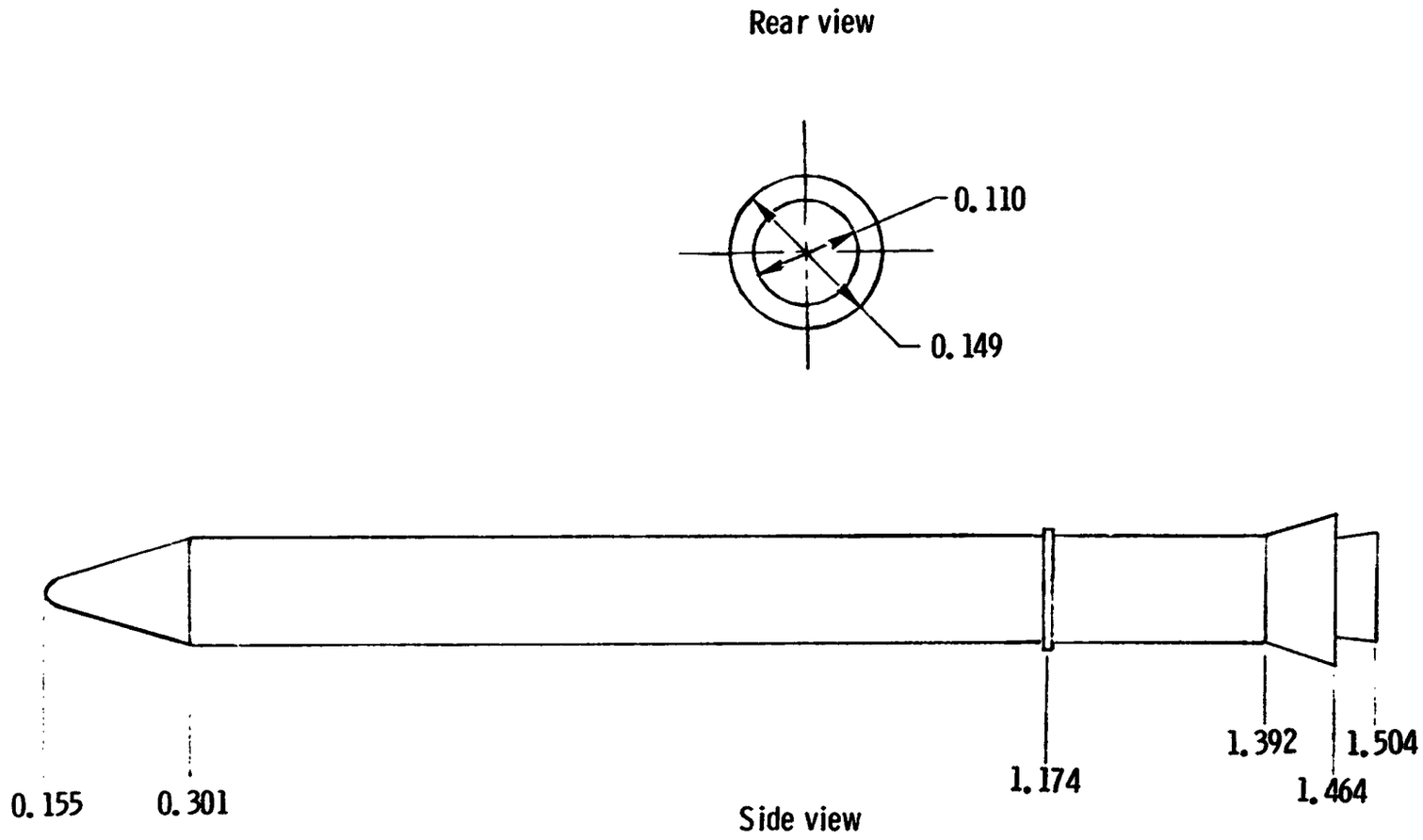

(b) Solid-rocket booster details.

Figure 3.- Continued.

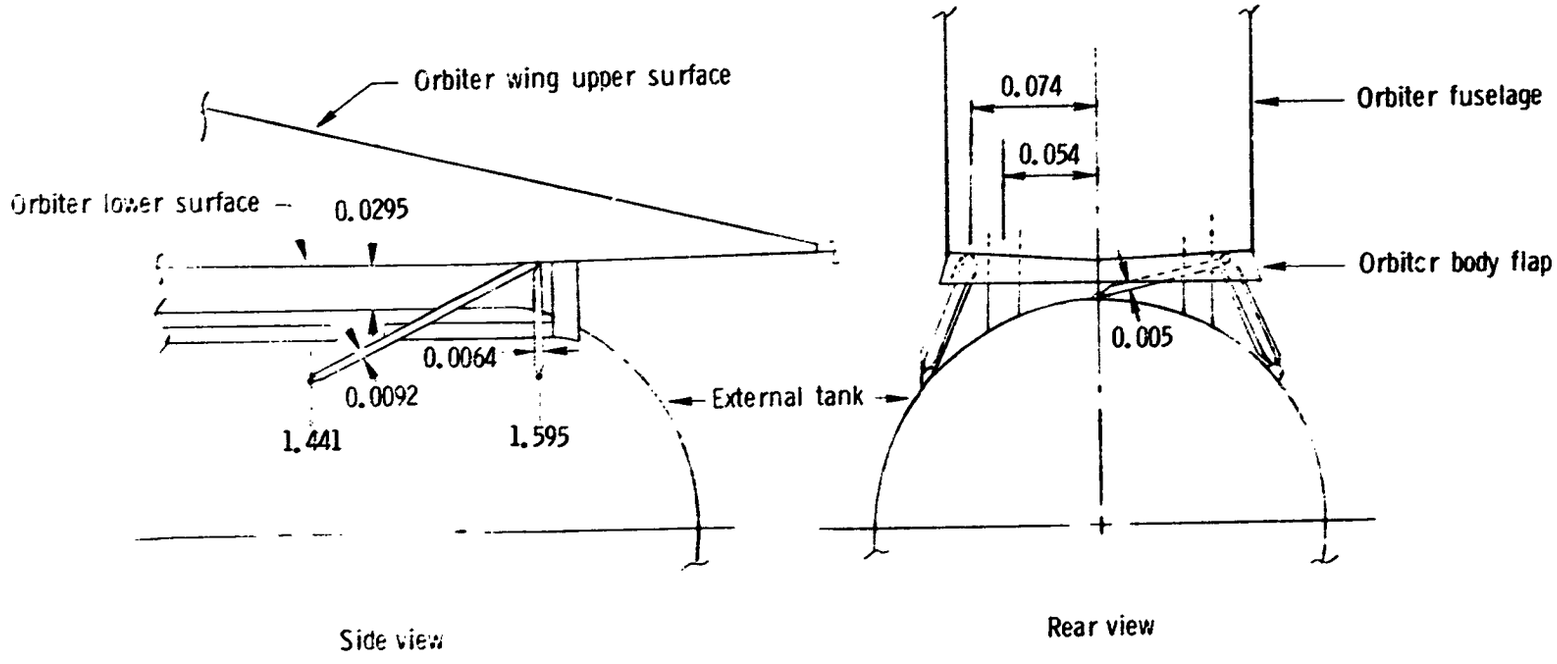

(c) Rear attachment structure details.

Figure 3.- Continued.

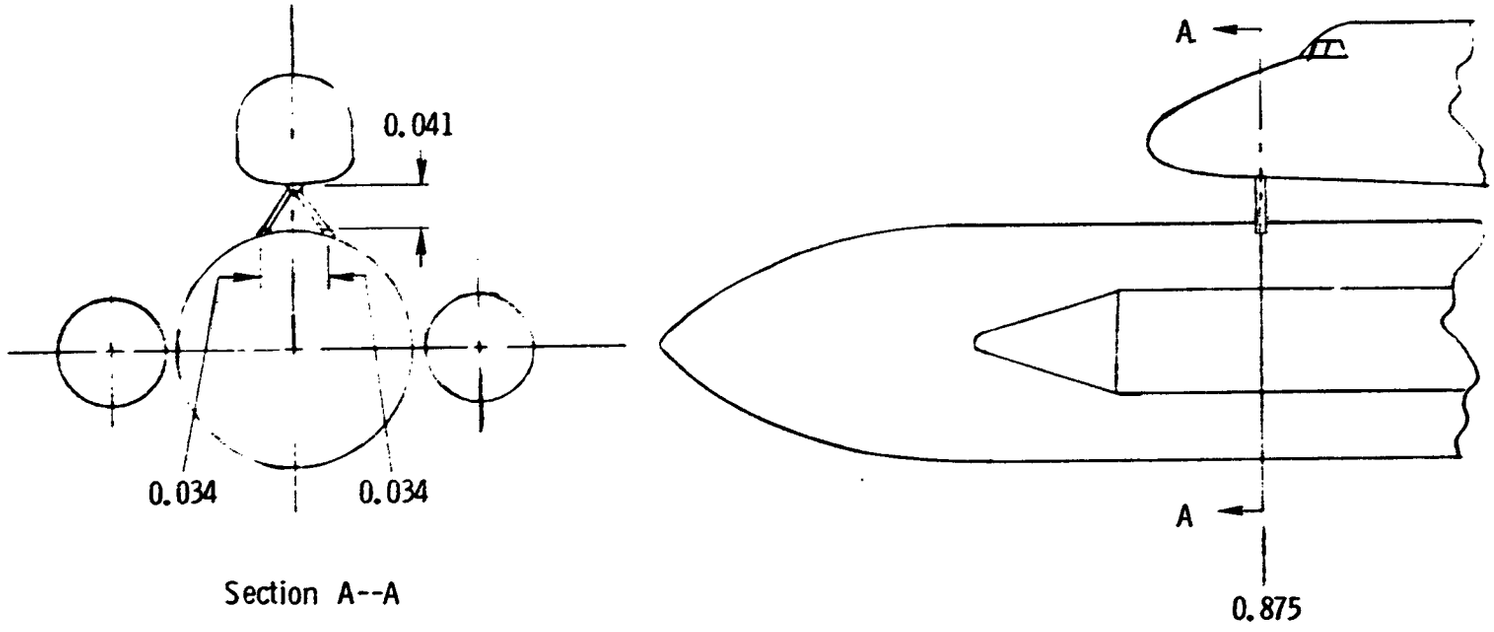

(d) Front attachment structure details.

Figure 3.- Concluded.

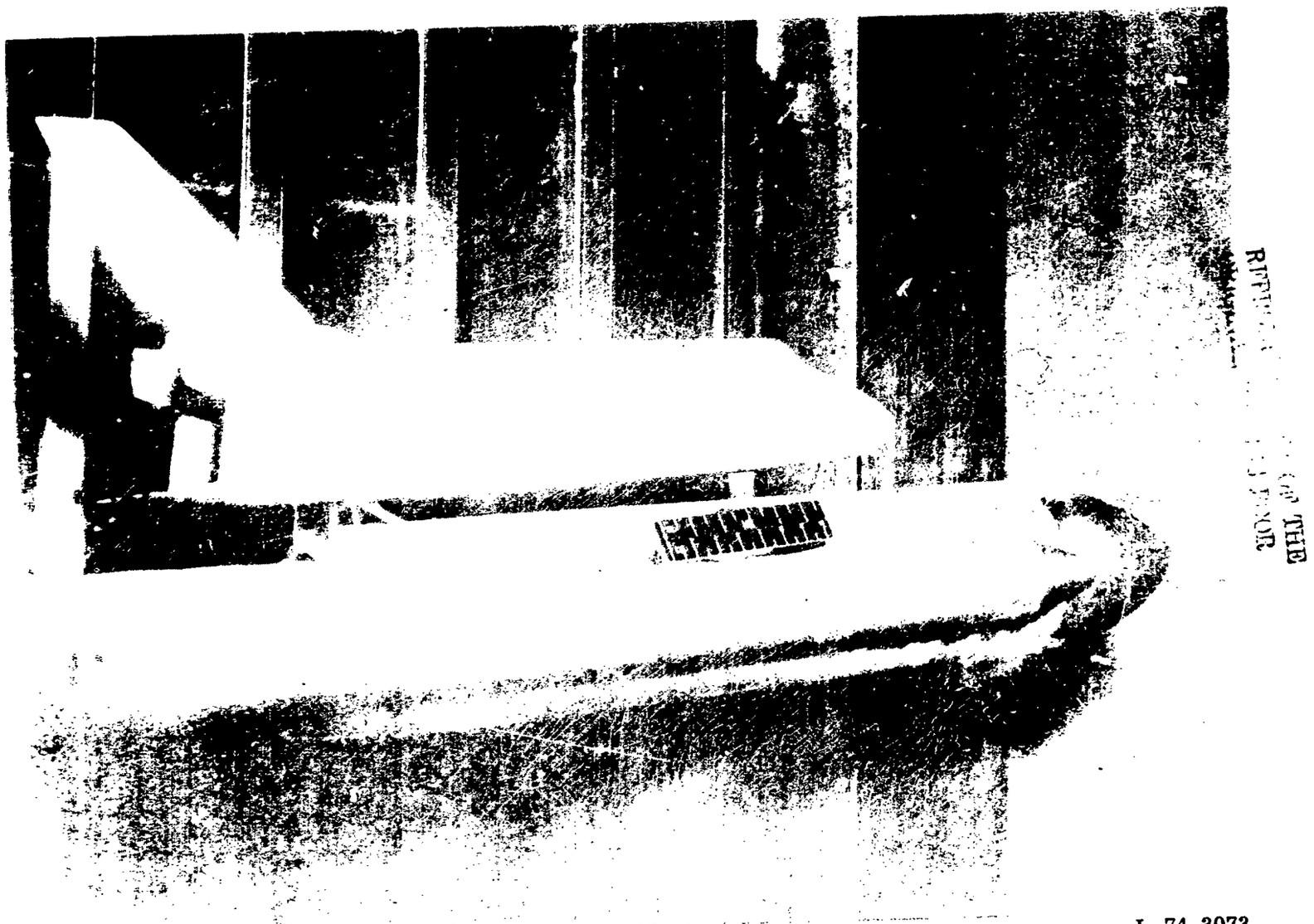

L-74-3073

Figure 4.- Photograph of model in the Unitary Plan wind tunnel.

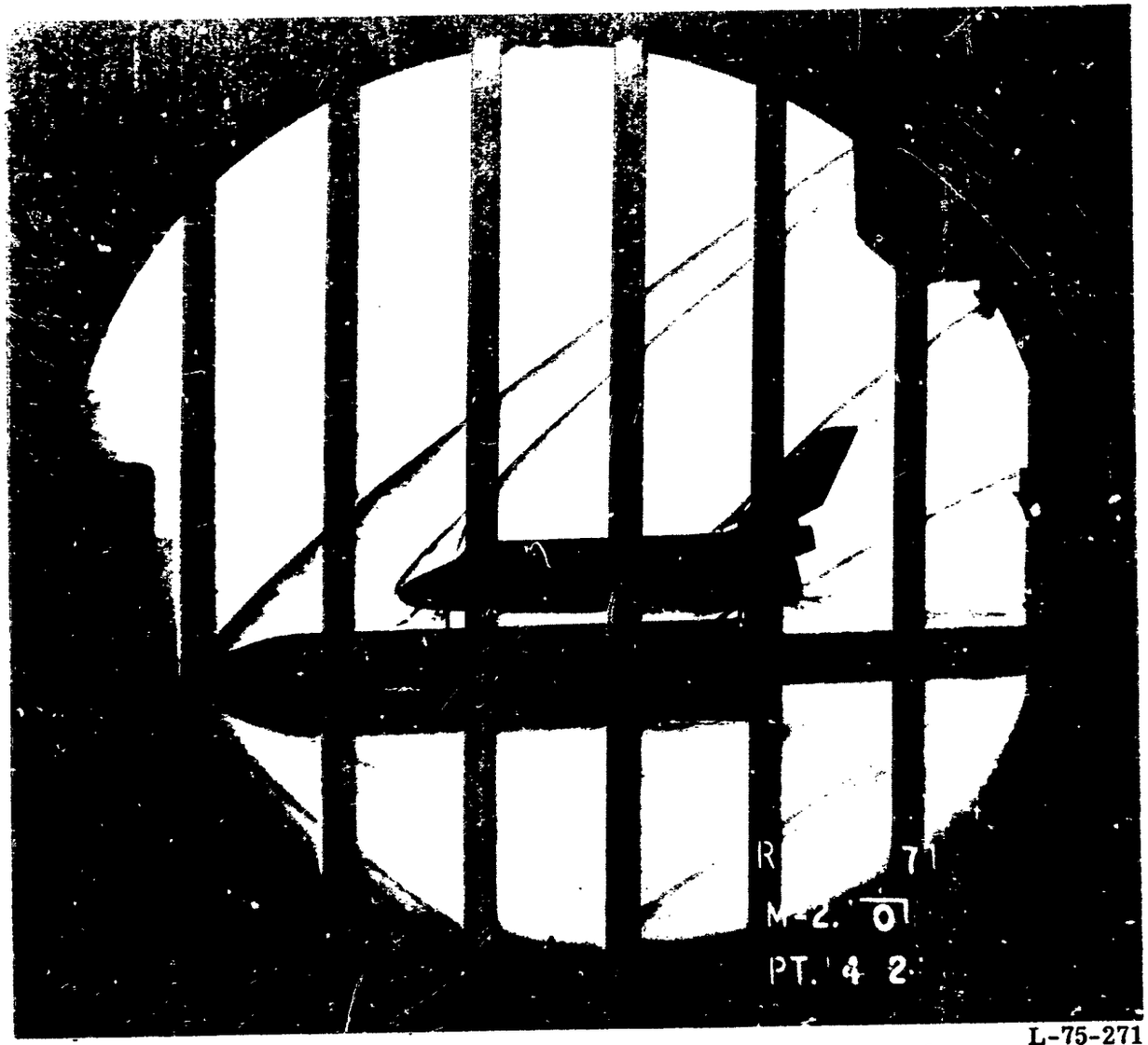

L-75-271

(a) Orbiter external-tank configuration, M = 2.00; $\alpha = -1.0^{o}$.

Figure 5.- Typical schlieren photographs of model.

L-75-272

(b) Orbiter external-tank configuration, $M = 3.96$; $\alpha = 1.3^{\circ}$.

Figure 5.- Continued.

L-75-273

(c) Complete launch configuration, M = 4.63; $\alpha = 2.1^{\circ}$.

Figure 5.- Concluded.

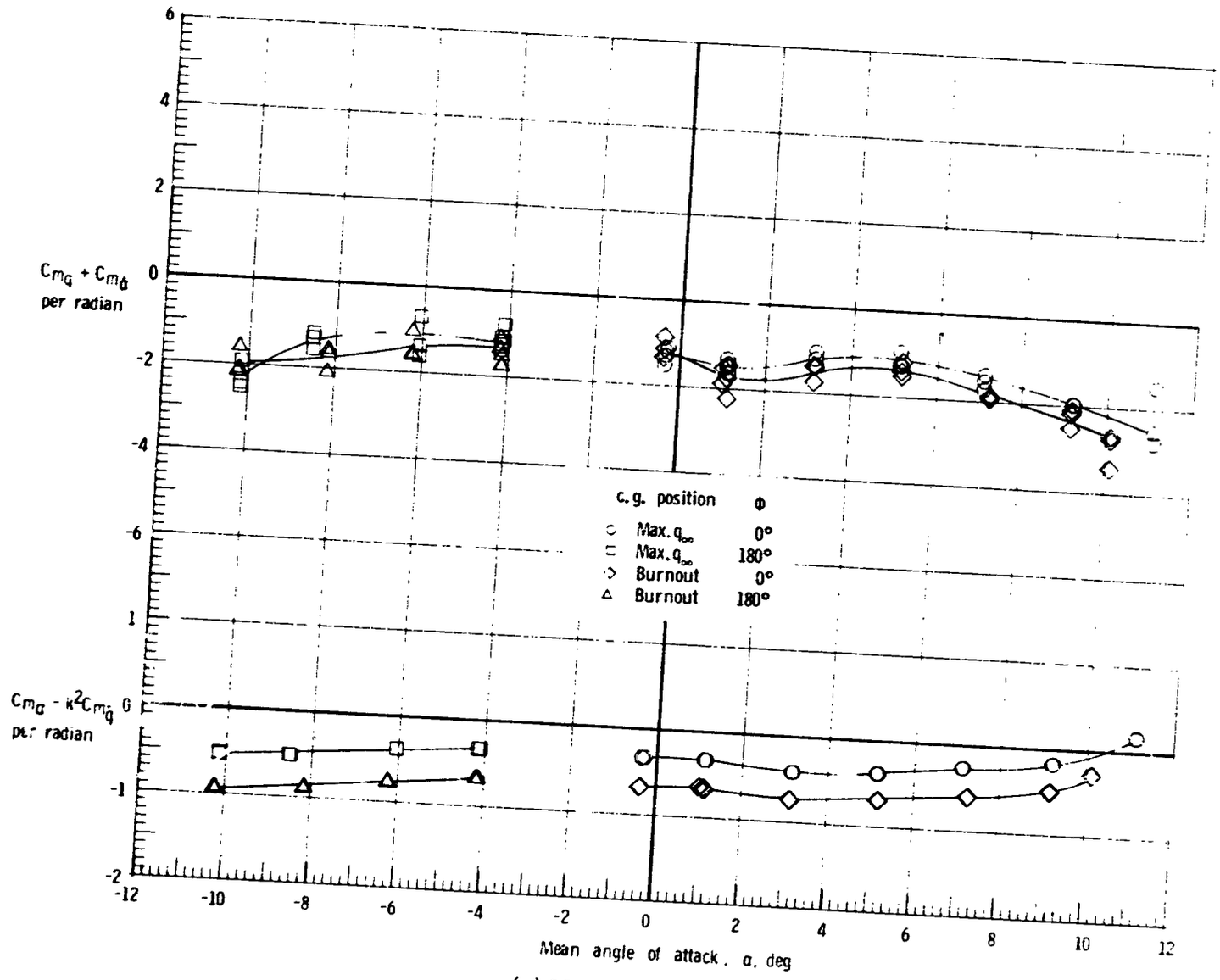

(a) M = 2.00.

Figure 6.- Effect of center-of-gravity position of the launch configuration on the damping-in-pitch parameter and on the oscillatory stability in pitch parameter.

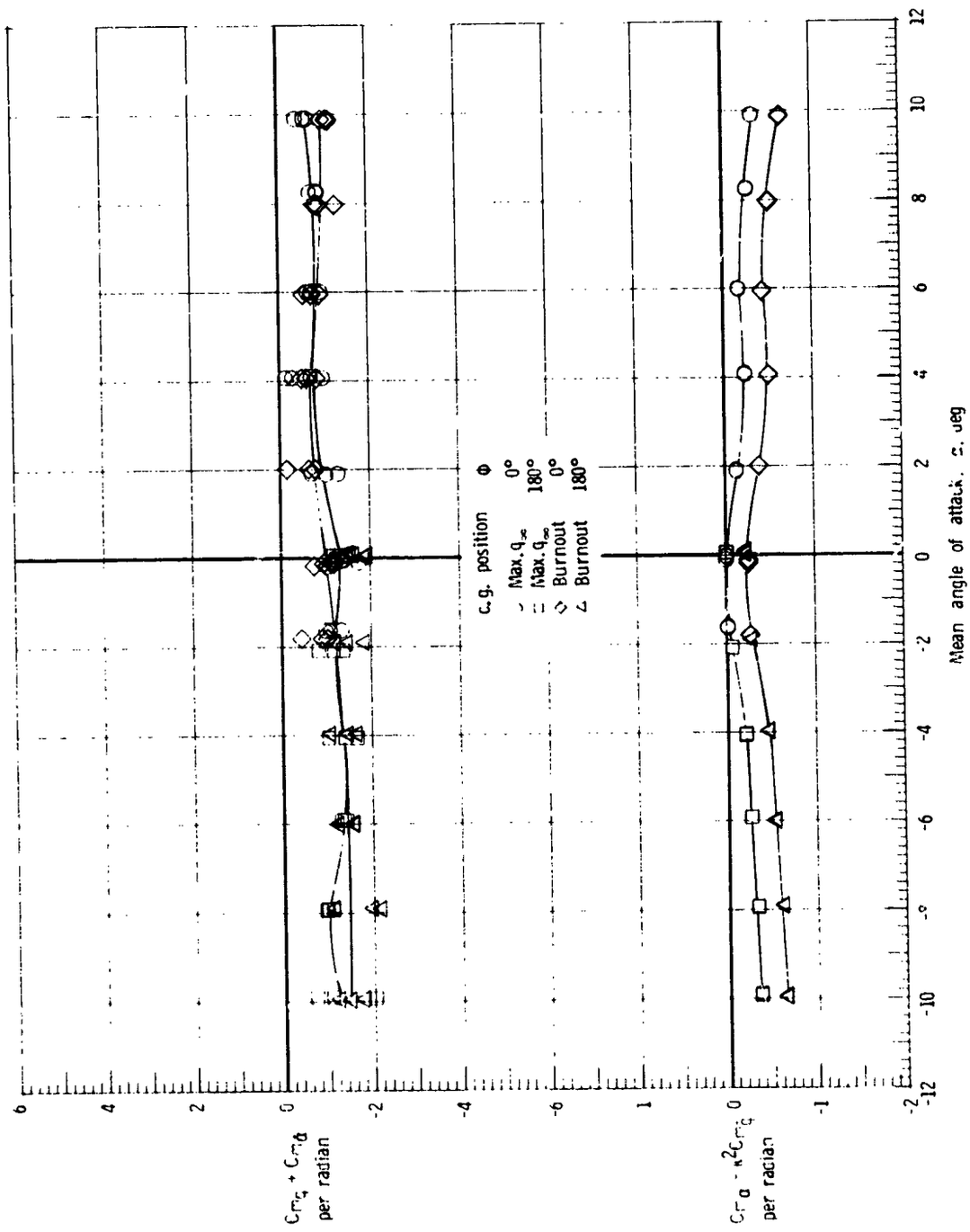

(b) M = 2.86.

Figure 6.- Continued.

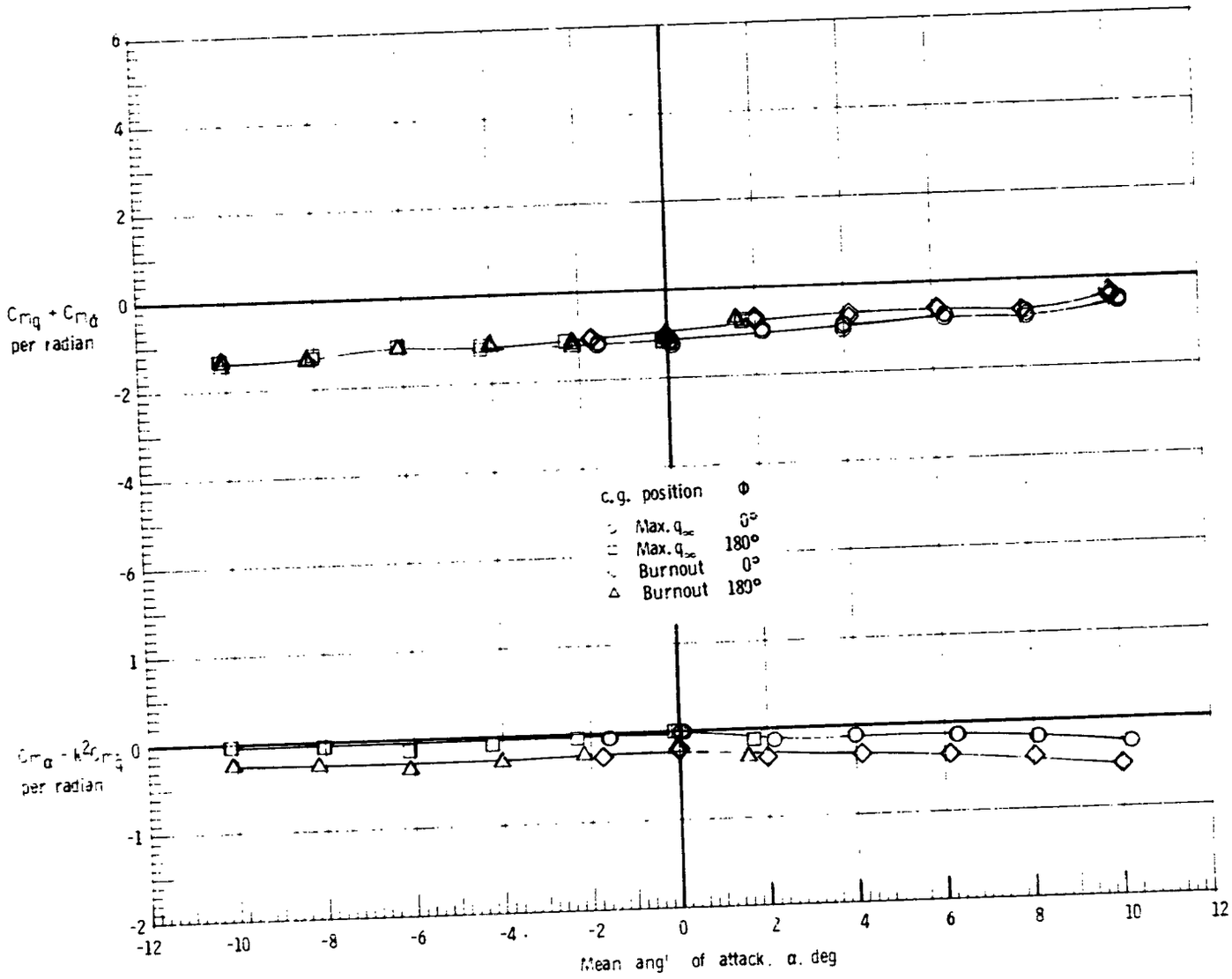

(c) M = 3.96.

Figure 6.- Continued.

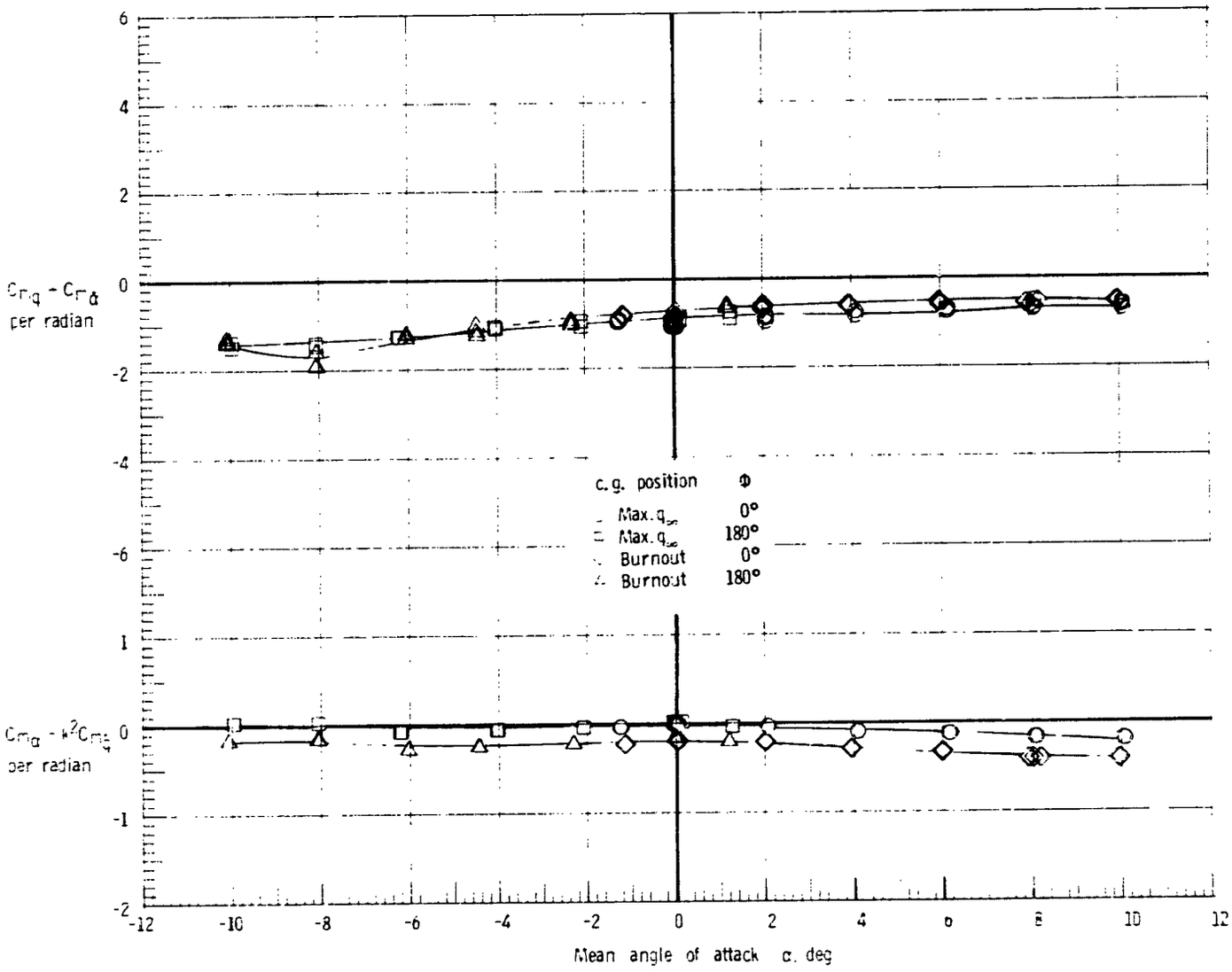

(d) M = 4.63.

Figure 6.- Concluded.

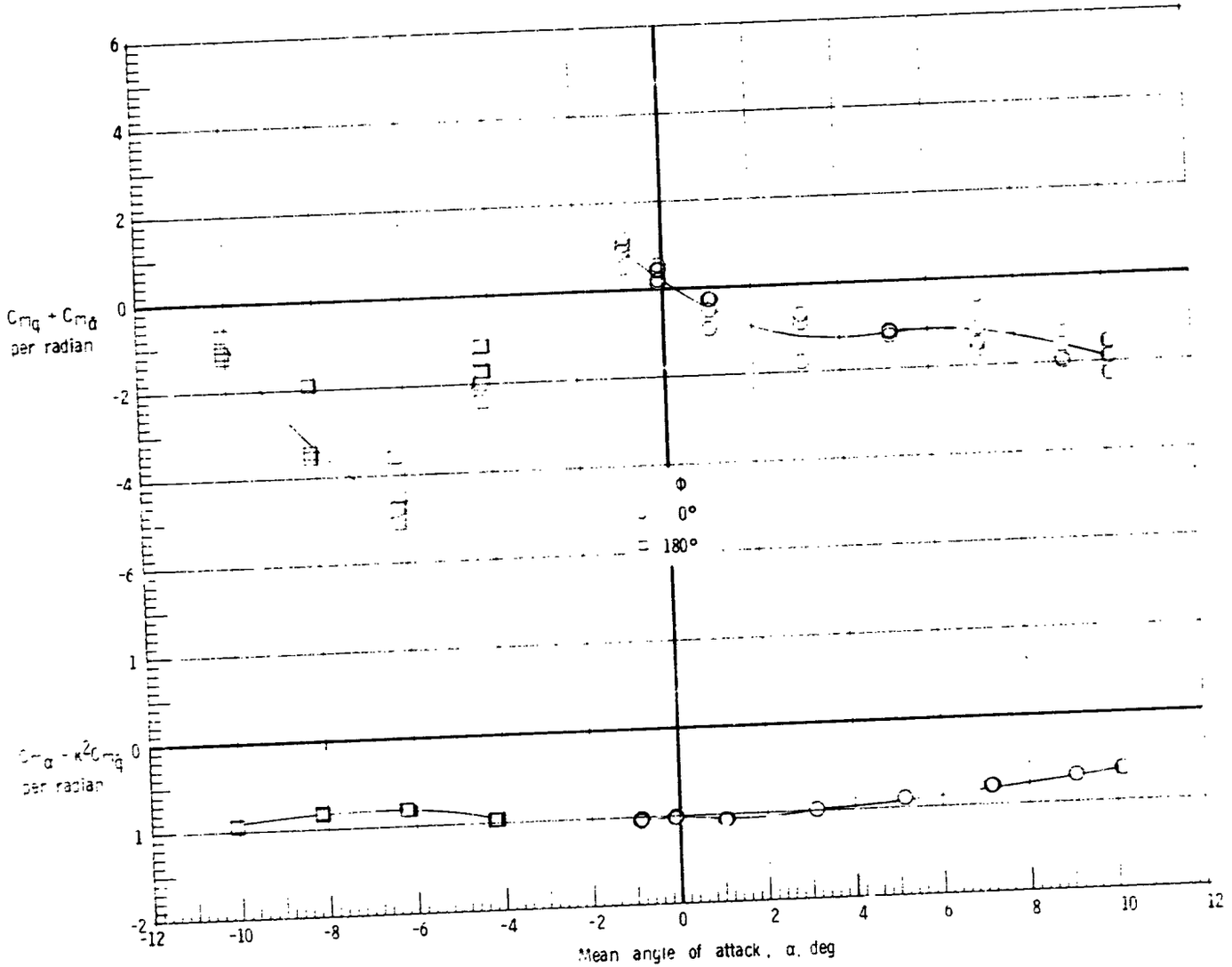

(a) M = 2.00.

Figure 7.- Damping-in-pitch parameter and oscillatory stability-in-pitch parameter for the orbiter external-tank configuration.

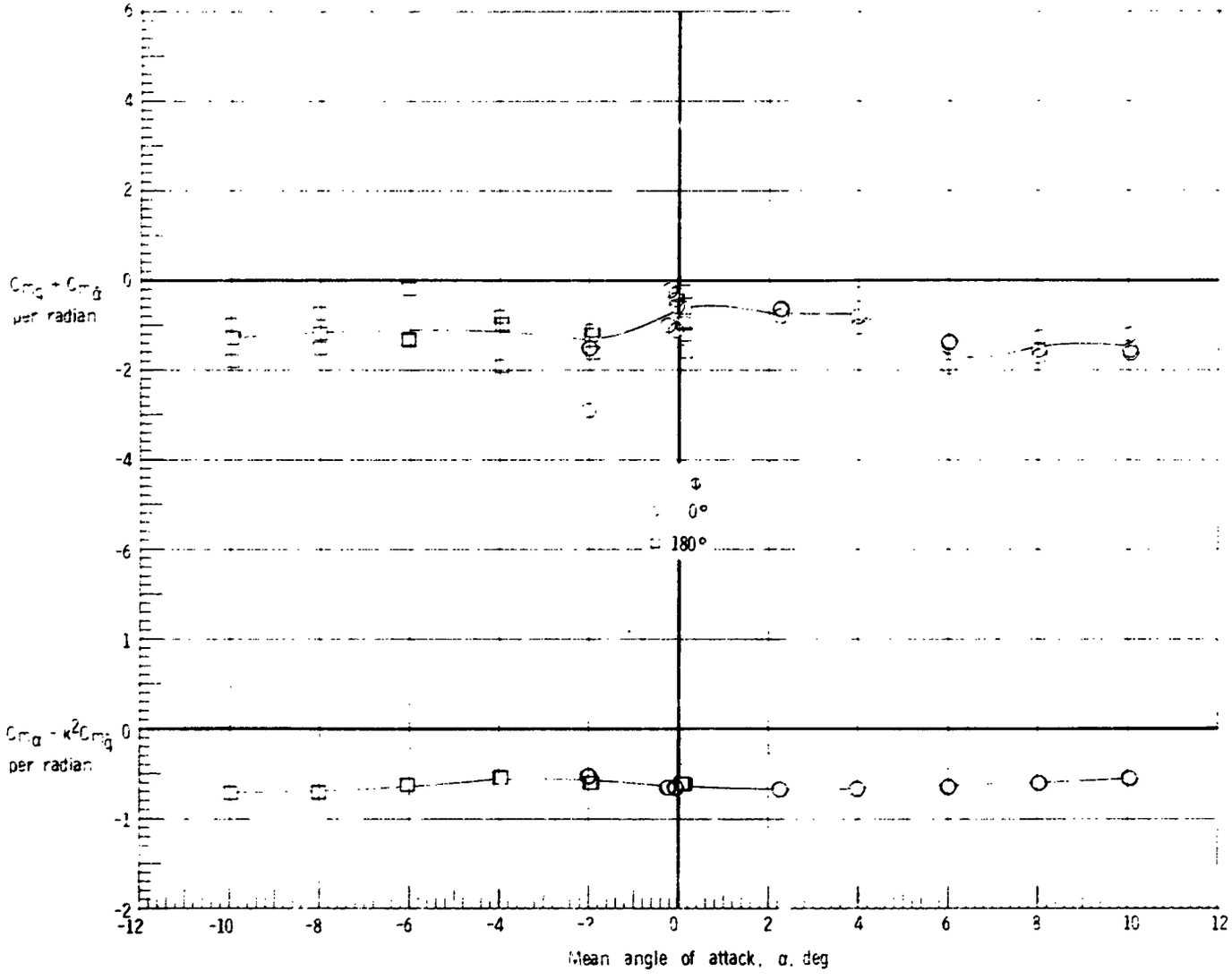

(b) M = 2.86.

Figure 7.- Continued.

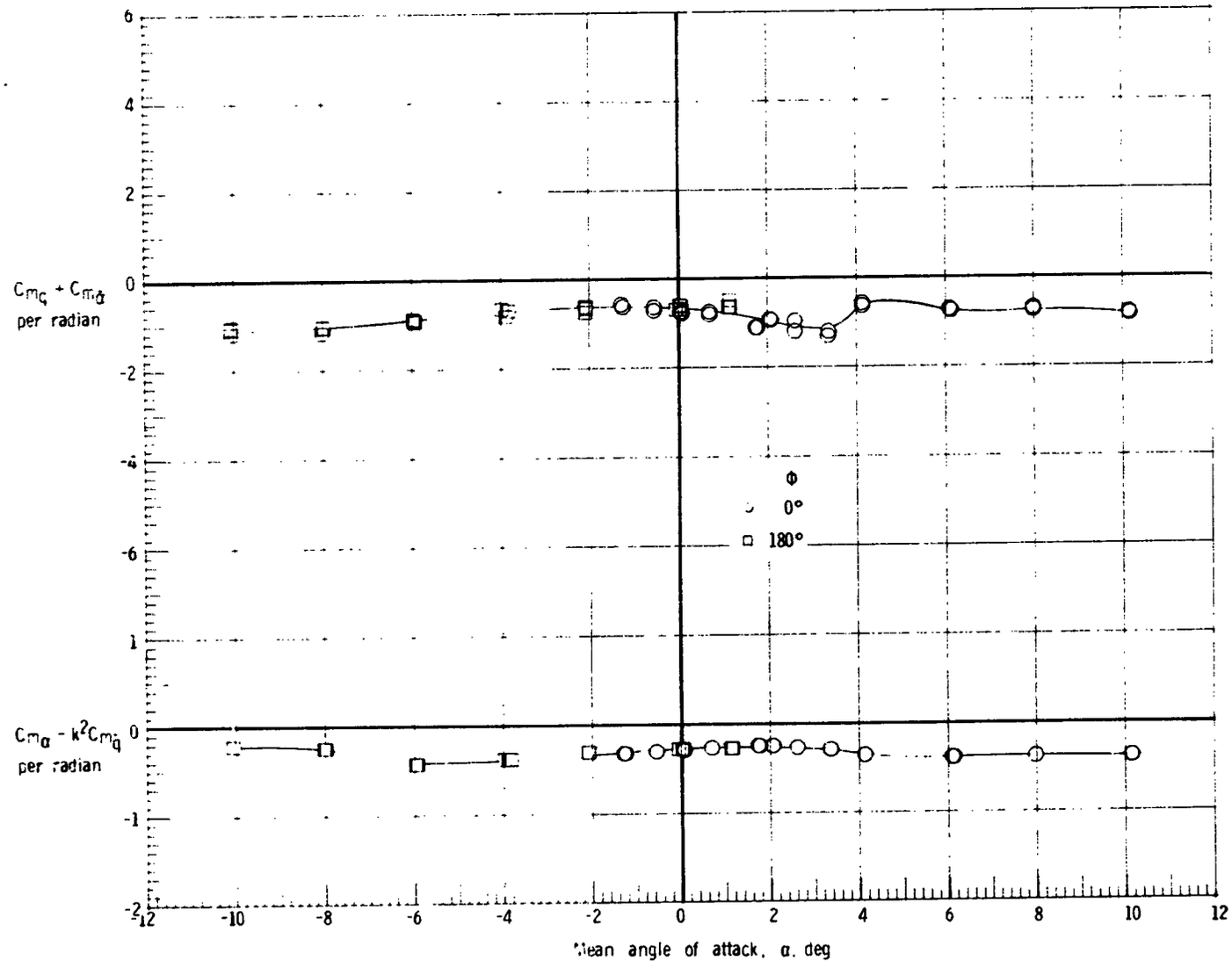

(c) M = 4.63.

Figure 7.- Concluded.

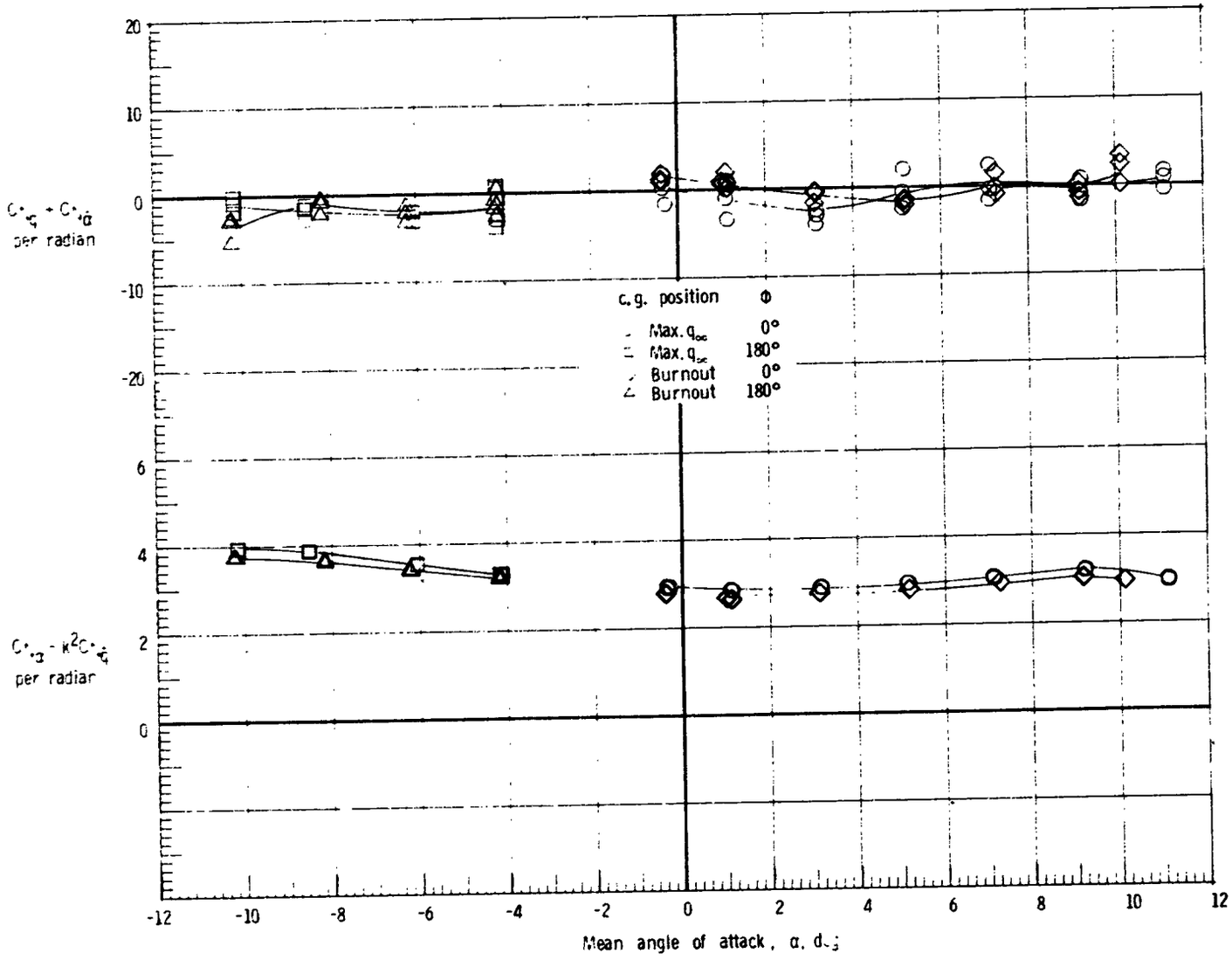

(a) M = 2.00.

Figure 8. Effect of center-of-gravity position of the launch configuration on the normal force due to pitch-rate parameter and on the normal force due to pitch-displacement parameter.

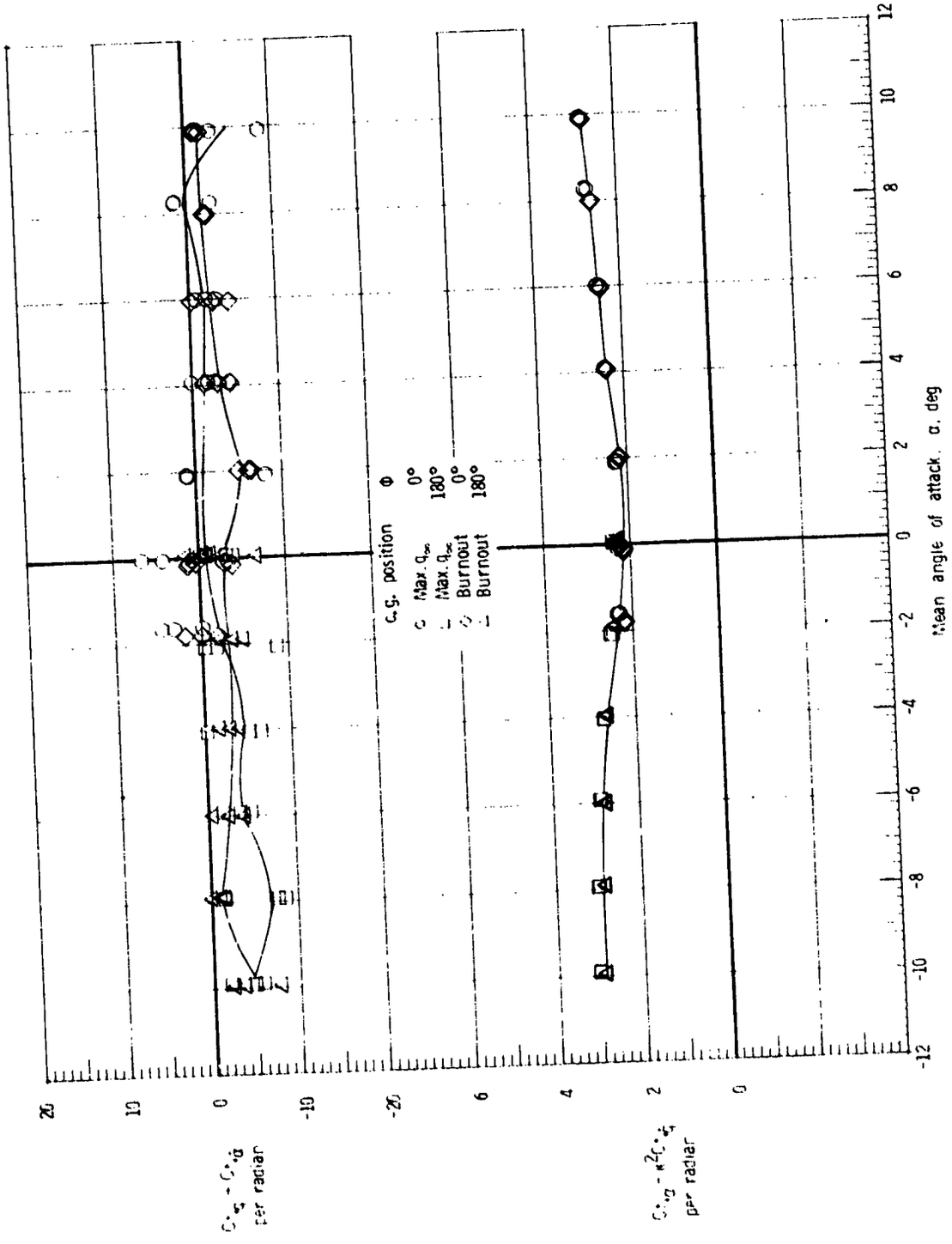

(b) M = 2.86.

Figure 8.- Continued.

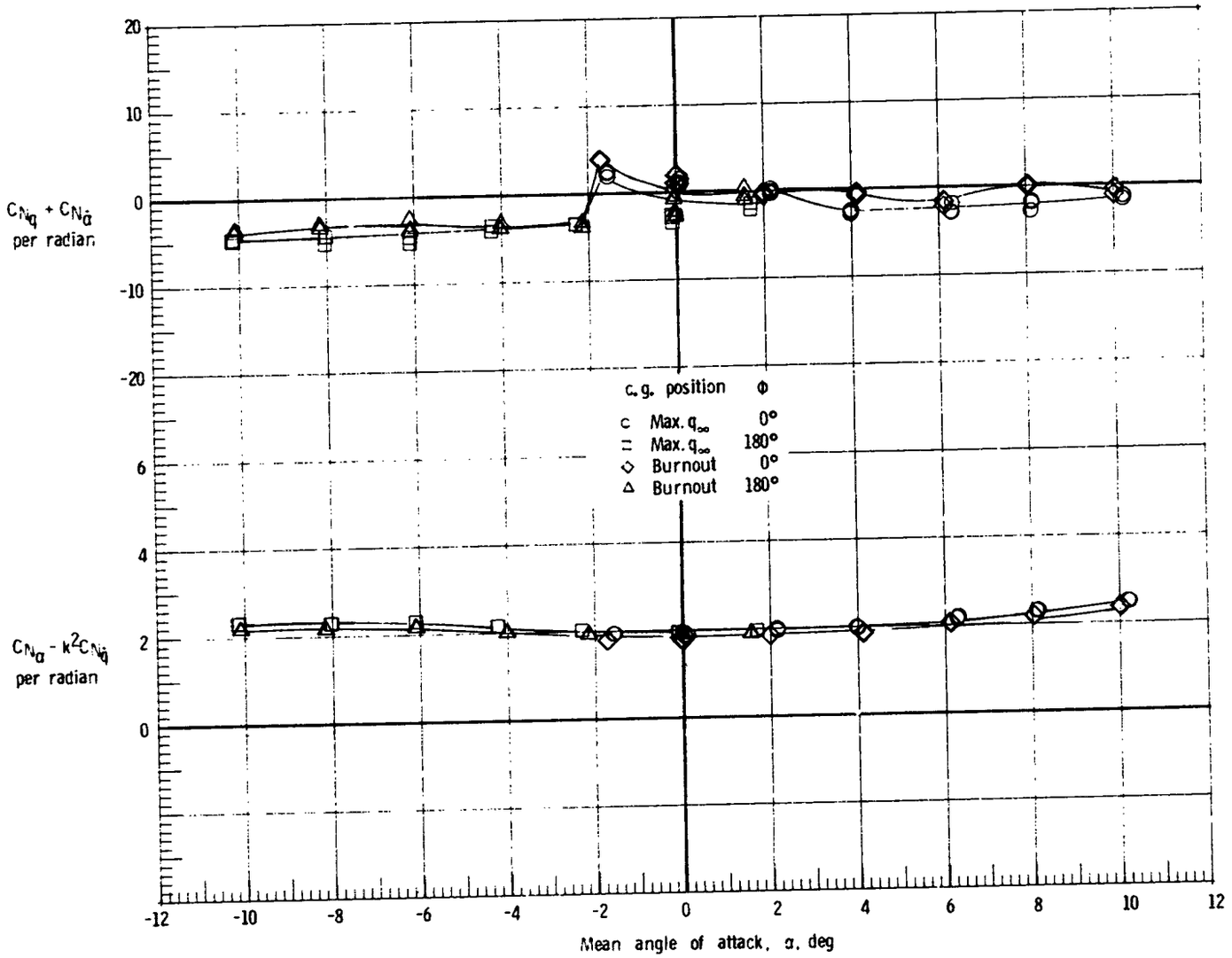

(c) M = 3.96.

Figure 8.- Continued.

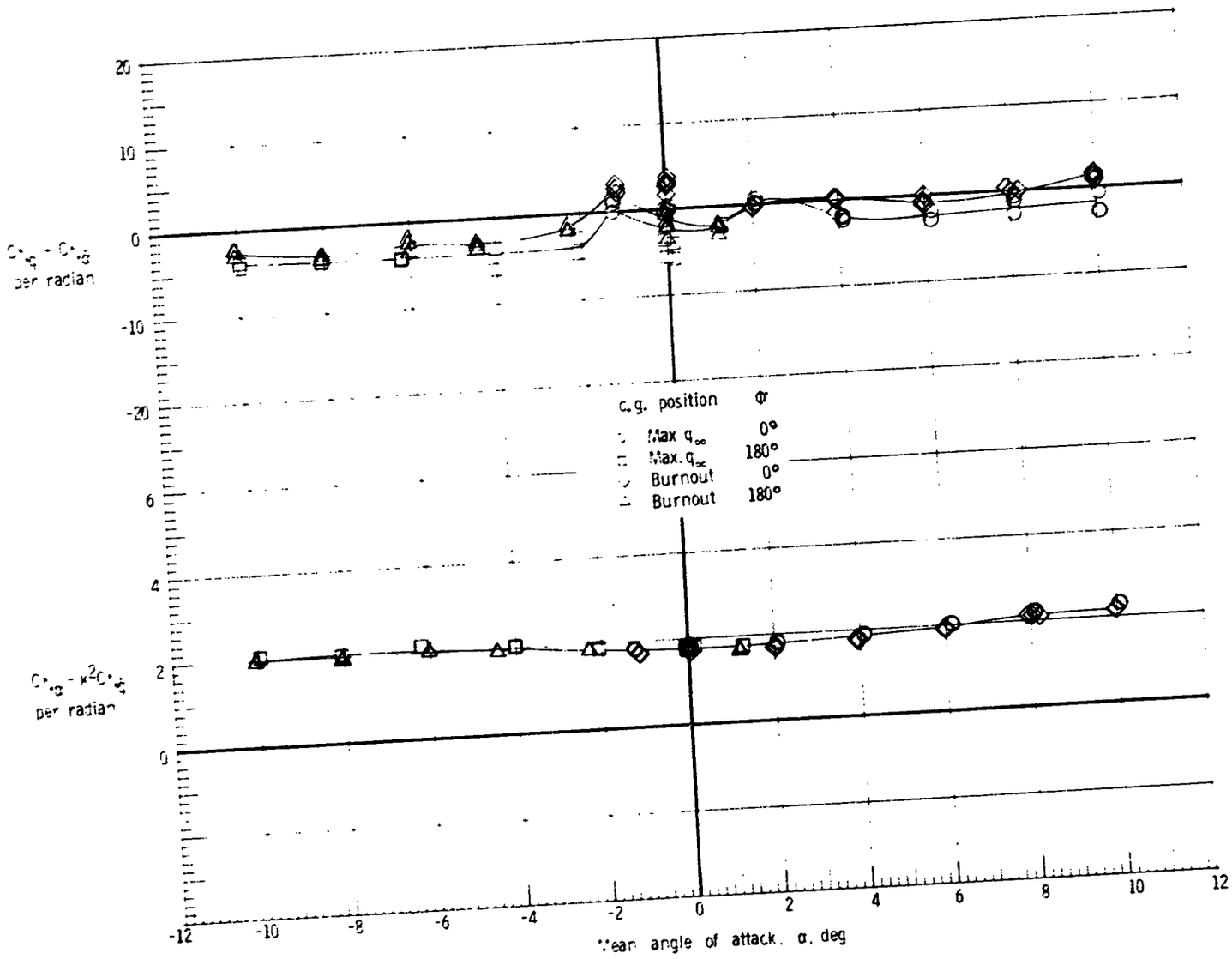

(d) M = 4.63.

Figure 8.- Concluded.

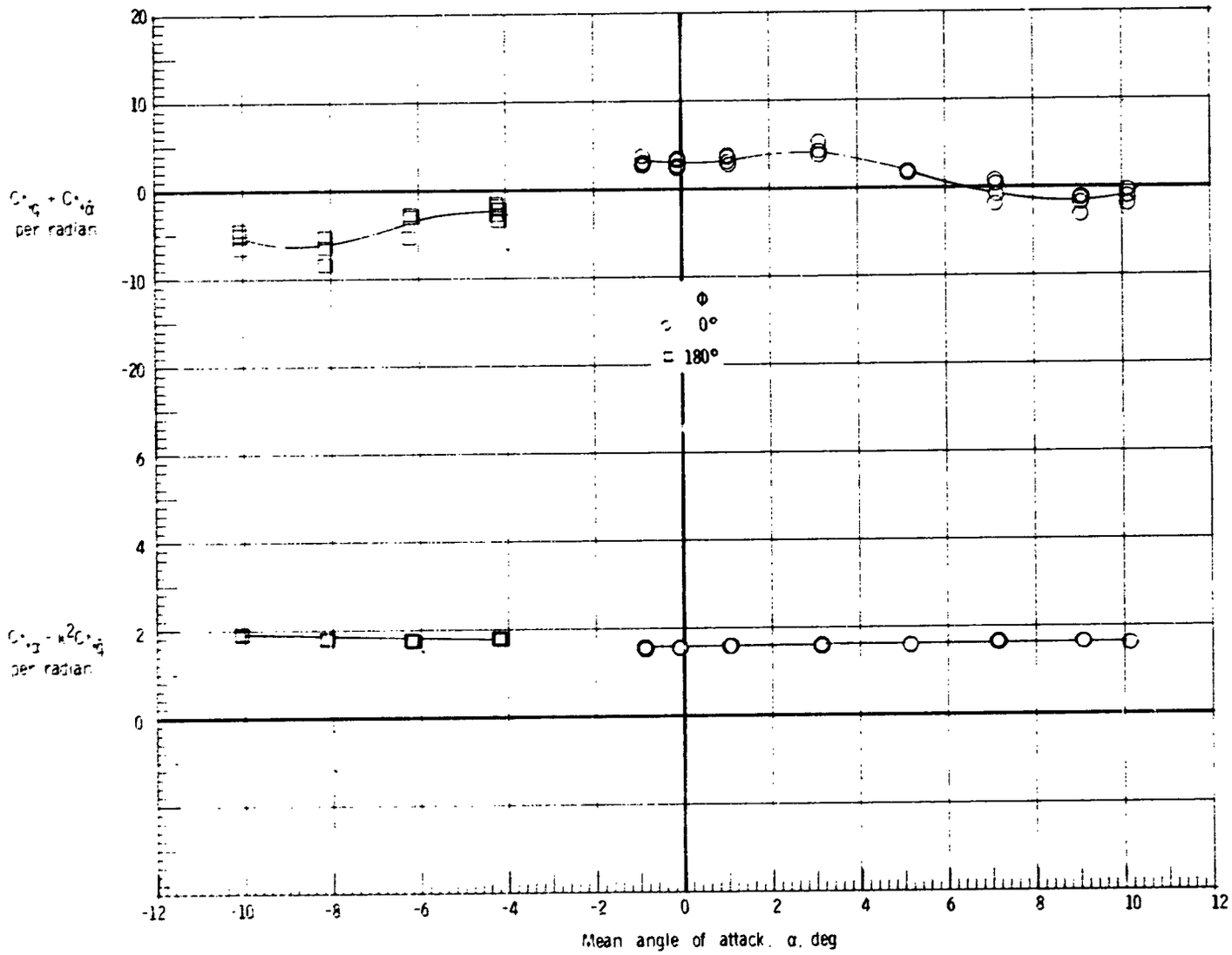

(a) M = 2.00.

Figure 9.- Normal force due to pitch-rate parameter and normal force due to pitch-displacement parameter for the orbiter external-tank configuration.

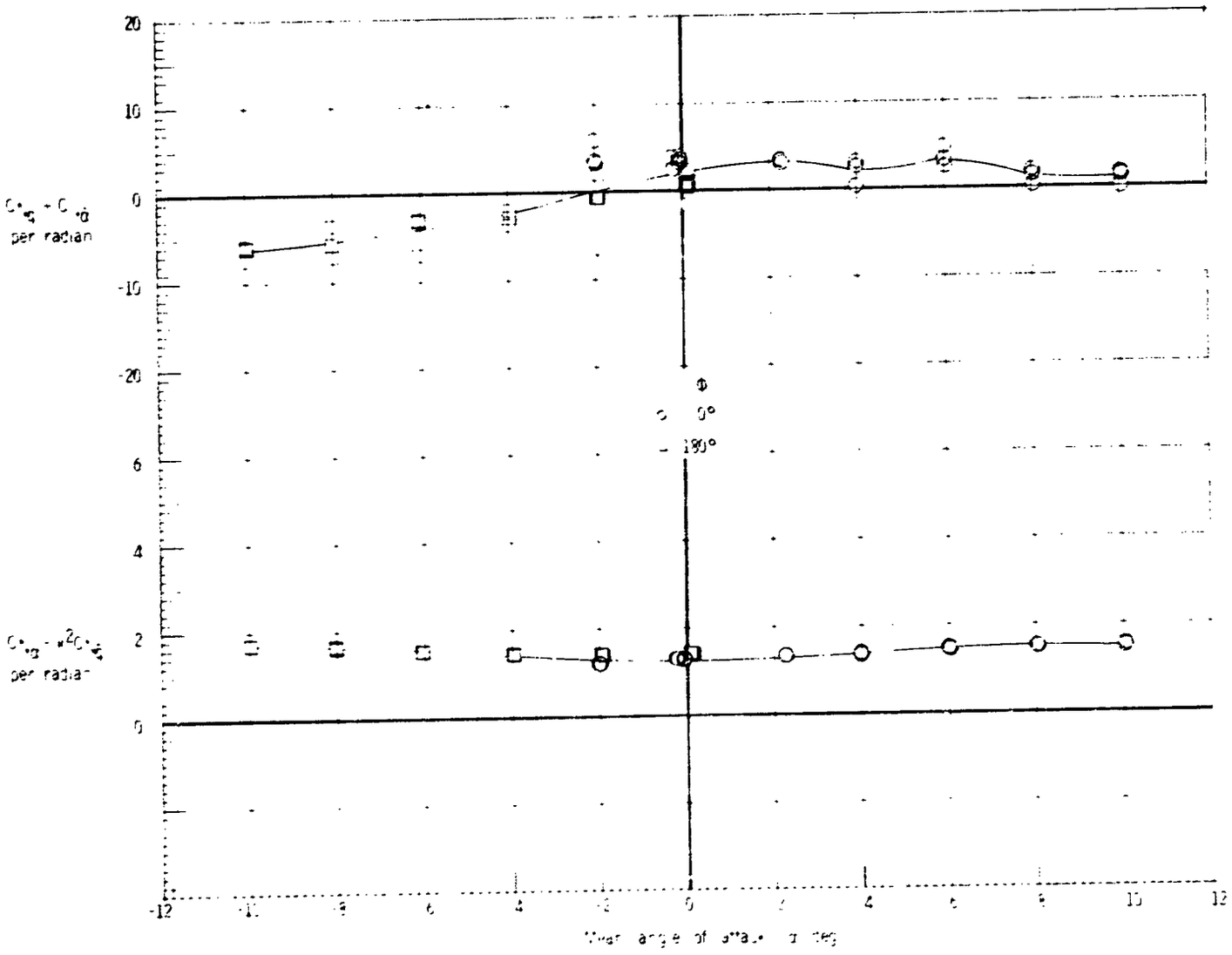

(b) M = 2.86.

Figure 9.- Continued.

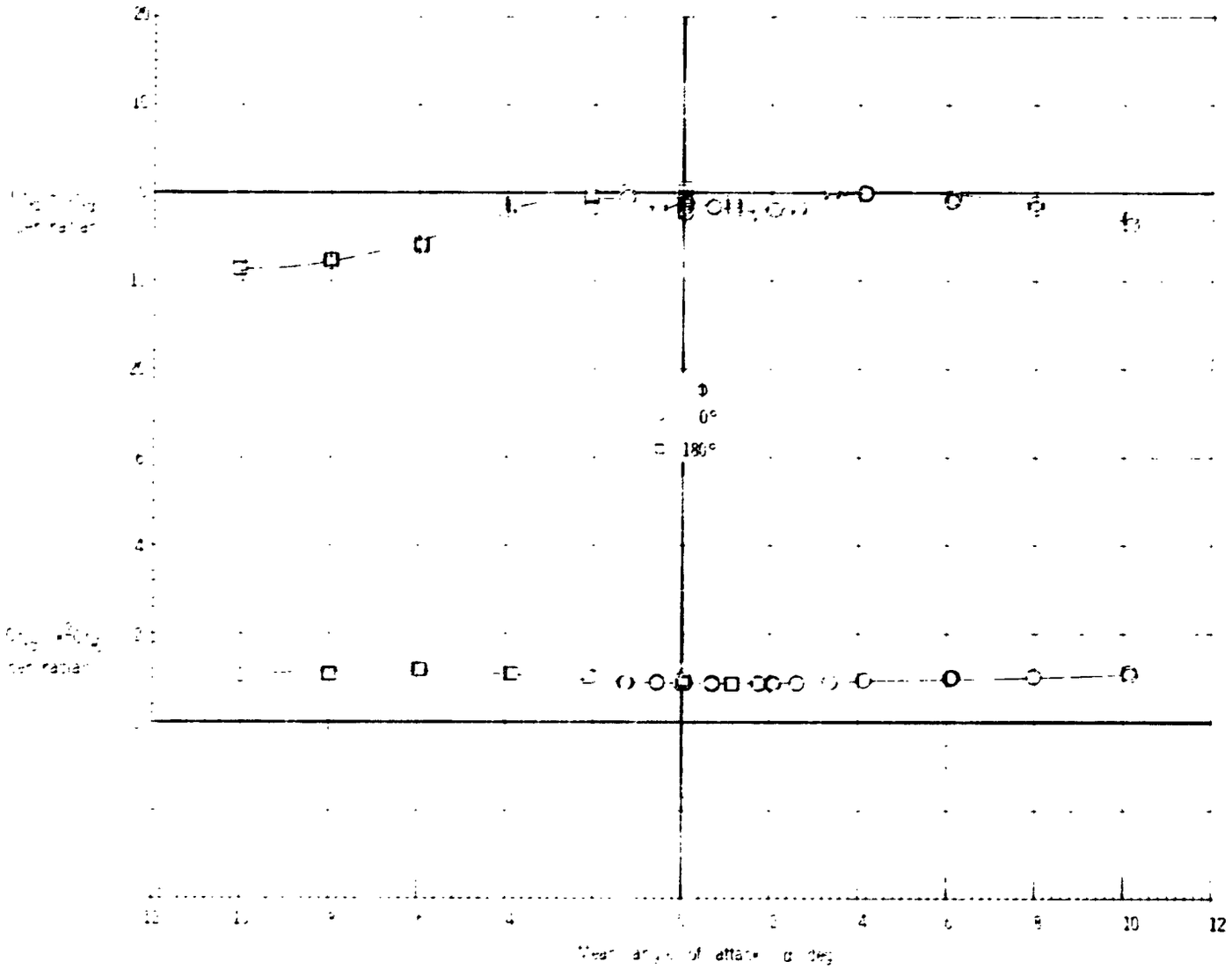

(c) M = 4.63.

Figure 9.- Concluded.

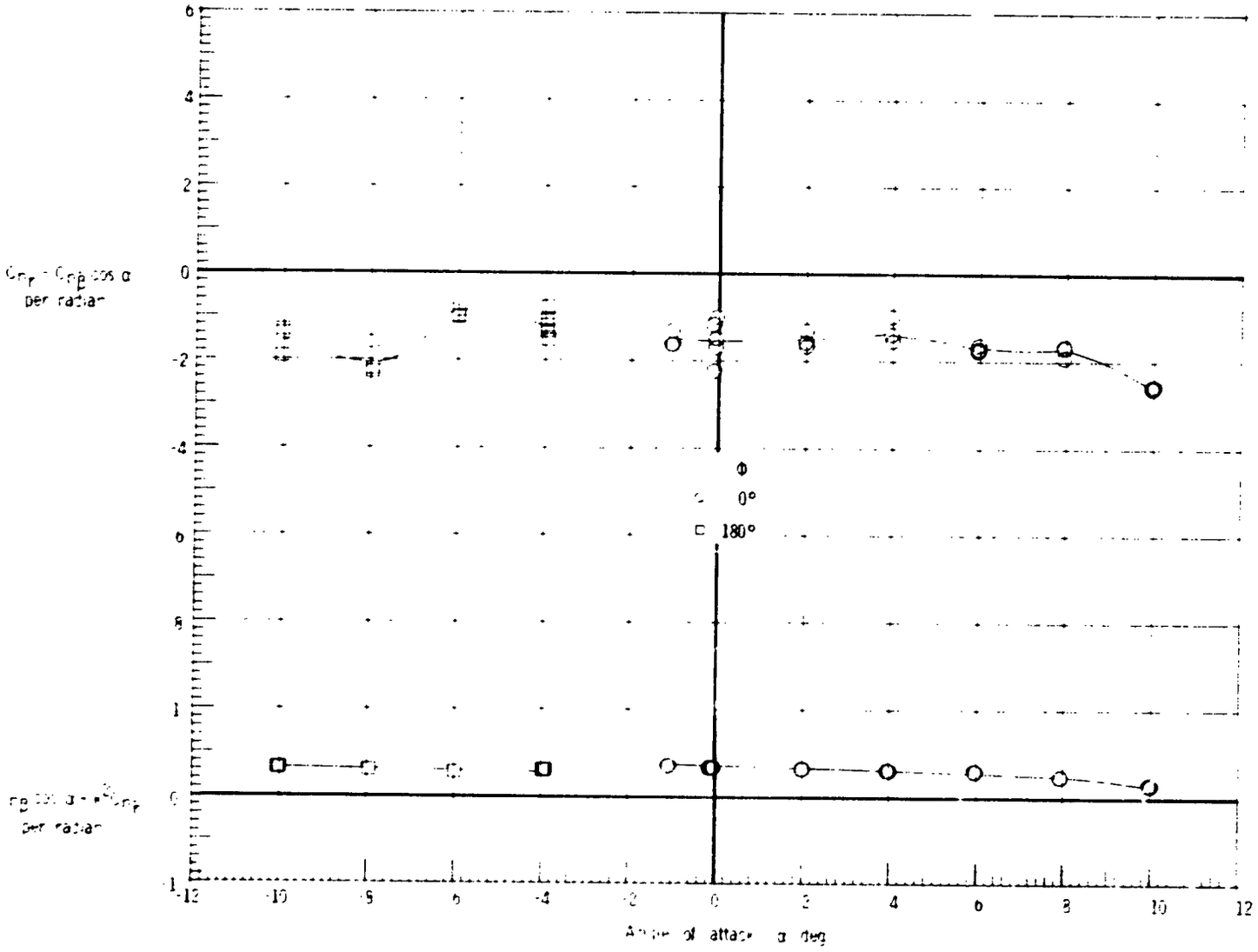

(a) M 2.00.

Figure 10.- Damping-in-yaw parameter and oscillatory directional-stability parameter for the launch configuration; maximum dynamic pressure center-of-gravity position.

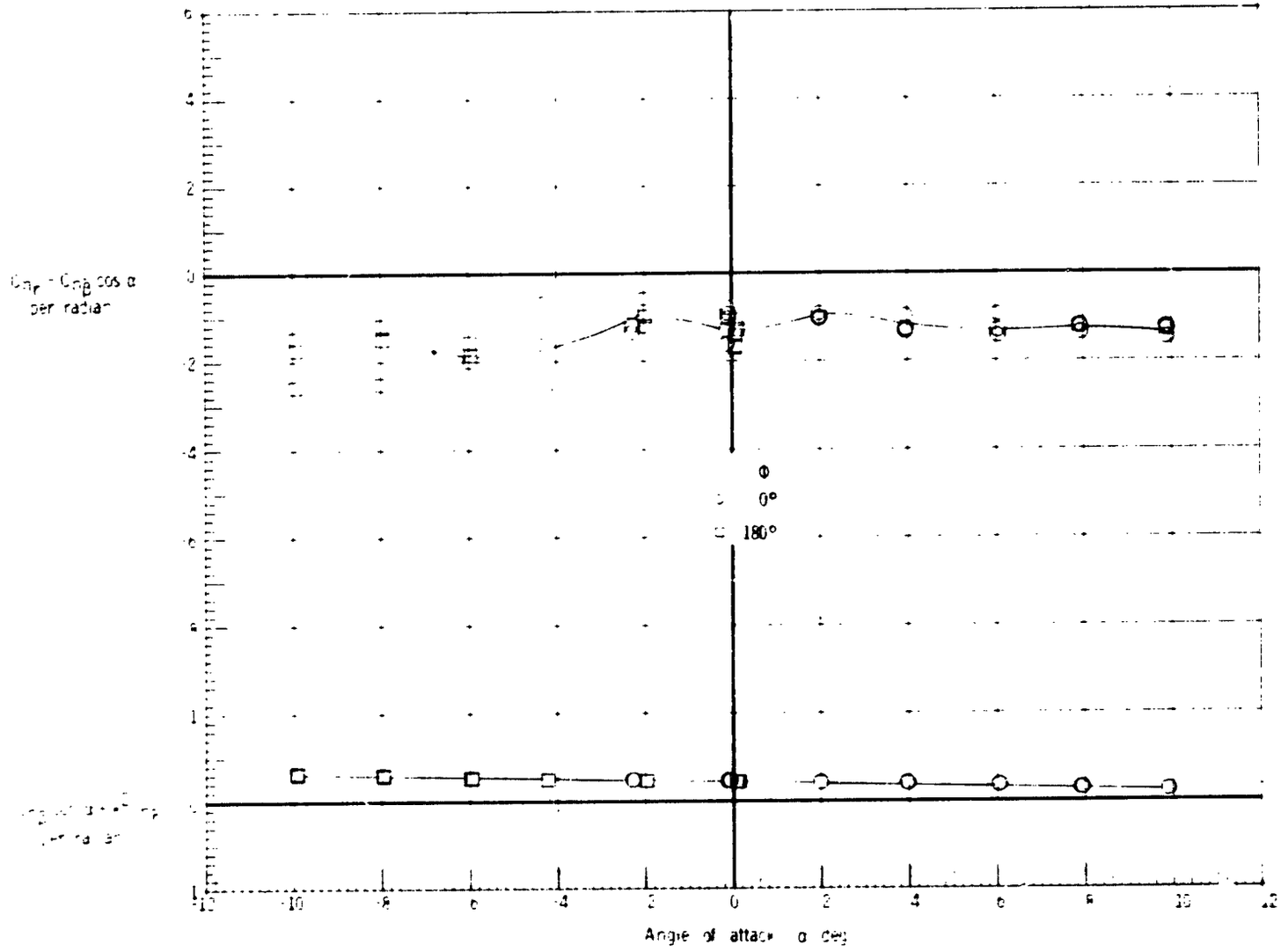

(b) M = 2.86.

Figure 10.- Continued.

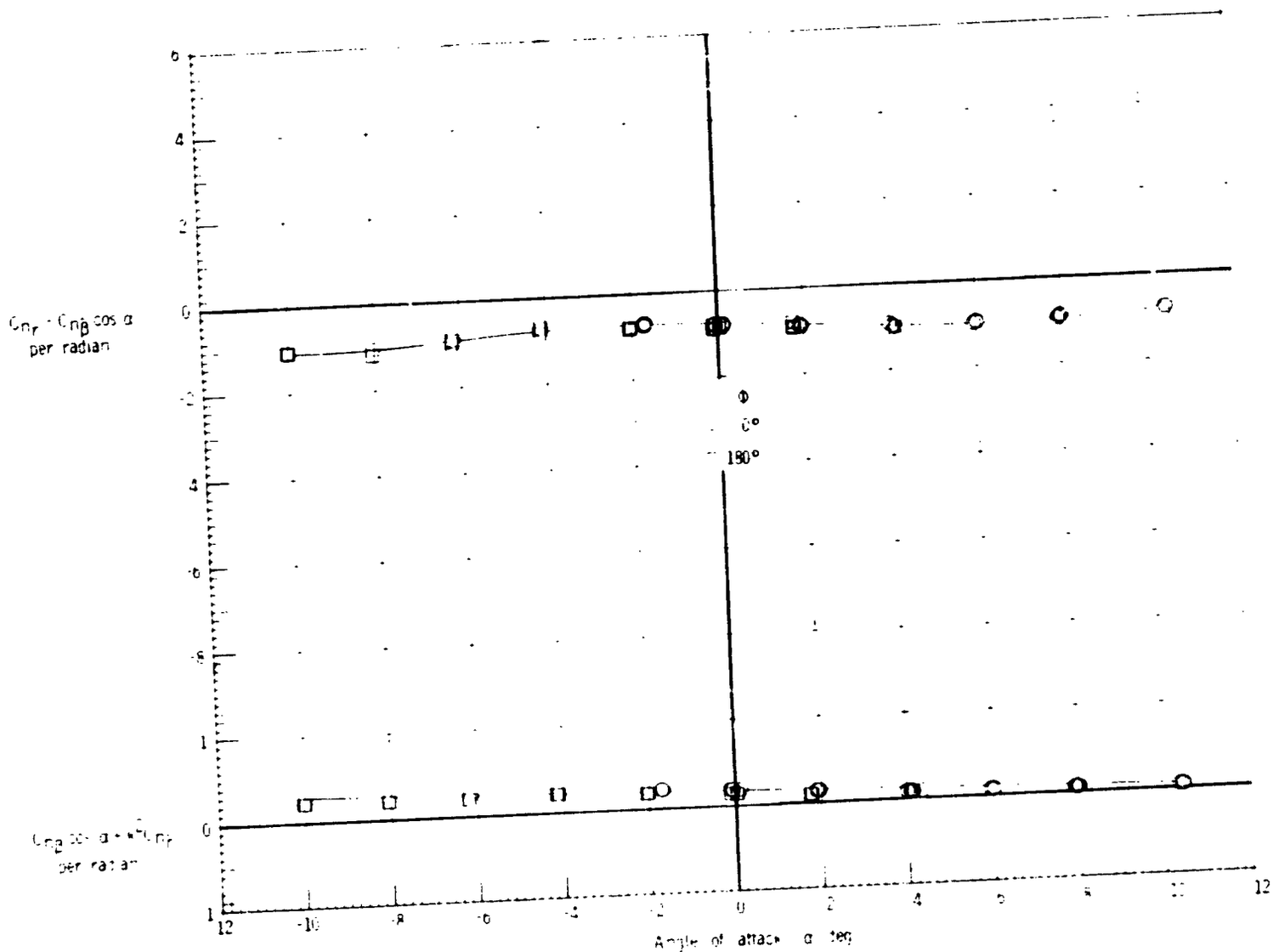

(c) M = 3.96.

Figure 10.- Continued.

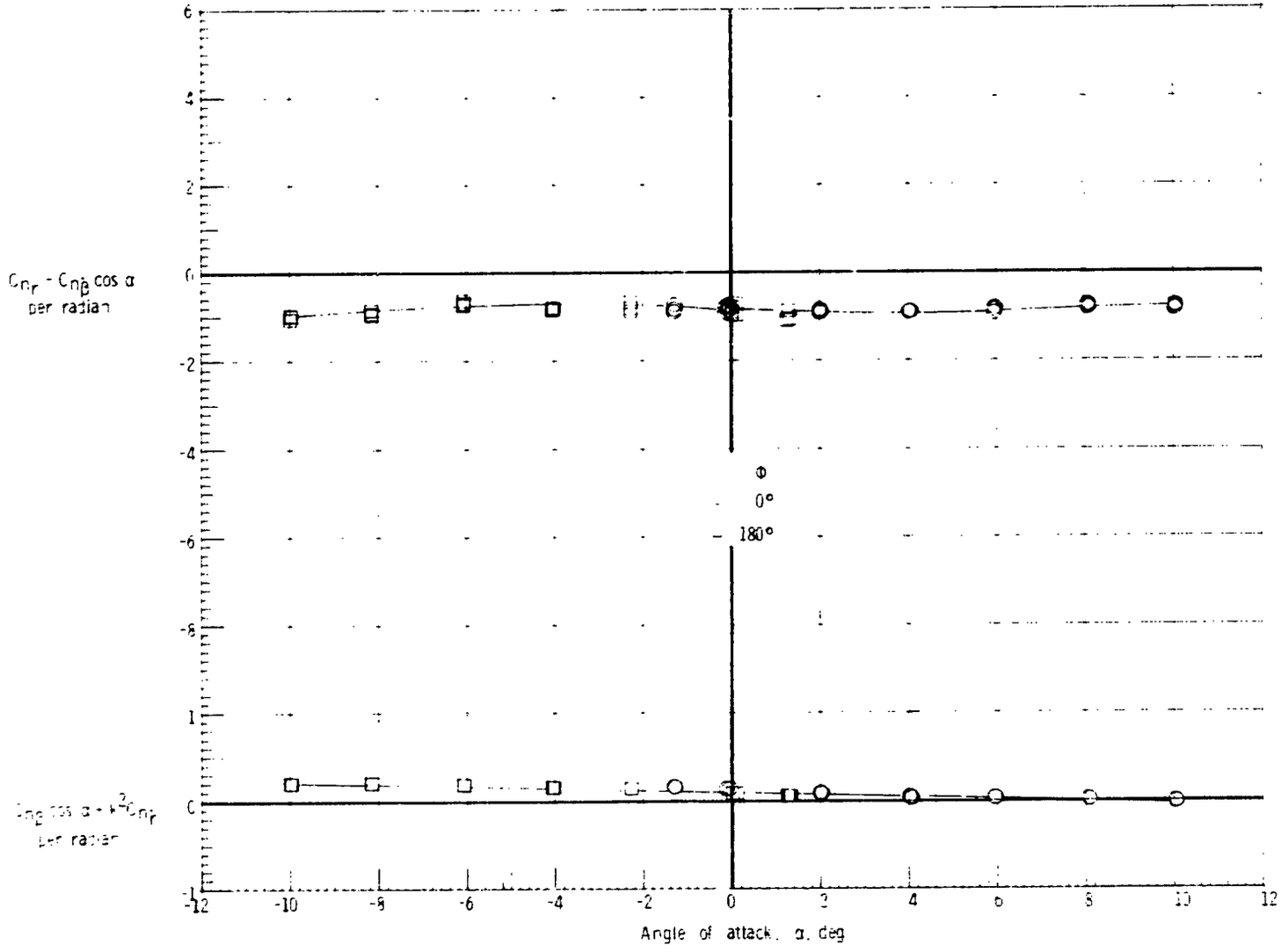

(d) M = 4.63.

Figure 10.- Concluded.

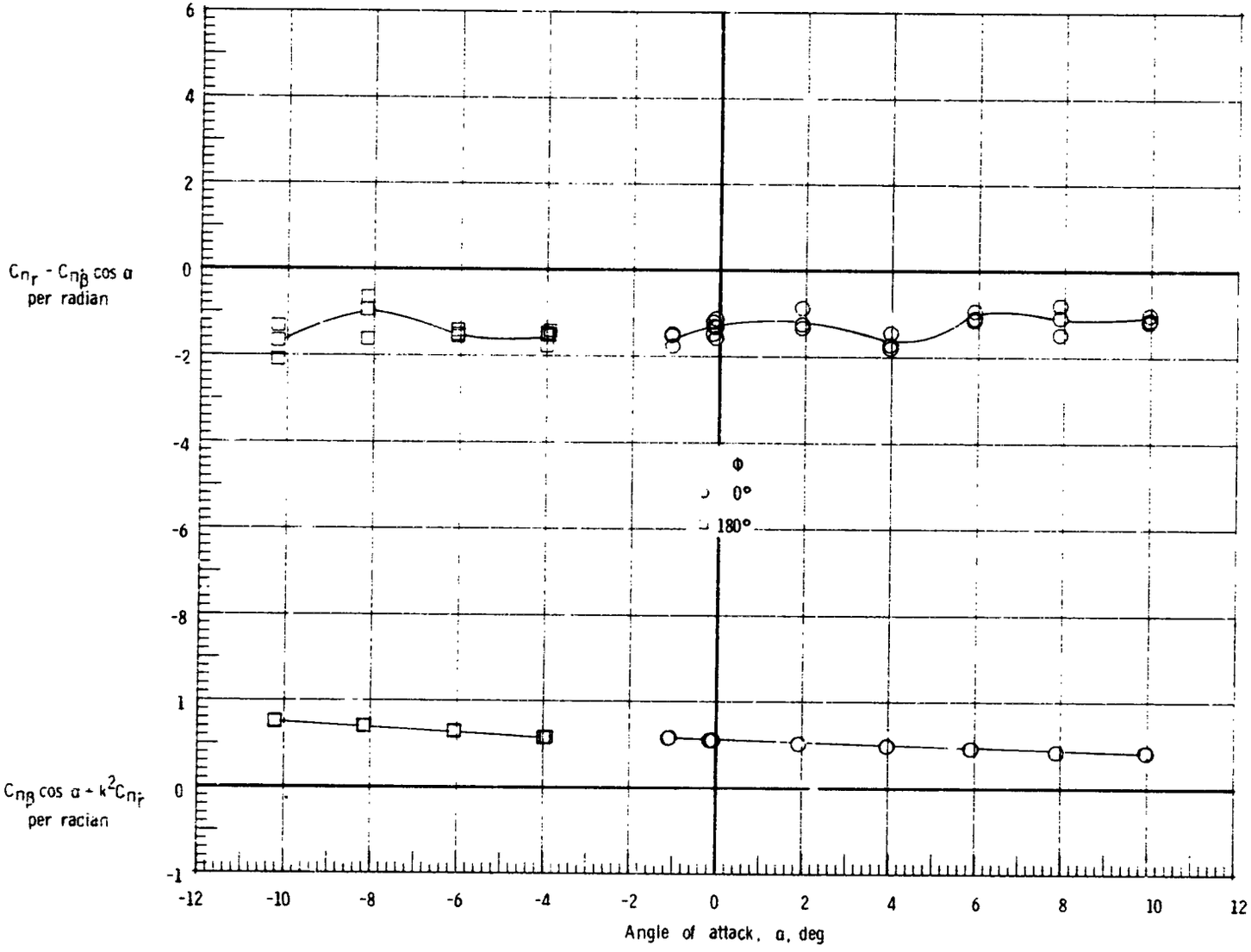

(a) M = 2.00.

Figure 11.- Damping-in-yaw parameter and oscillatory directional-stability parameter for the orbiter external-tank configuration.

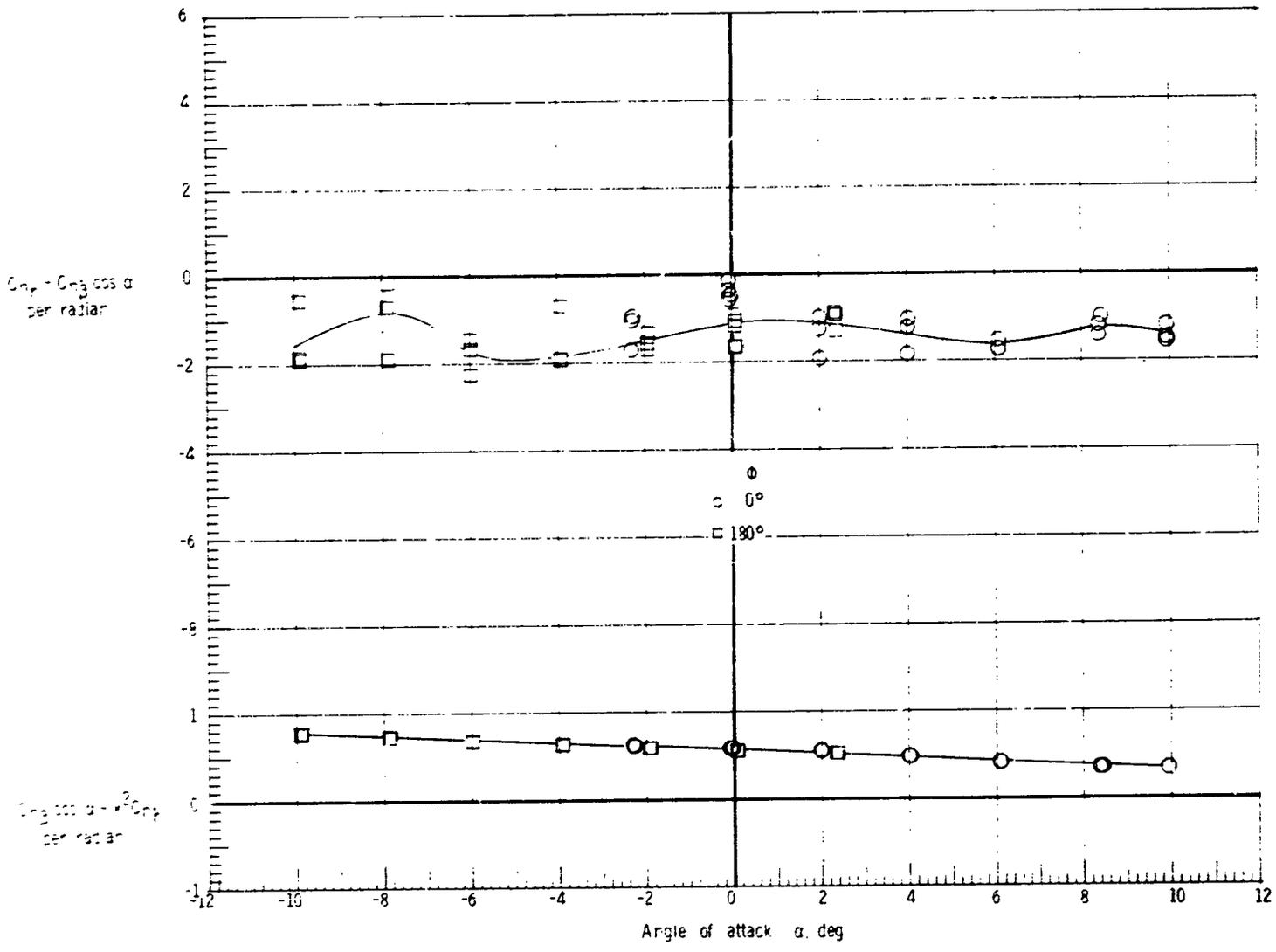

(b) M = 2.86.

Figure 11.- Continued.

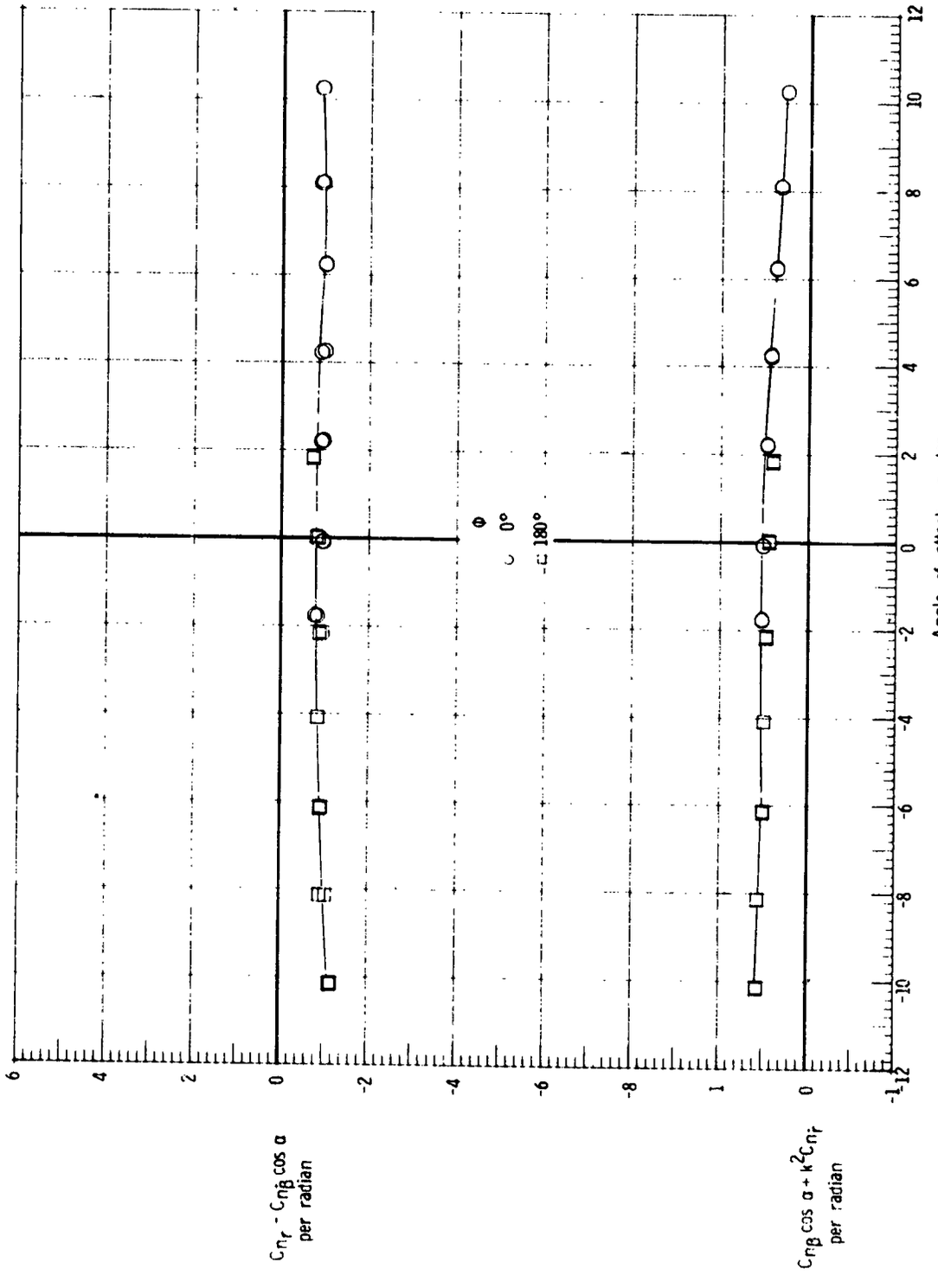

(c) M = 3.96.

Figure 11.- Continued.

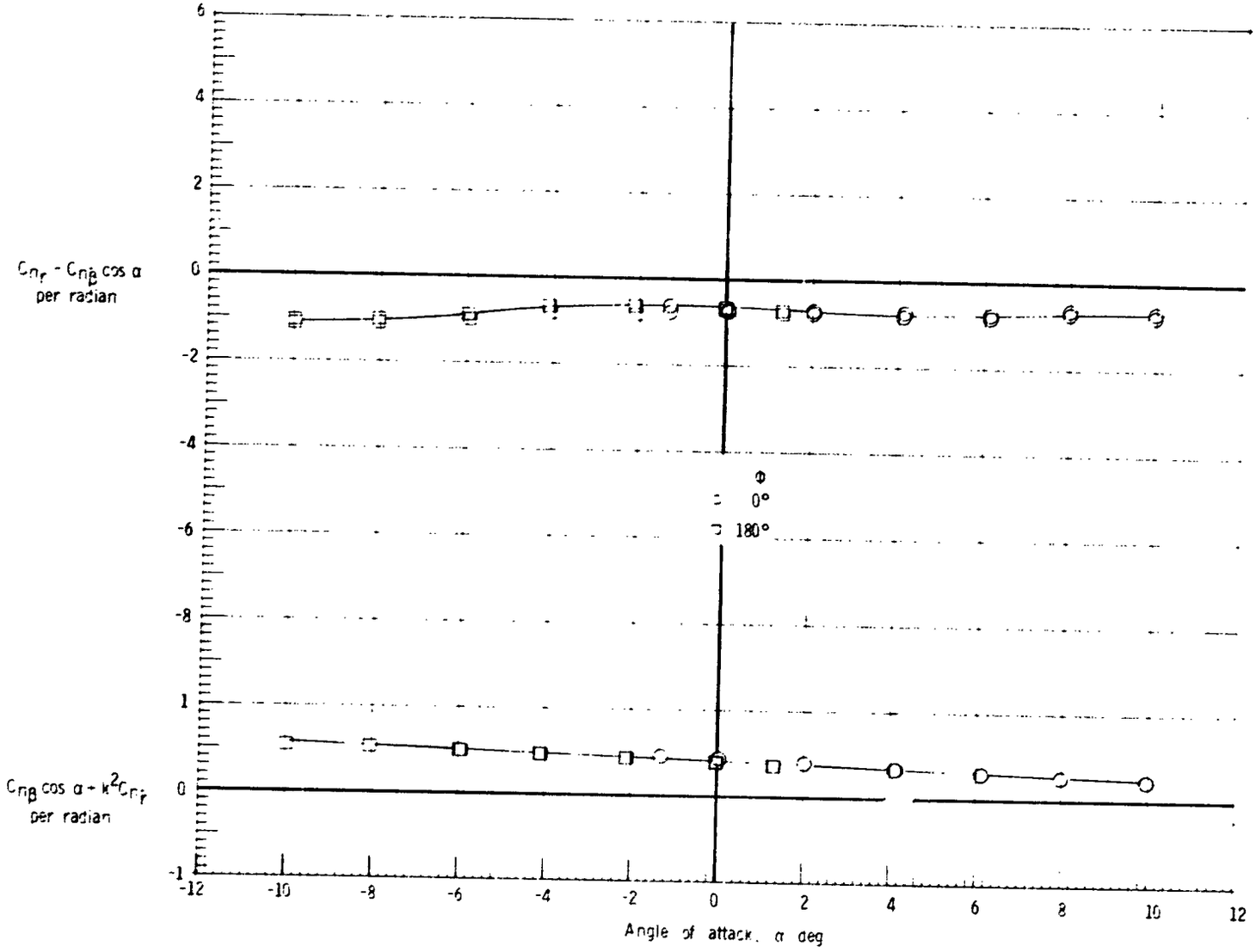

(d) M = 4.63.

Figure 11.- Concluded.

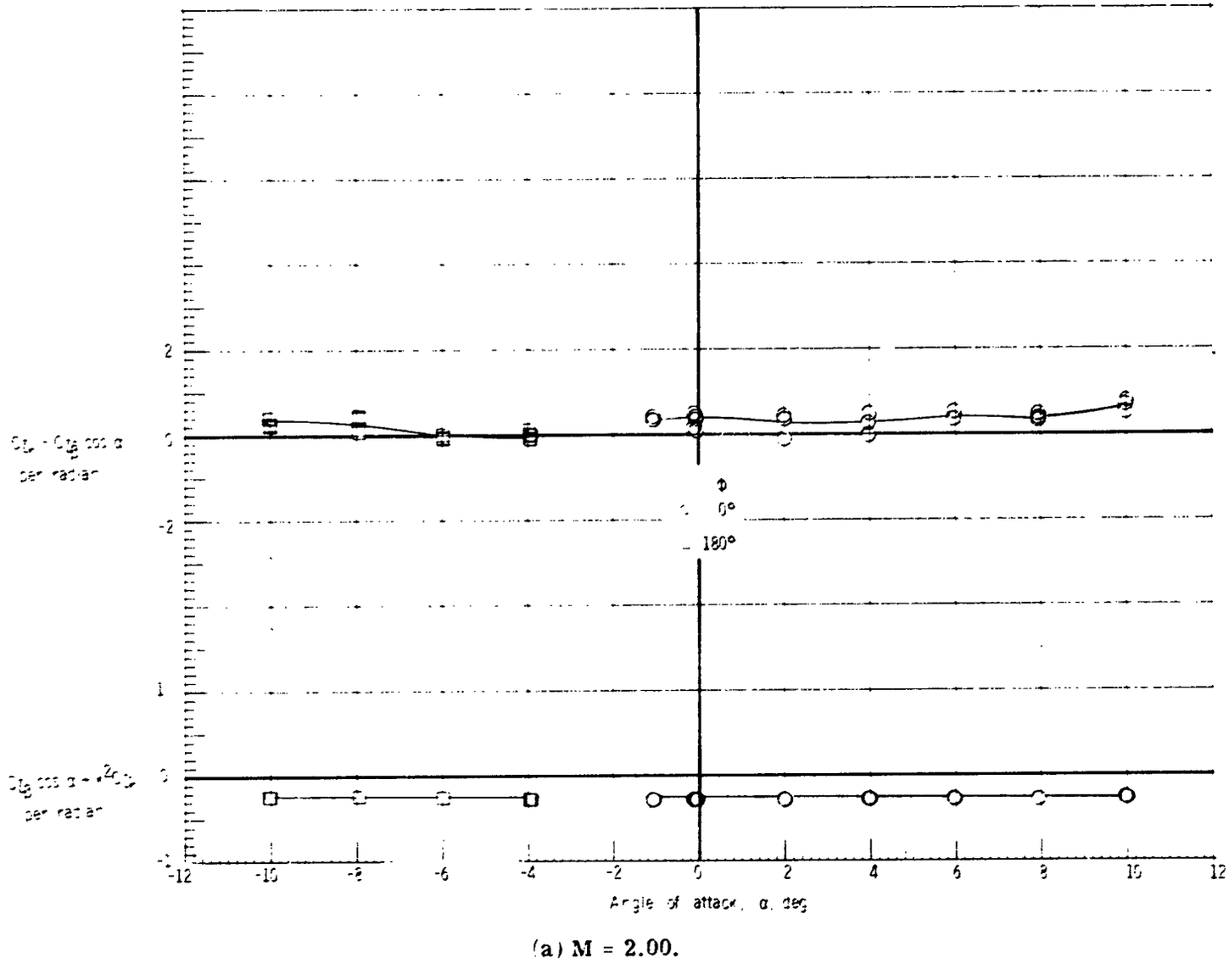

(a) M = 2.00.

Figure 12.- Rolling moment due to yaw-rate parameter and effective dihedral parameter for the launch configuration; maximum dynamic pressure center-of-gravity position.

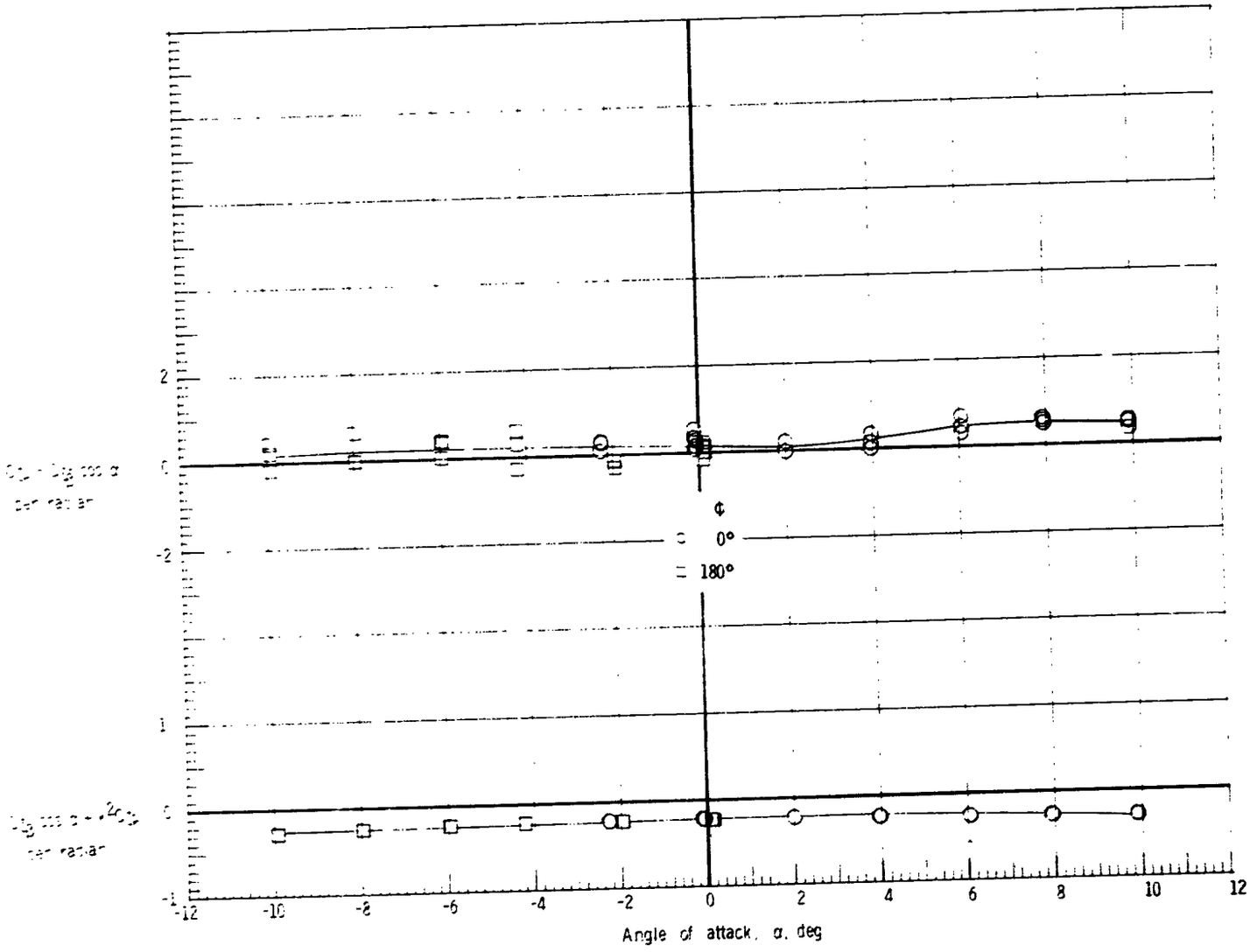

(b) M = 2.86.

Figure 12.- Continued.

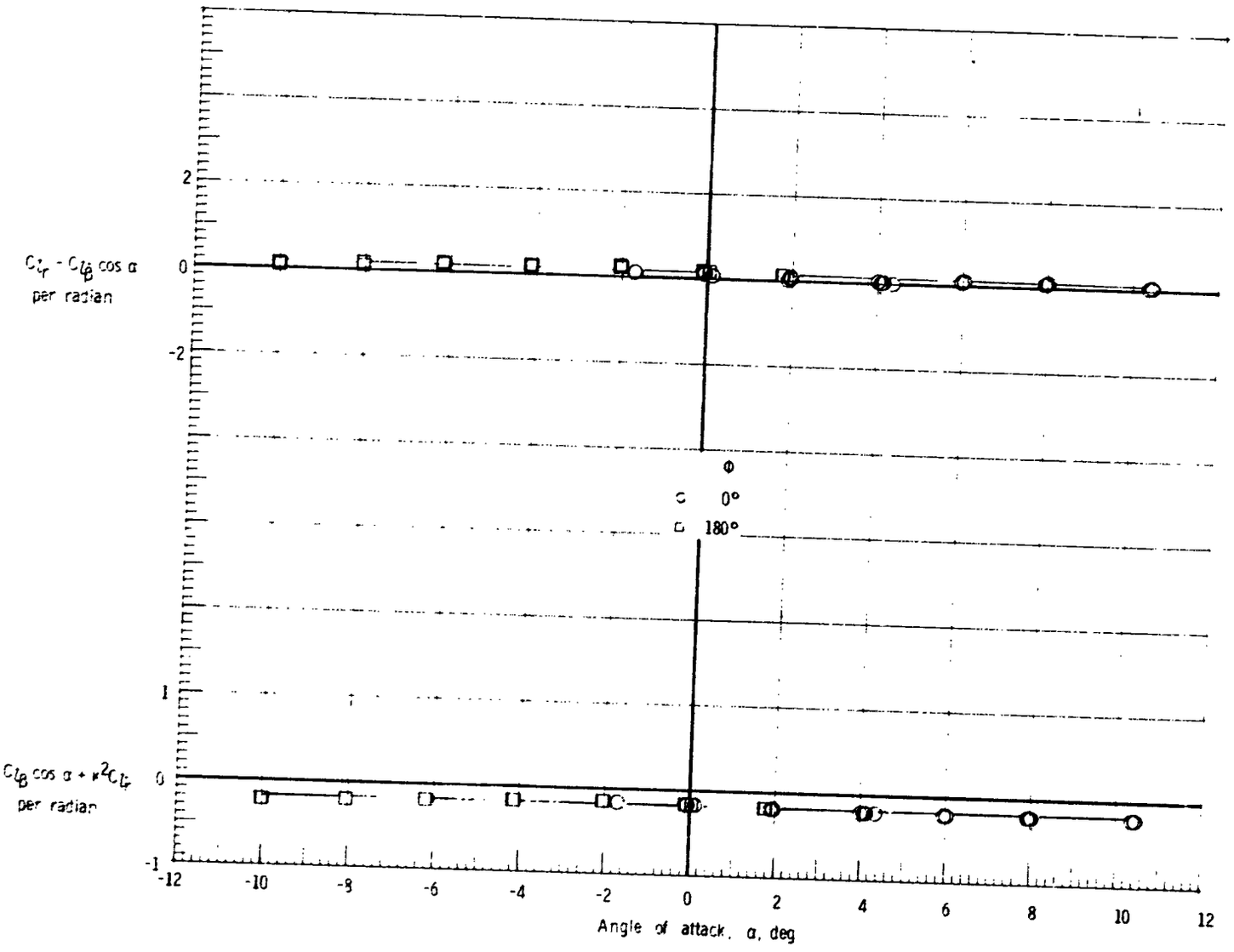

(c) M = 3.96.

Figure 12.- Continued.

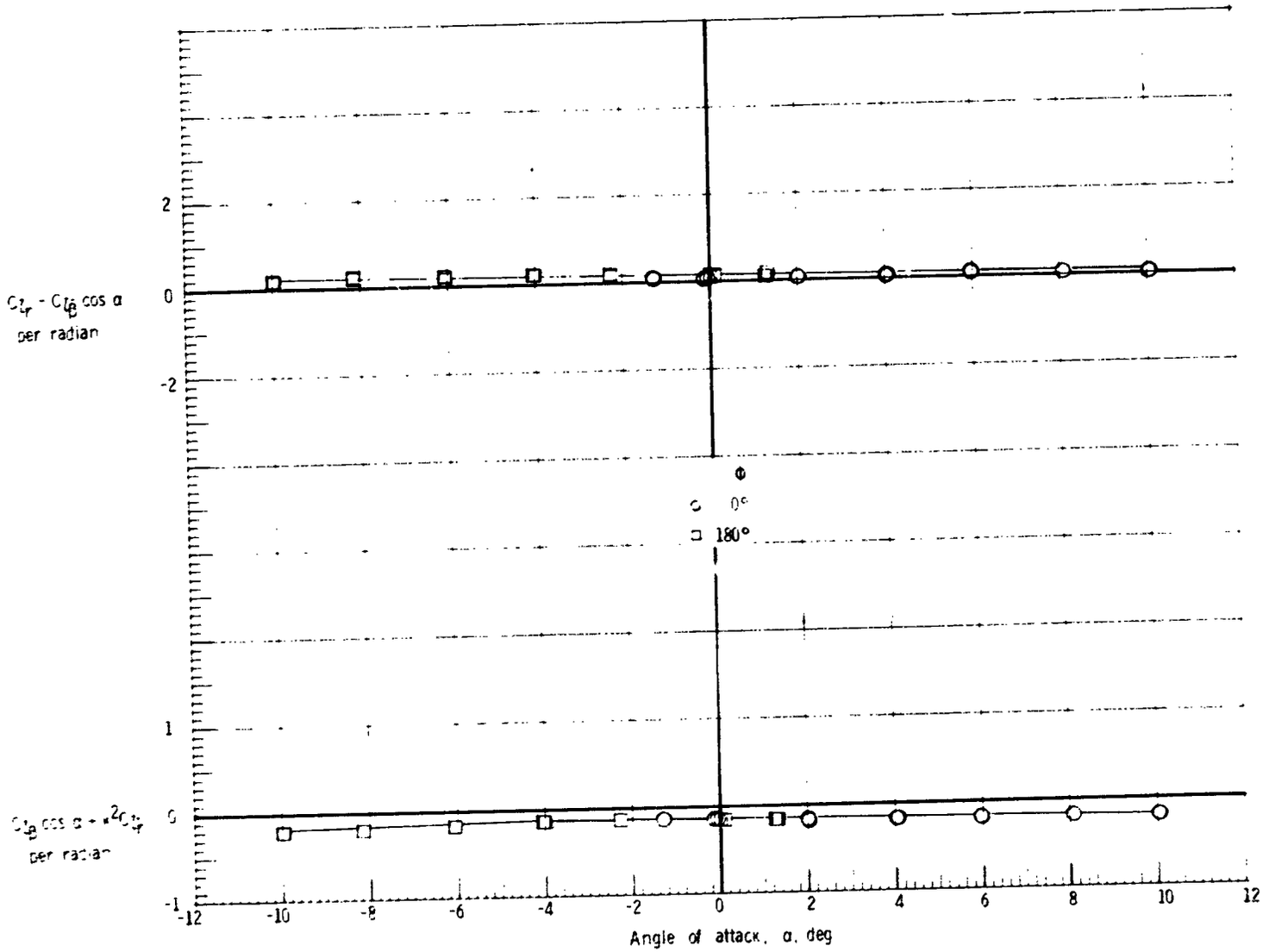

(d) M = 4.63.

Figure 12.- Concluded.

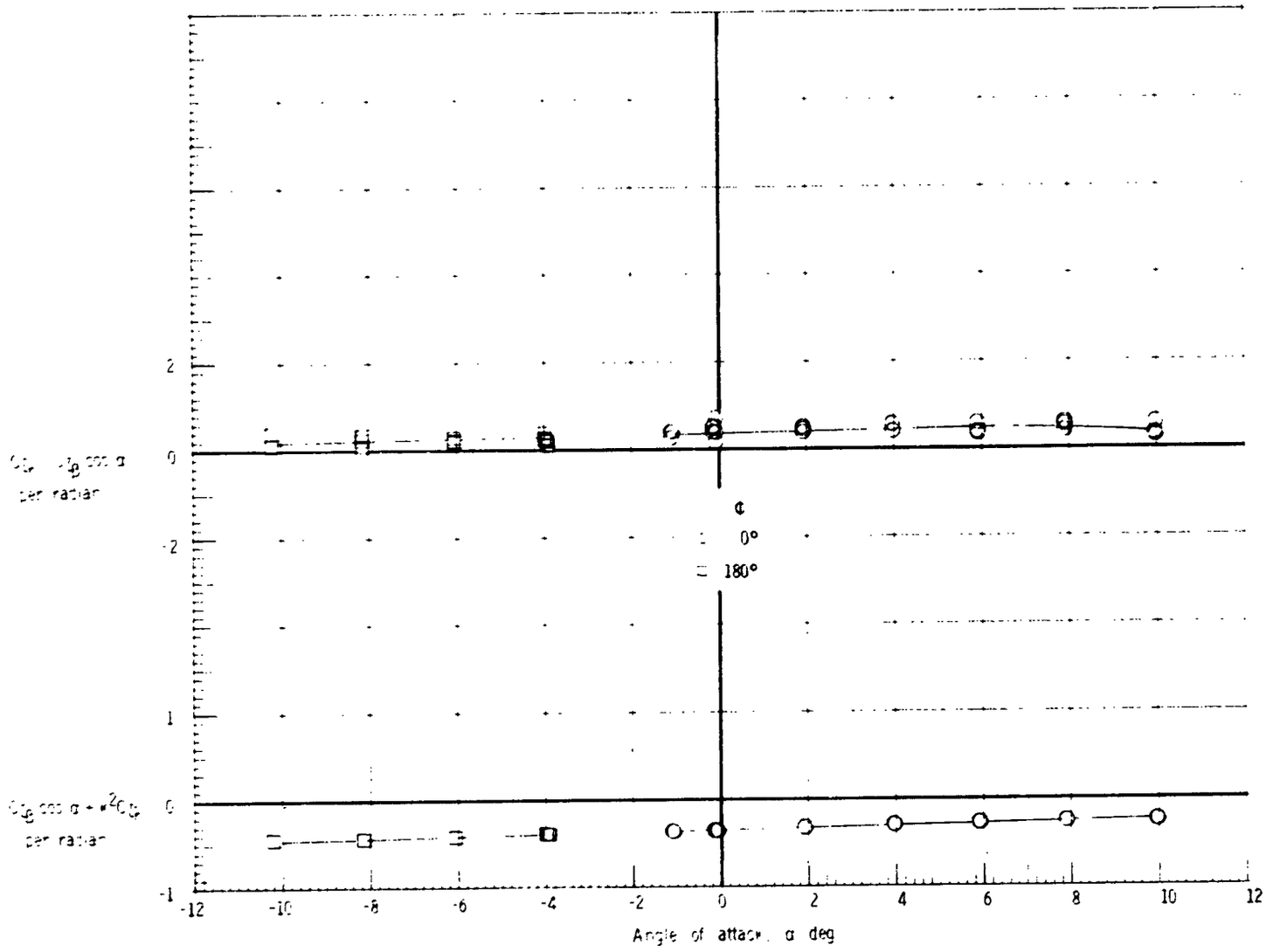

(a) M = 2.00.

Figure 13.- Rolling moment due to yaw-rate parameter and effective dihedral parameter for the orbiter external-tank configuration.

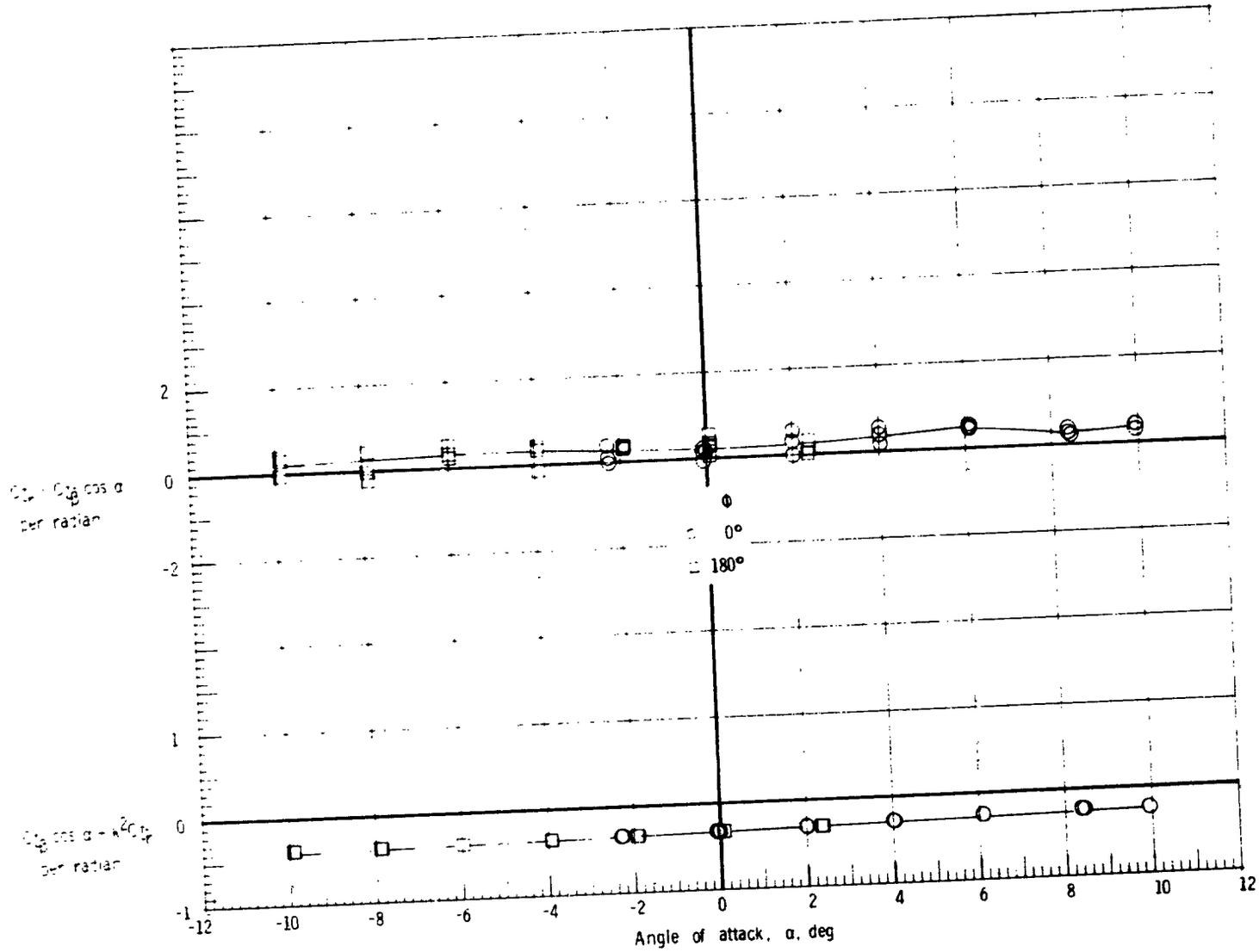

(b) M = 2.86.

Figure 13.- Continued.

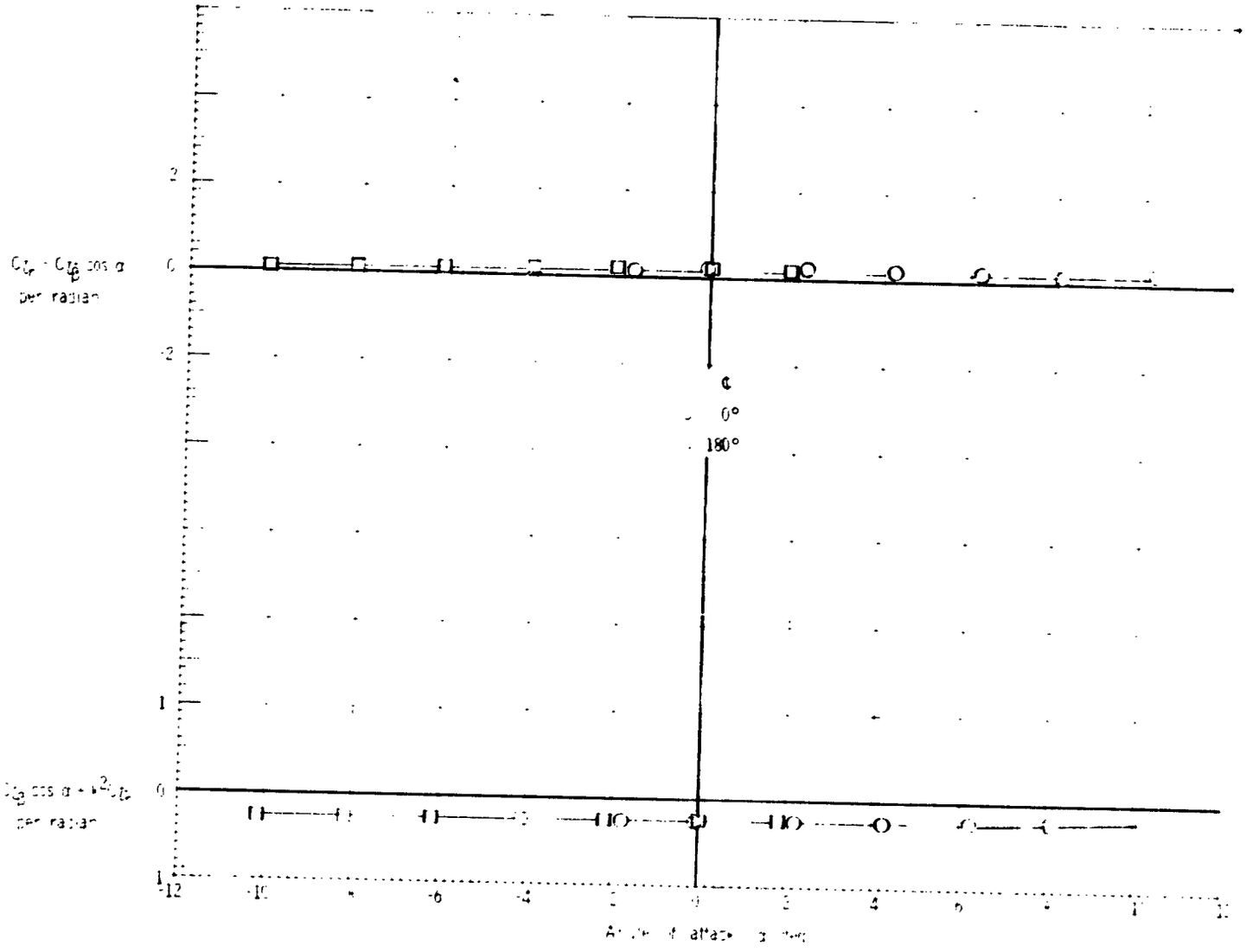

(c) M = 3.96.

Figure 13.- Continued.

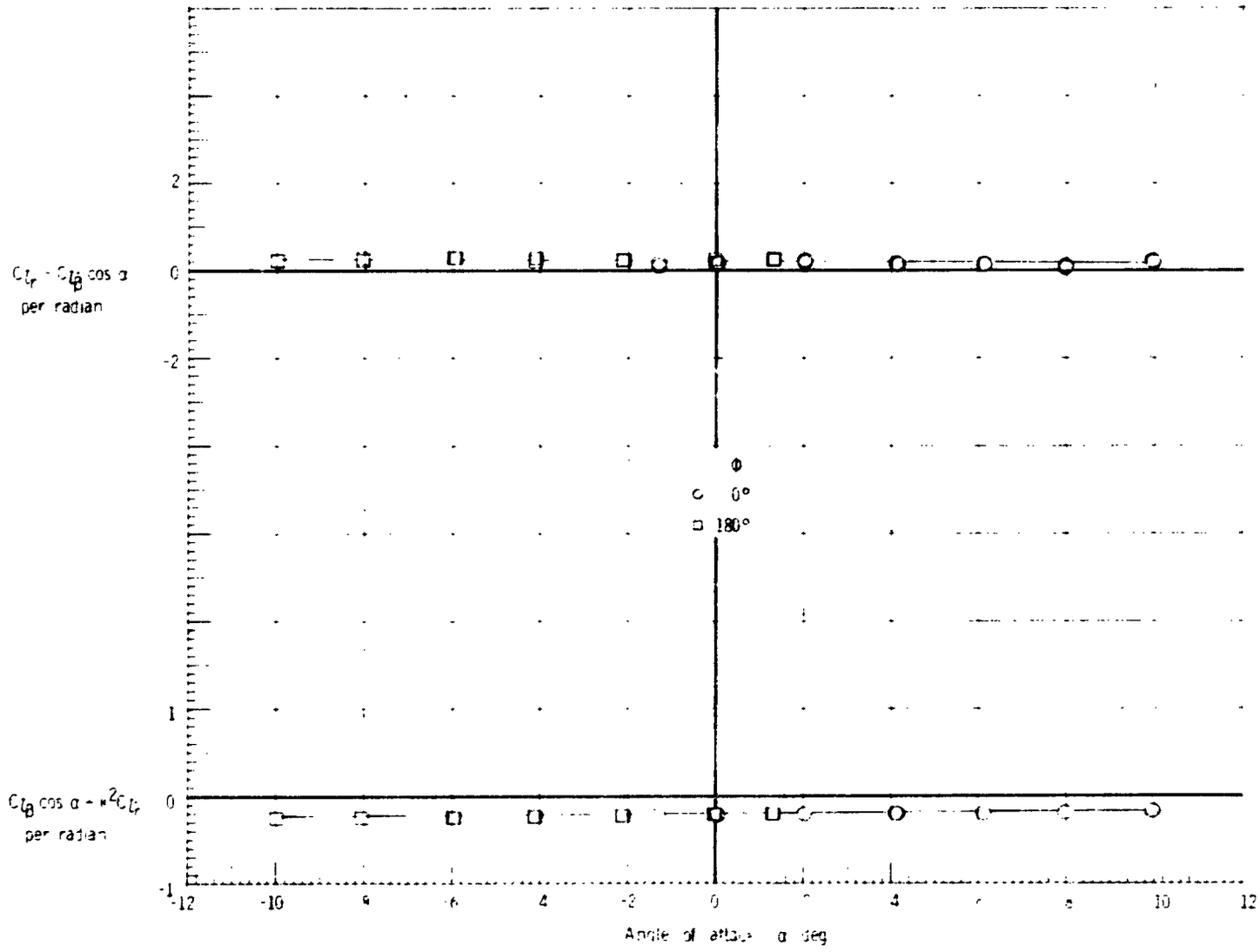

(d) M = 4.63.

Figure 13.- Concluded.

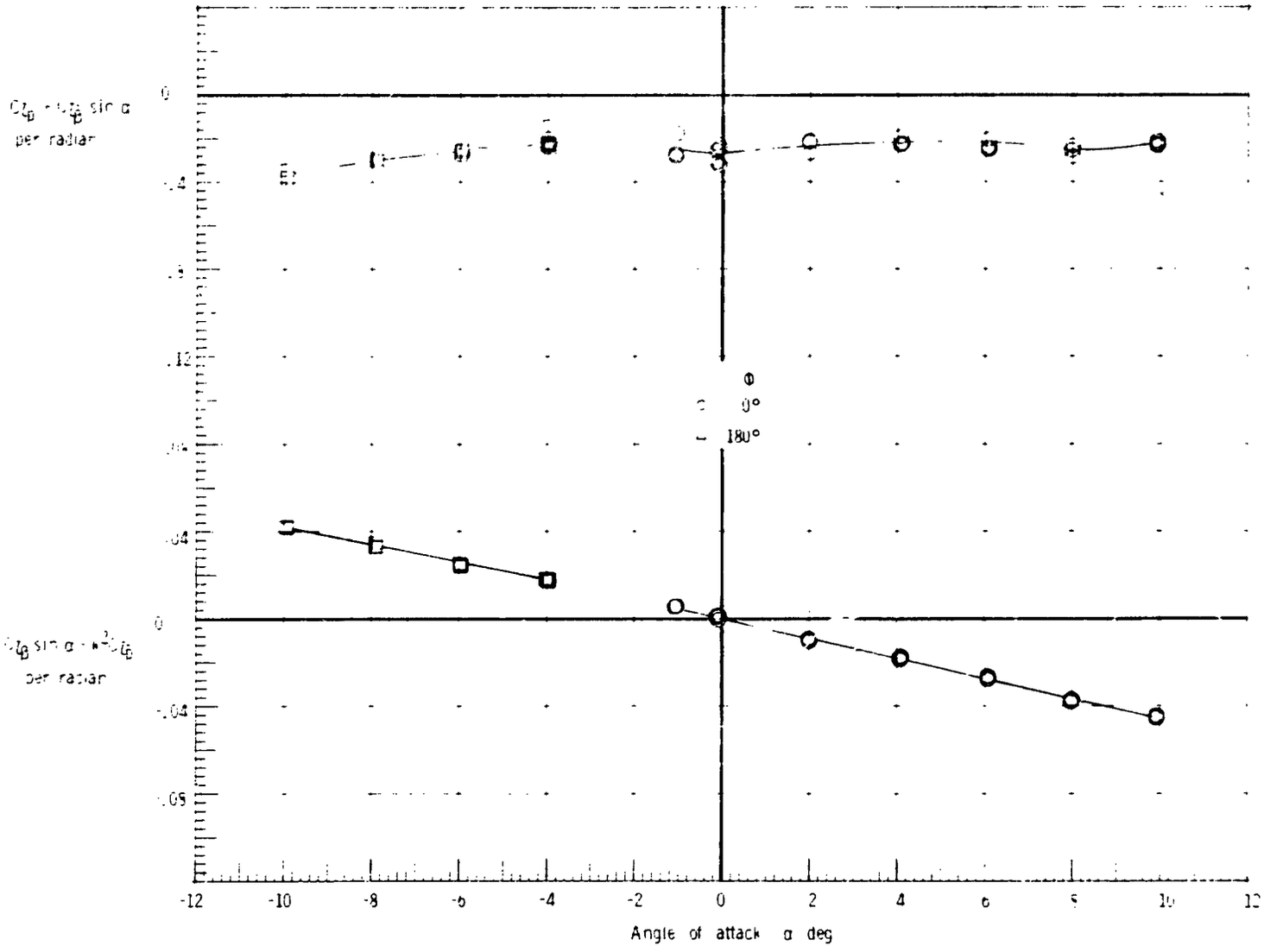

(a) M = 2.00.

Figure 14.- Damping-in-roll parameter and rolling moment due to roll-displacement parameter for the launch vehicle; maximum dynamic pressure center-of-gravity position.

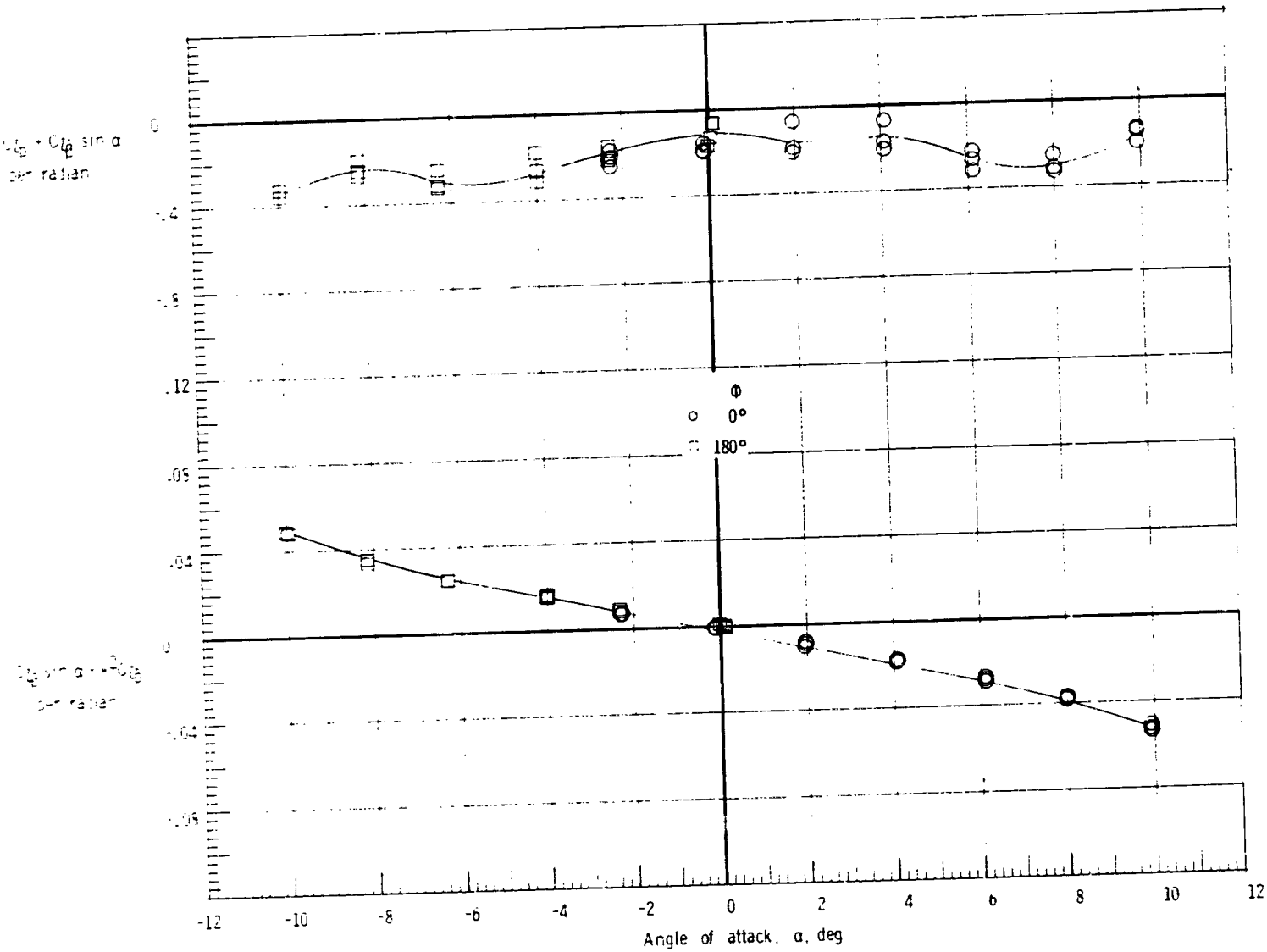

(b) M = 2.86.

Figure 14.- Continued.

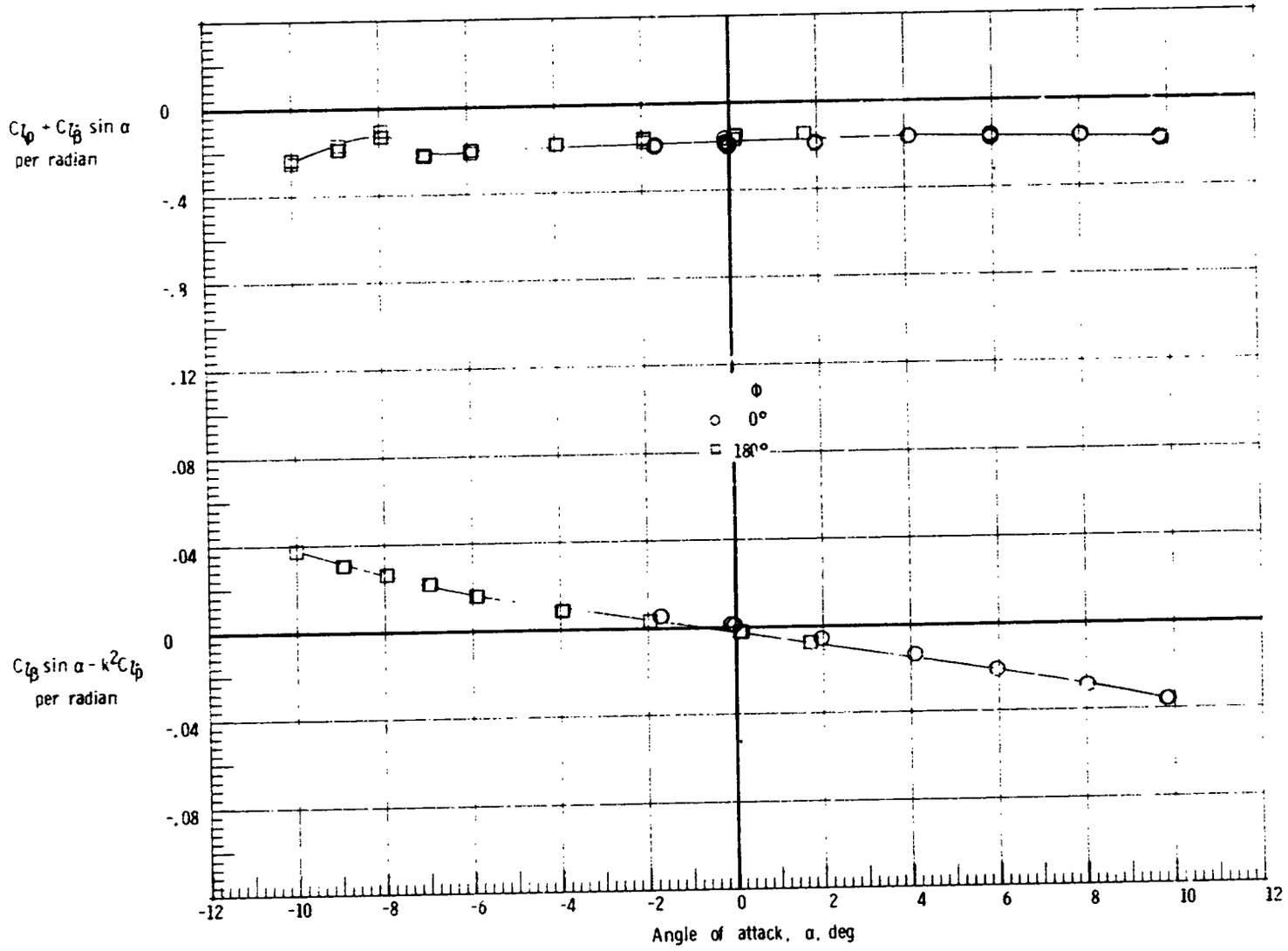

(c) M = 3.96

Figure 14.- Continued.

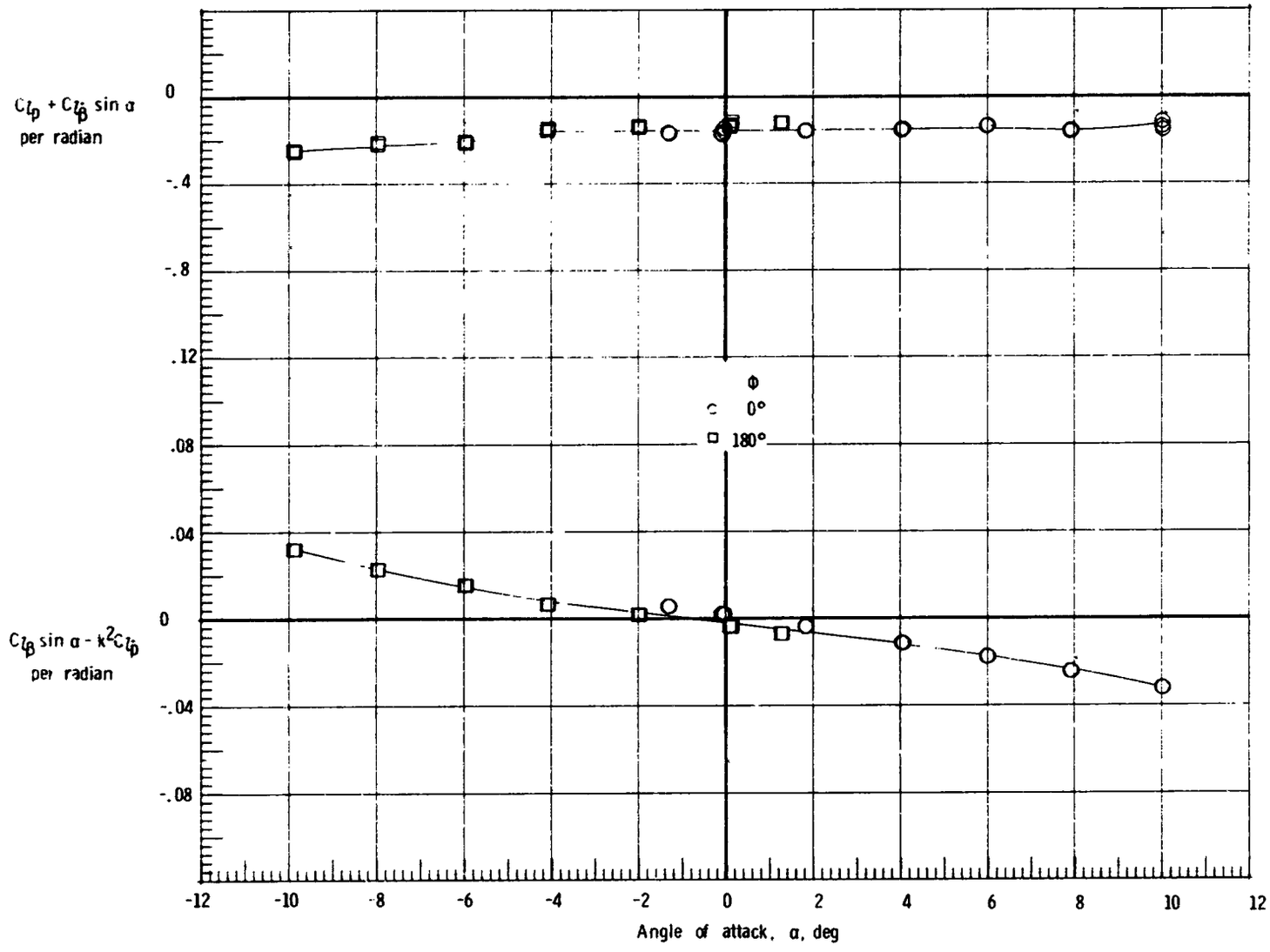

(d) M = 4.63.

Figure 14.- Concluded.

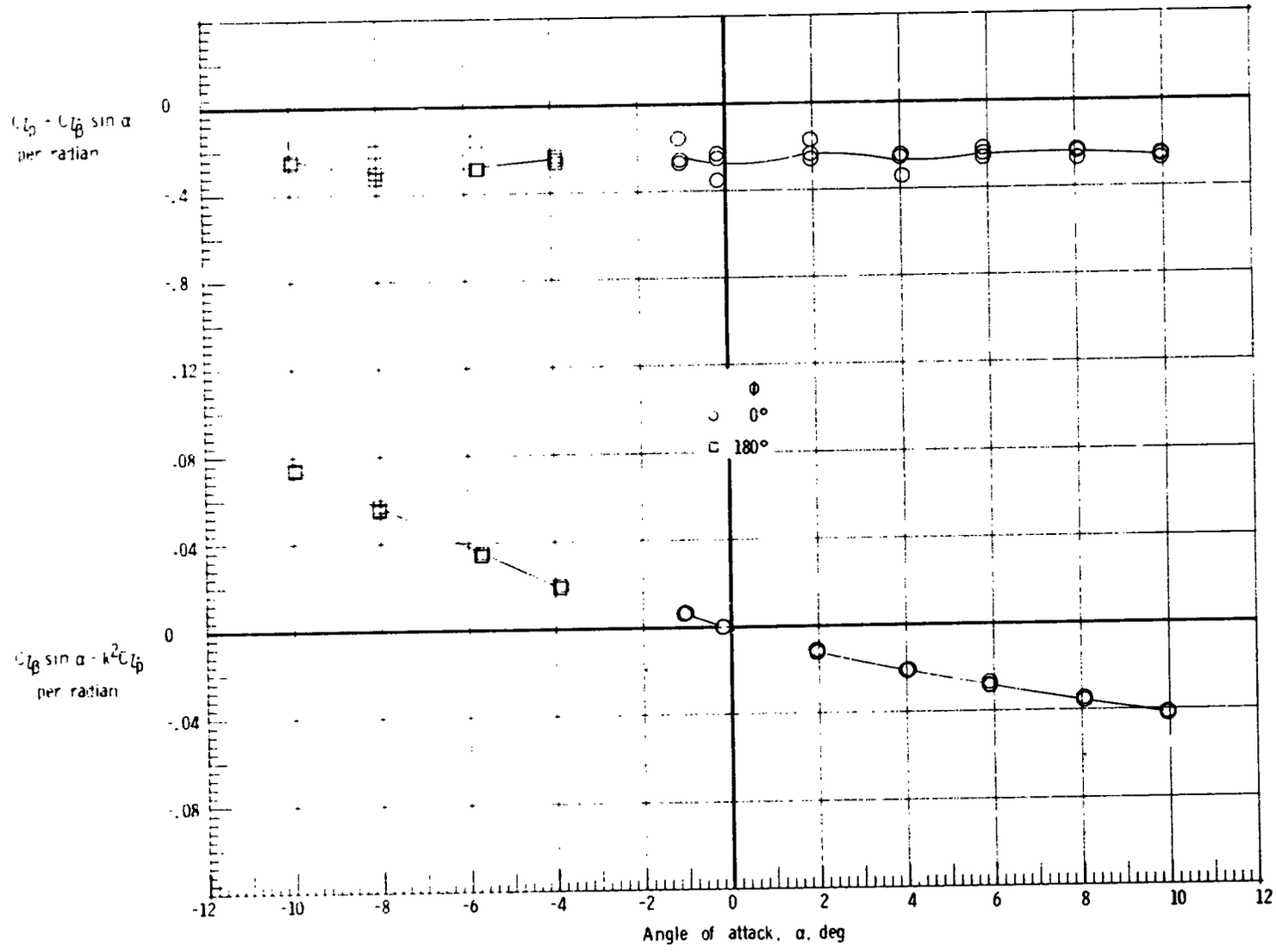

(a) M = 2.00.

Figure 15.- Damping-in-roll parameter and rolling moment due to roll-displacement parameter for the orbiter external-tank configuration.

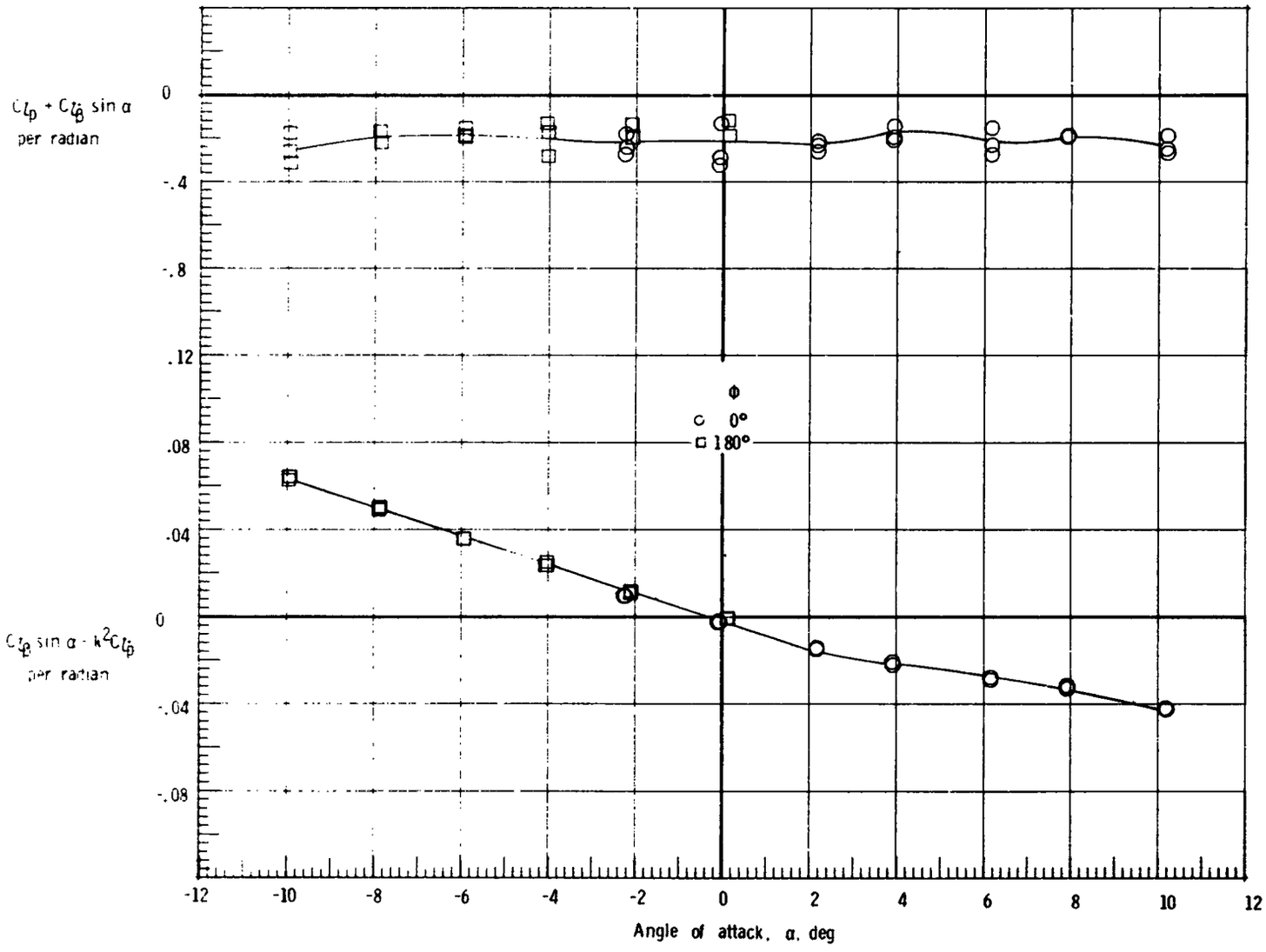

(b) M = 2.86.

Figure 15.- Continued.

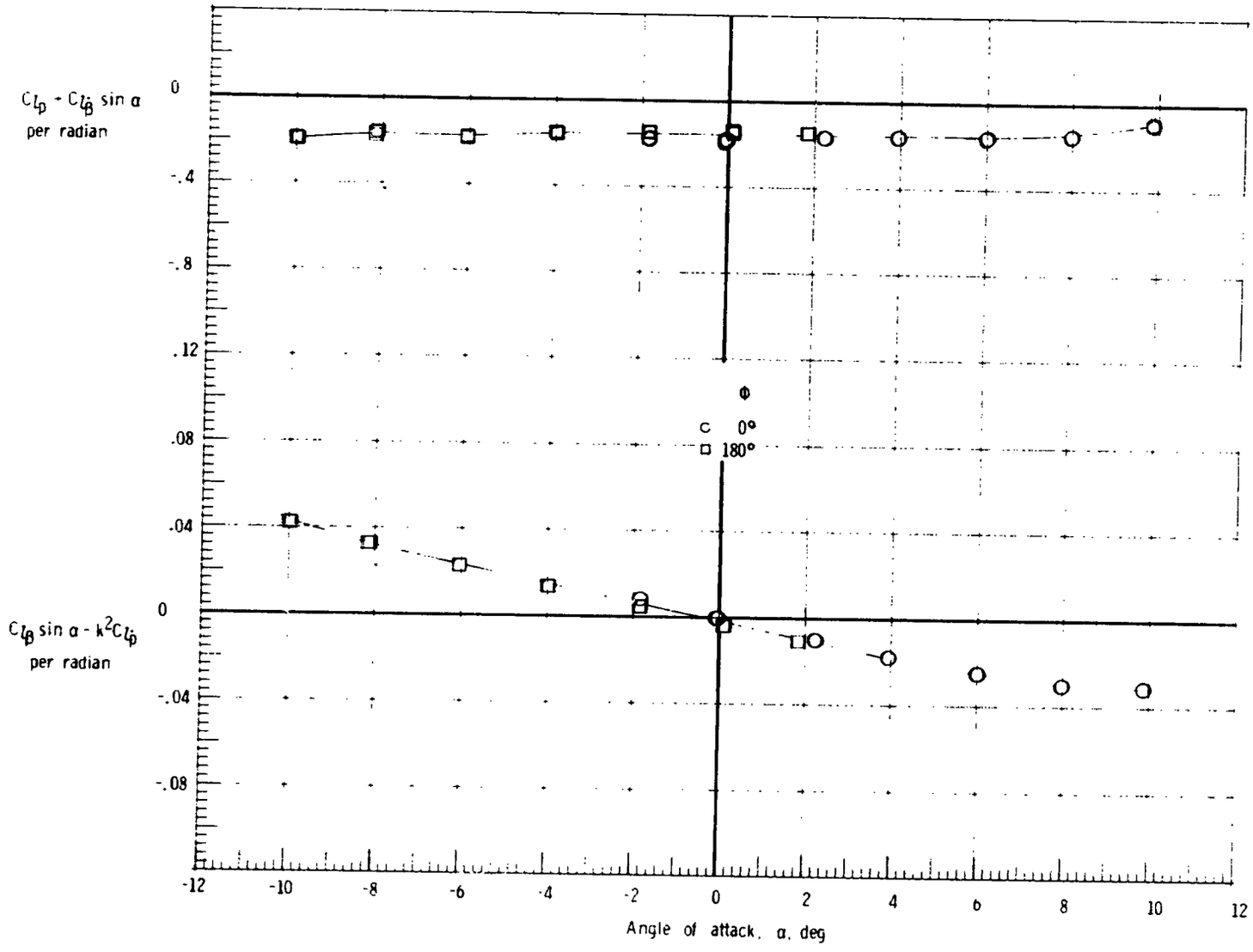

(c) M = 3.96.

Figure 15. Continued.

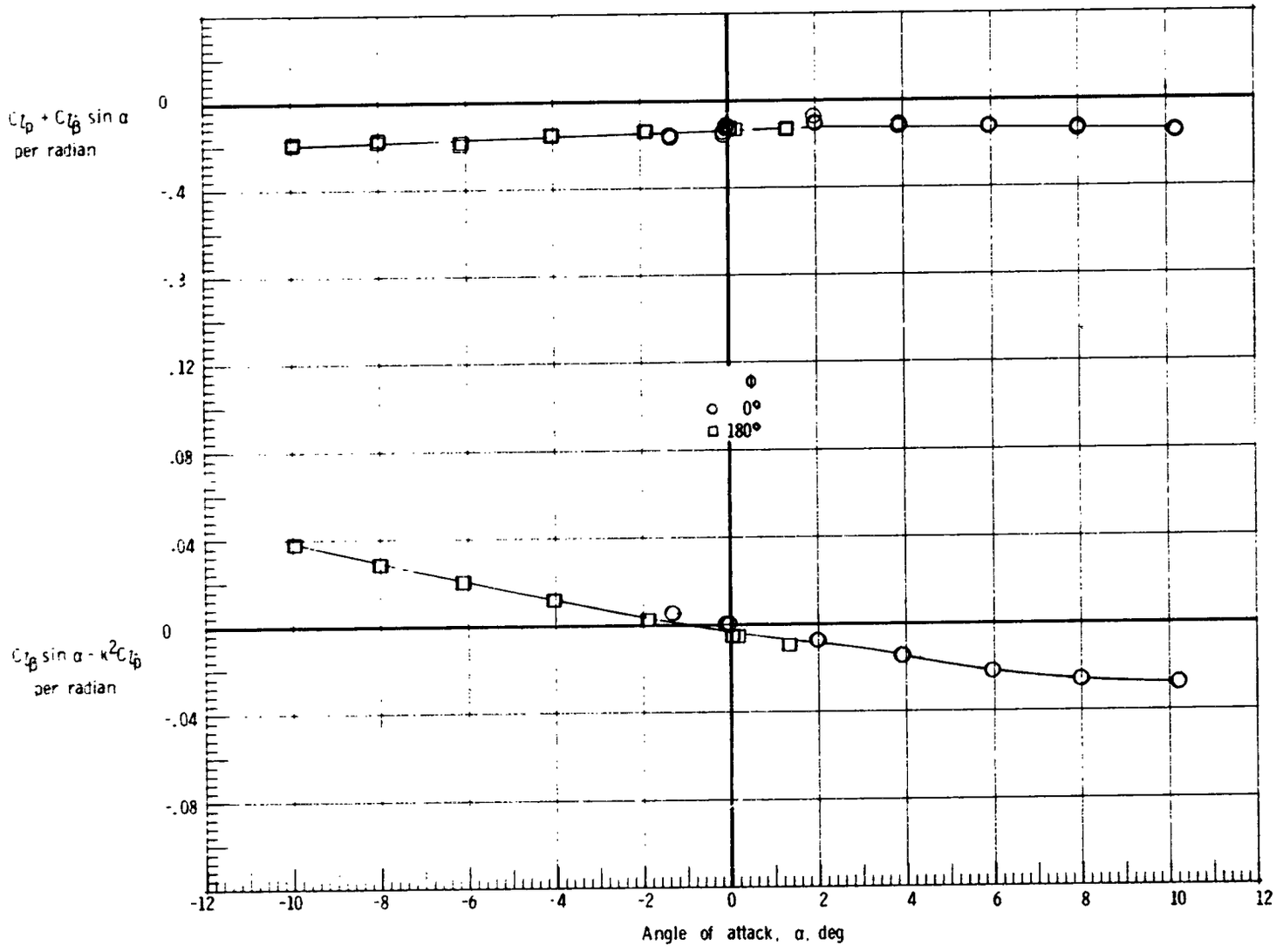

(d) M = 4.63.

Figure 15.- Concluded.

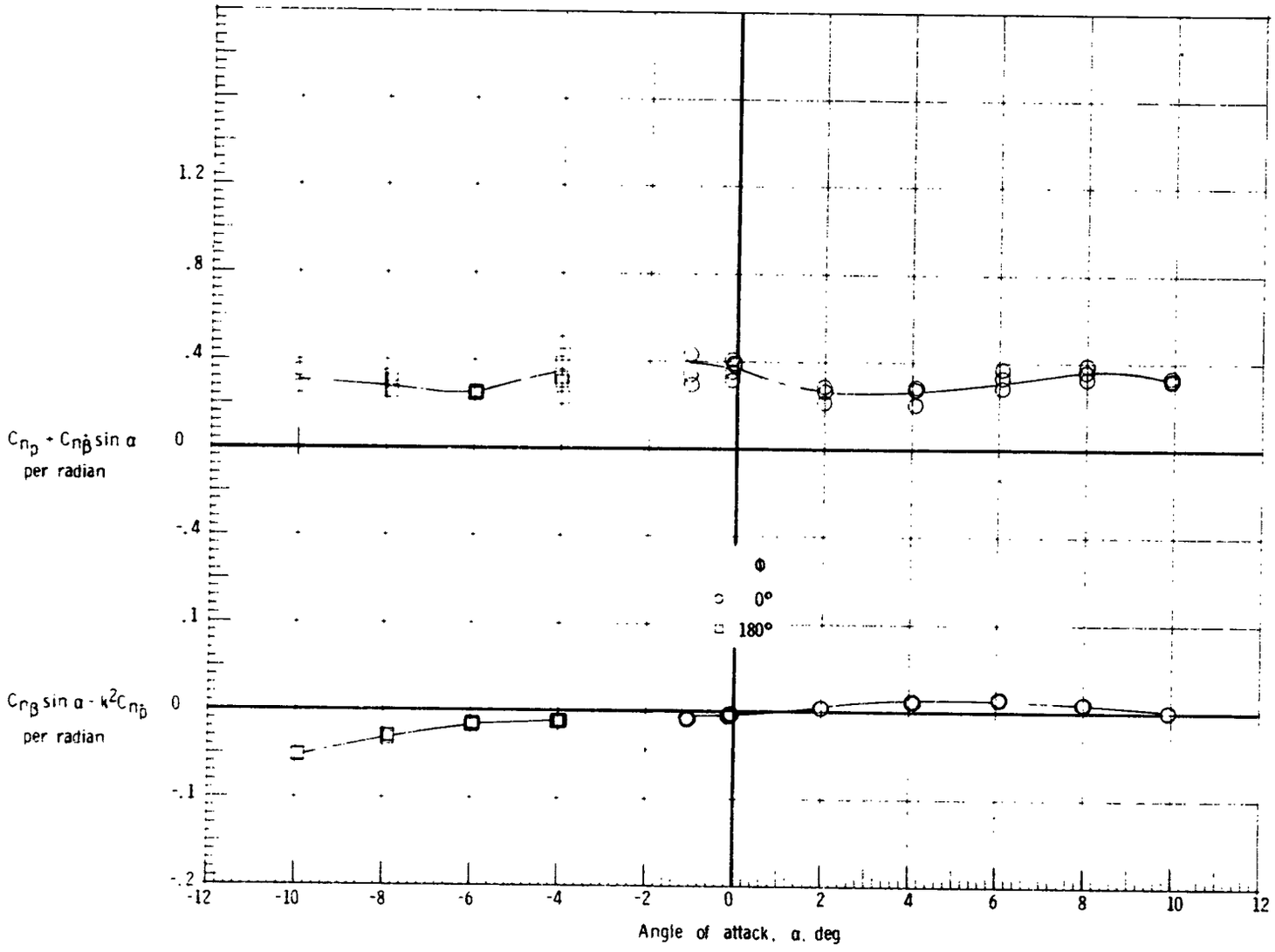

(a) M = 2.00.

Figure 16.- Yawing moment due to roll-rate parameter and yawing moment due to roll-displacement parameter for the launch configuration; maximum dynamic pressure center-of-gravity position.

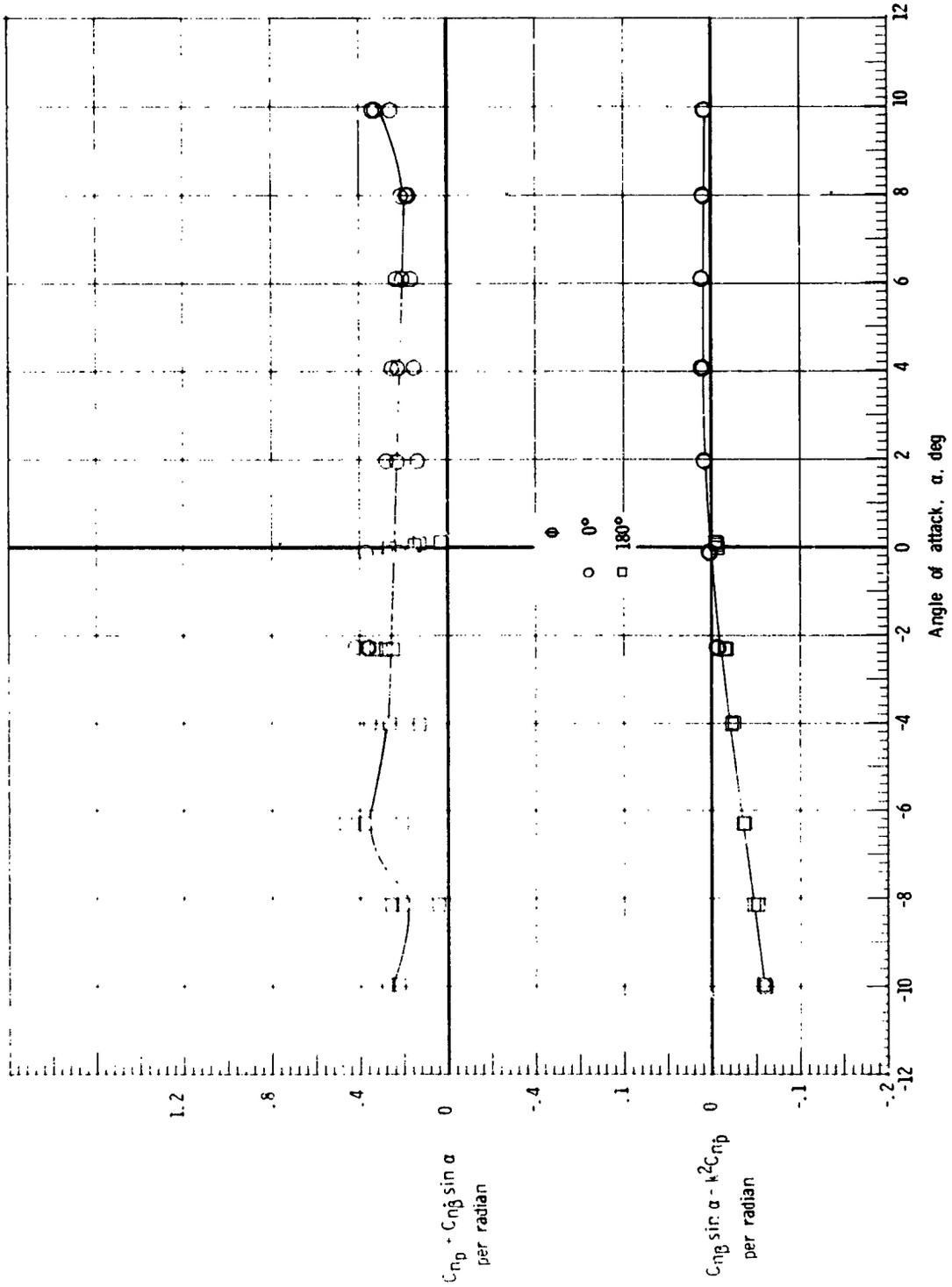

(b) M = 2.86.

Figure 16.- Continued.

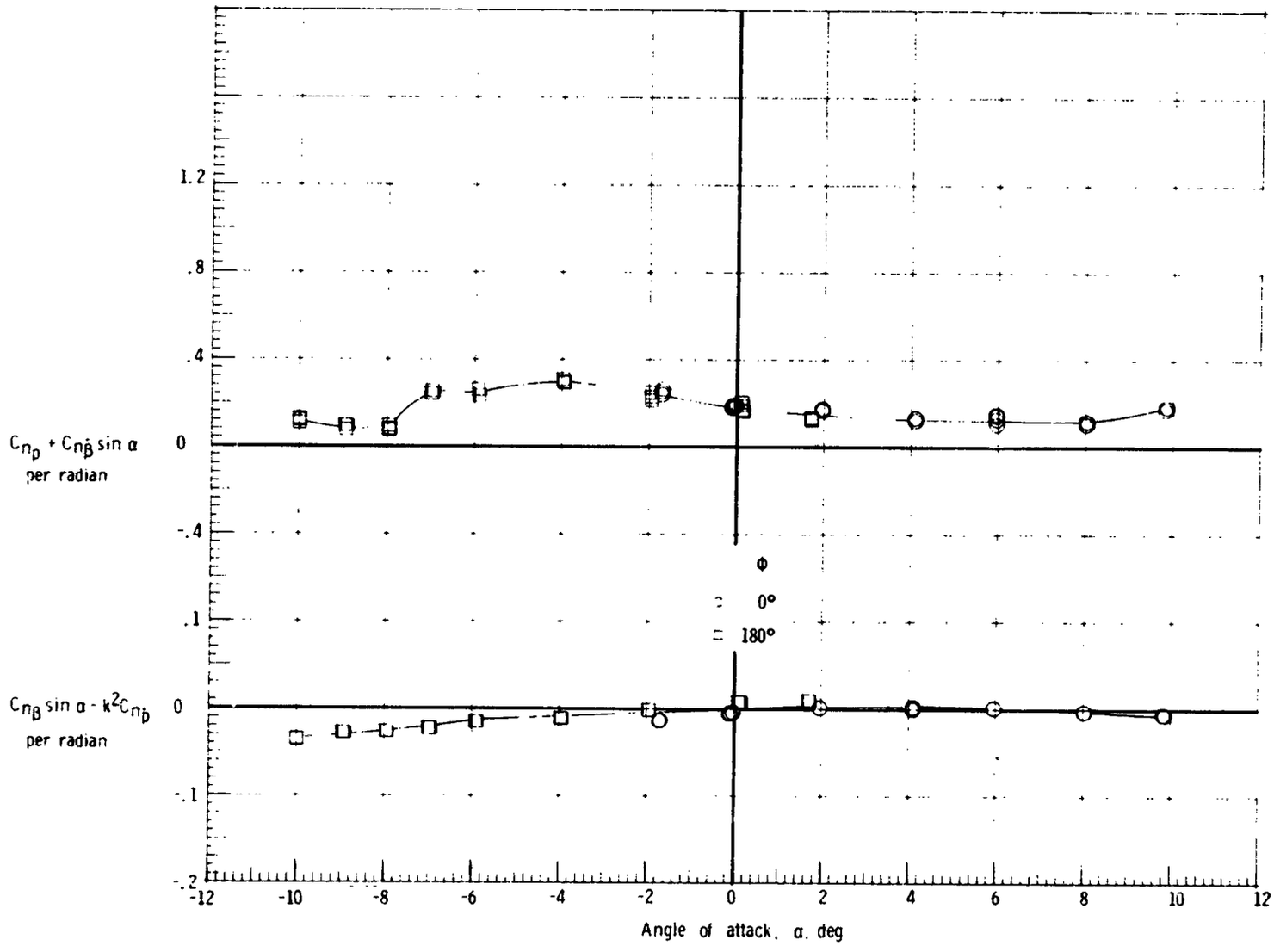

(c) M = 3.96.

Figure 16.- Continued.

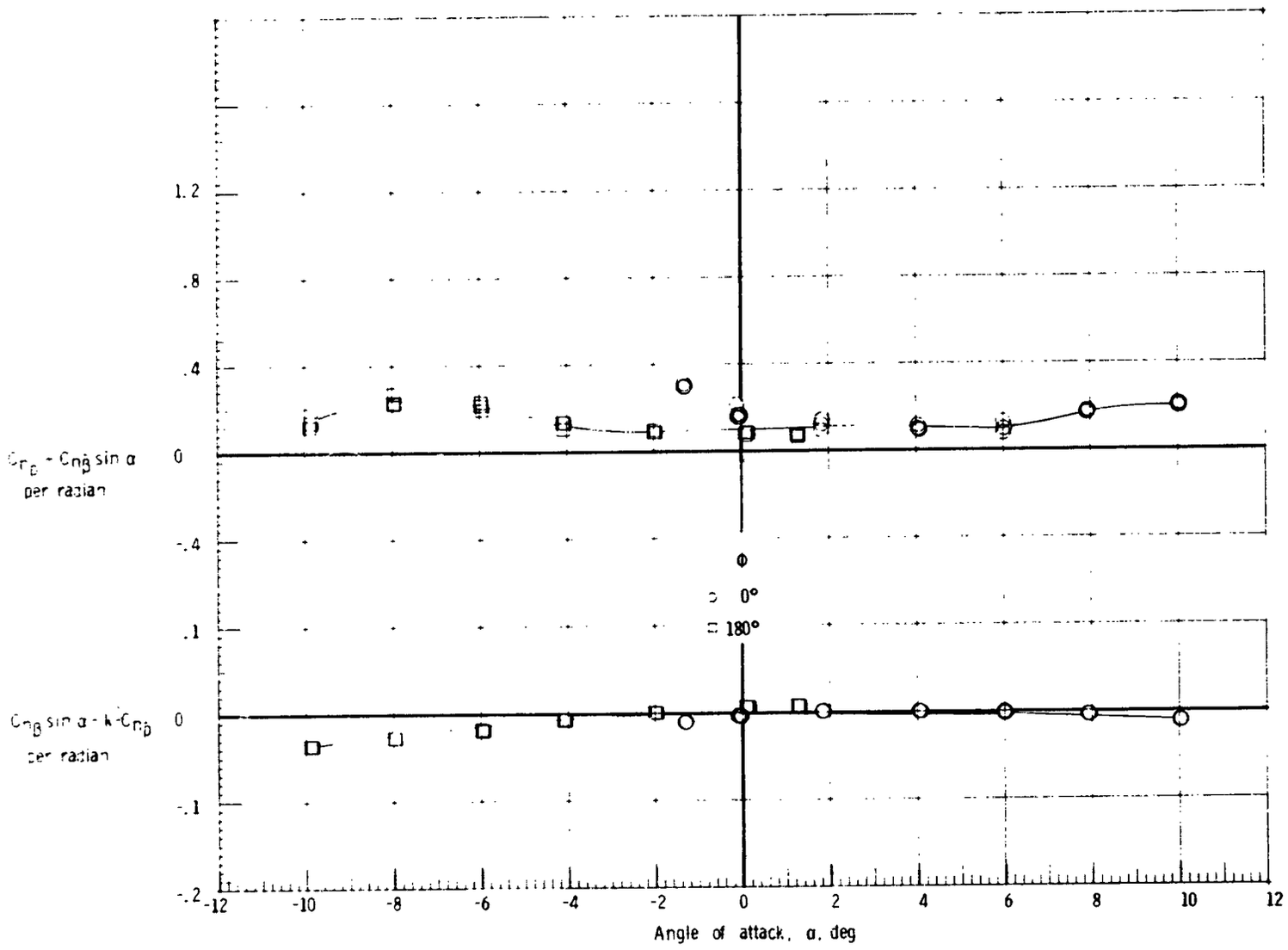

(d) M = 4.63.

Figure 16.- Concluded.

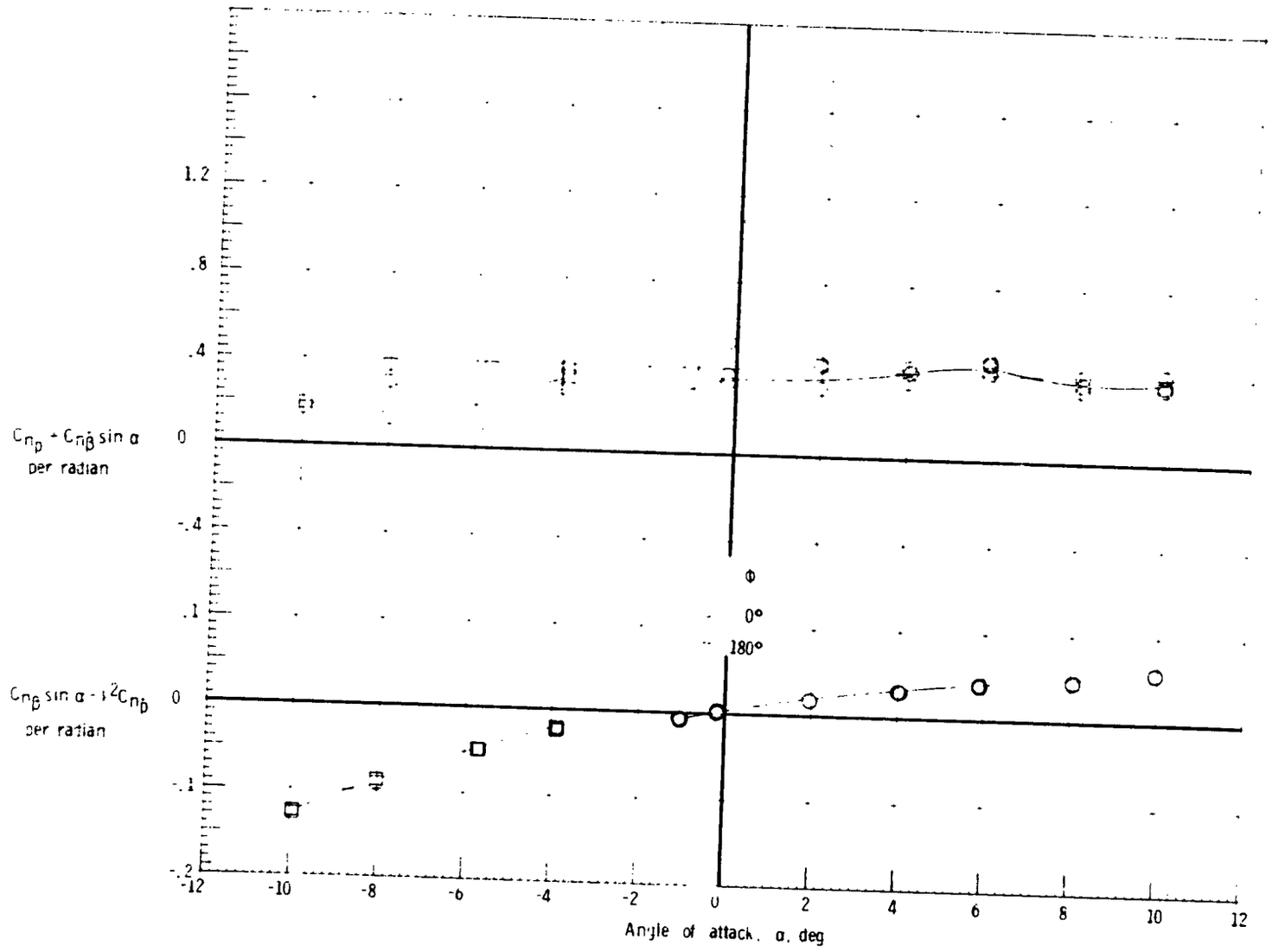

(a) M = 2.00.

Figure 17.- Yawing moment due to roll-rate parameter and yawing moment due to roll-displacement parameter for the orbiter external-tank configuration.

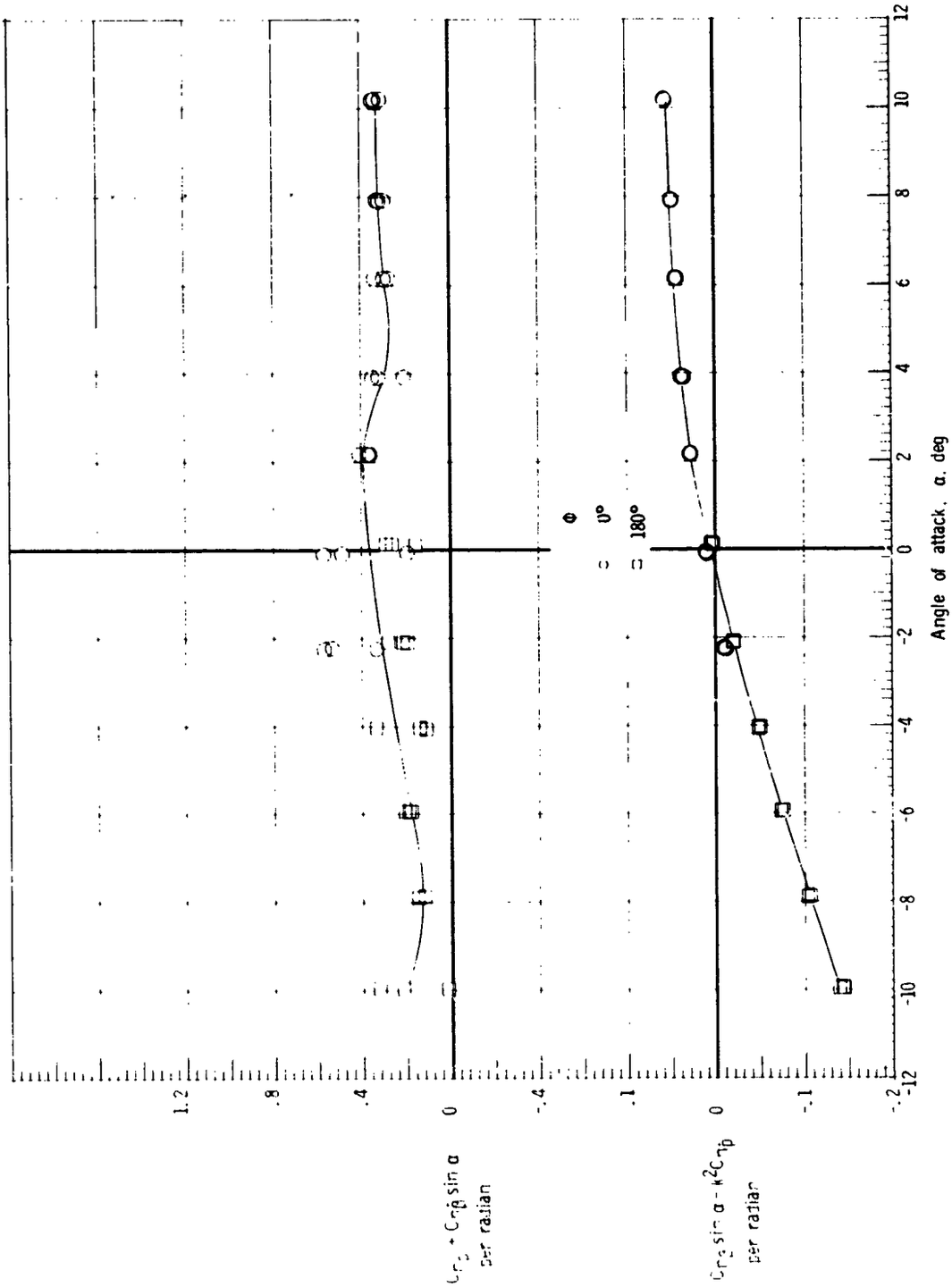

(b) M = 2.86.

Figure 17.- Continued.

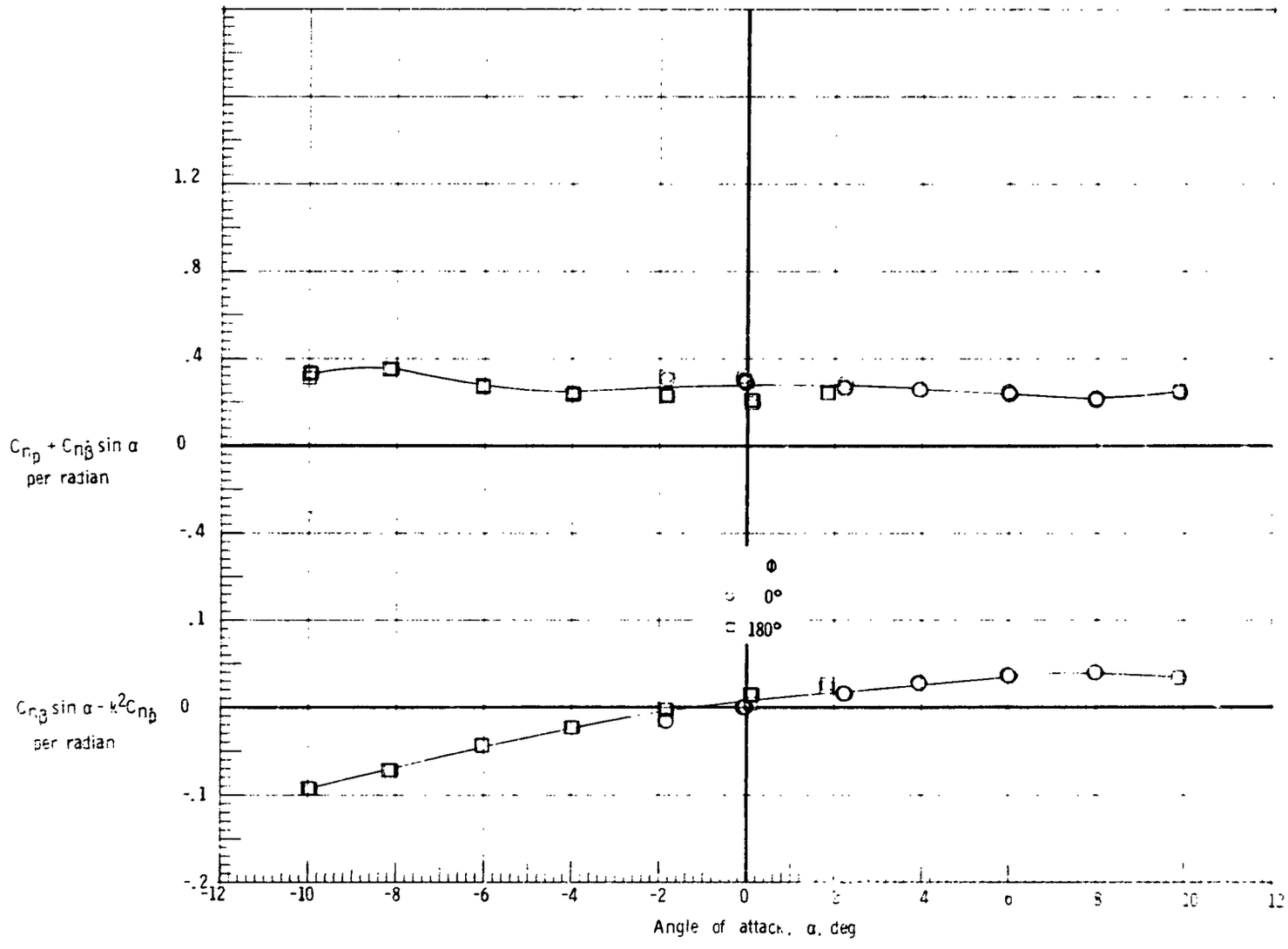

(c) M = 3.96.

Figure 17.- Continued.

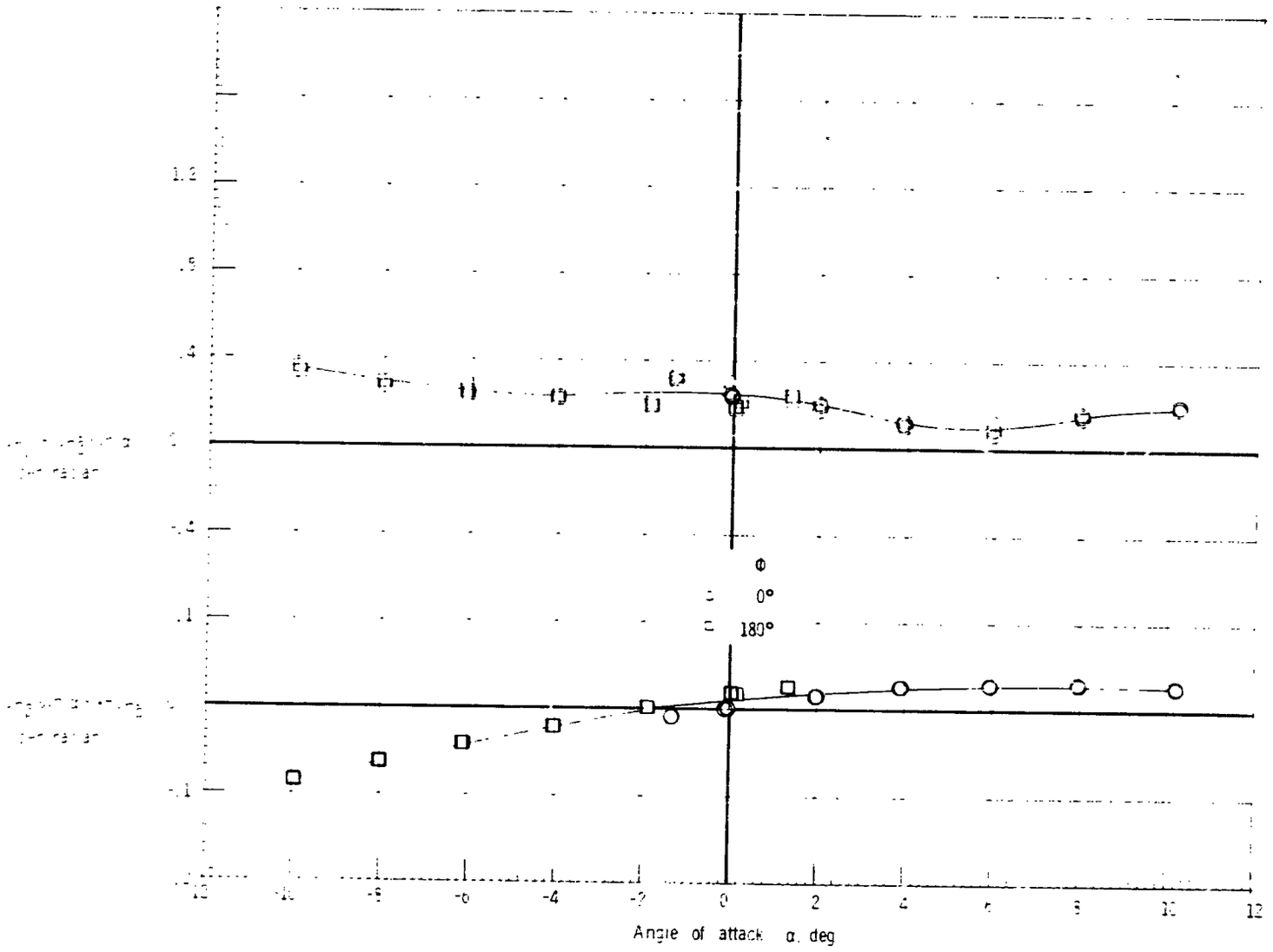

(d) M = 4.63.

Figure 17.- Concluded.